The Dissertation Committee for Vladimir Alexandrovich Zyuzin certifies that this is the approved version of the following dissertation:

One-dimensional bosonization approach to higher dimensions

Committee:

Gregory A. Fiete, Supervisor

Alexander A. Demkov

Allan H. MacDonald

Qian Niu

Lorenzo Sadun

One-dimensional bosonization approach to higher dimensions

by

Vladimir Alexandrovich Zyuzin, B.S., M.Phy.

DISSERTATION

Presented to the Faculty of the Graduate School of

The University of Texas at Austin

in Partial Fulfillment

of the Requirements

for the Degree of

DOCTOR OF PHILOSOPHY

THE UNIVERSITY OF TEXAS AT AUSTIN

May 2012

Dedicated to my father and mother

Acknowledgments

I thank my research advisor Gregory A. Fiete for inspiring discussions with him, his support and for raising me as an independent researcher. I thank my previous academic advisors E.G. Mishchenko, M.E. Raikh, and A.Yu. Zyuzin for patiently educating me. Discussions with condensed matter theory professors at the University of Texas at Austin, Allan H. MacDonald and Qian Niu are greatly acknowledged.

I thank my father and mother for their support and care they gave me. I thank my brothers Alexander and Dmitry.

A very big thanks to my friends, Peter Bagrov, Rostislav Bukasov, Abdul Haque Chang, Victor Chua, Andrey Danilenko, Apollo Ellis, Mariya Fetisova, Suhas Gangadharaiah, Mikhail Glazov, Maksim Gorokhov, Andrey Greshnov, Moe Jangda, Sergey Karasev, Jogendro Kshetrimayum, Rafael Moreira, Evgeny Makshanov, Marina Semina, Mikhail Sharkov, Peter Shternin and Alexander Slepko for their support and for inspiring me to see other interesting and beautiful possibilities in life.

One-dimensional bosonization approach to higher dimensions

Publication No. _____

Vladimir Alexandrovich Zyuzin, Ph.D.
The University of Texas at Austin, 2012

Supervisor: Gregory A. Fiete

This dissertation is devoted to theoretical studies of strongly interacting one-dimensional and quasi one-dimensional electron systems. The properties of one-dimensional electron systems can be studied within the bosonization technique, which presents fermions as collective bosonic density excitations. The power of this approach is the ability to treat electron-electron interaction exactly in the low-energy limit. The approach predicts the failure of Fermi liquid and an absence of long-range order in one-dimensions. The low-energy description of one-dimensional interacting systems is called the Tomonaga-Luttinger liquid theory.

For example, the edges of quantum Hall systems are one-dimensional and described by a chiral Tomonaga-Luttinger liquid. Another example is a quantum spin Hall system with helical edge states, which are also described

by a Tomonaga-Luttinger liquid. In our first work, a study of magnetized edge states of quantum spin-Hall system is presented. A magnetic field dependent signature of such edges is obtained, which can be verified in a Coulomb drag experiment.

The second part of the dissertation is devoted to quasi-one dimensional antiferromagnetic lattices. A spatially anisotropic lattice antiferromagnet can be viewed as an array of one dimensional spin chains coupled in a way to match the lattice symmetry. This allows to use the non-Abelian bosonization technique to describe the low-energy physics of spin chains and study the inter-chain interactions perturbatively. The work presented in the dissertation studies the effect of Dzyaloshinskii-Moriya interaction on the magnetic phase diagram of the spatially anisotropic kagome antiferromagnet. We predict a Dzyaloshinskii-Moriya interaction driven phase transition from Neel to Neel+dimer state.

In the third work, a novel model of the fractional quantum Hall effect is given. Wave functions of two-dimensional electrons in strong and quantizing magnetic field are essentially one-dimensional. That invites one to use the one-dimensional phenomenological bosonization to describe the density fluctuations of the two-dimensional interacting electrons in magnetic field. Remarkably, the constructed trial bosonized fermion operator describing the electron states with a fixed Landau gauge momentum is effectively two-dimensional.

Table of Contents

List of Figures

Chapter 1

Introduction

1.1 Bosonization in one dimension

The statistics of particles, namely fermionic or bosonic, which the system is composed of define the physical properties of the whole system. In fermion systems, due to Pauli exclusion principle, no two particles can occupy the same energy state. Because of that the Fermi gases are characterized by an occupation number which has a discontinuous jump at the Fermi energy. In two and three dimensions, the electron-electron interactions simply renormalize the Fermi occupation number keeping a discontinuous jump at the Fermi momentum. Essentially, all the excitations above the ground state of a Fermi liquid behave as free electrons, but with renormalized mass. These excitations are called quasi-particles, and can be seen as a free electron "dressed" by a surrounding cloud of charge density. However, in one-dimensional electron system the electron interactions are crucial in the description of the collective behavior. For an electron to propagate, it has to interact with its neighbors, creating a collective density fluctuation. Therefore, any excitations can not be seen as quasi-particles, or almost free electrons with renormalized mass. Alternative description of such system was developed based on the bosonization [30, 62, 86–88, 93].

It can be shown that in one-dimensions one can present fermions in form of bosonic charge and spin density excitations. The electron interactions being quadratic in charge density can then be diagonalized within this description. The resulting liquid of electrons is called the Tomonaga-Luttinger (TL) liquid. It indeed shows a non-Fermi liquid behavior with no discontinuous jump at the Fermi energy. Another peculiarity in one-dimensions the TL liquid predicts is the spin-charge separation, meaning that the spin and charge degree of freedom and their excitations are independent from each other. Another important advance of the TL liquid is the analytical theory for the interaction driven metal-insulator transition (Mott transition).

Examples of the TL liquid naturally occurring in nature include edges of the integer quantum Hall and quantum spin Hall systems, quasi one-dimensional wires, carbon nanotubes and arrays of weakly coupled spin chains. Even though there are not that many one-dimensional electron systems, the theoretical predictions of the TL liquid can give a tremendous insight in to the physics of strongly interacting two or three dimensional electron systems. For example, the knowledge of the mechanism of the one-dimensional Mott transition can be used to draw analogies to think of a breakdown of the Fermi liquid in higher dimensions.

This dissertation presents three separate works on application of a one-dimensional approach to study the properties and phase diagrams of quasi one-dimensional structures. Quasi one-dimensional systems are composed of weakly coupled one dimensional sub-systems, such as quantum wires or spin

chains. The low energy description of every one-dimensional sub-system is a TL liquid. All interactions between the sub-systems, such as tunneling or electron-electron interactions, are then treated perturbatively to understand the resulting phase diagram of the quasi one-dimensional system.

There are not that many exact analytical techniques to tackle the strongly interacting two-dimensional systems. Among them are widely used mean field theories, effective field theories, such as Chern-Simons and non-linear sigma model, various exactly-solvable toy-models, such as XY-model, the Kitaev model for a spin-liquid on a honeycomb and other lattices, semi-classical spin-wave theory and Jordan-Wigner transformation for the spin system and many others [1, 3, 7, 17, 124]. The advantage of the method presented in this dissertation is the ability to solve for the ground state analytically with a reliable technique, namely bosonization. The quantum fluctuations which are important in low-dimensional systems are also included in the formalism. Even though, there are not that many truly quasi one-dimensional systems, the understanding of their phase diagrams and physical properties within the bosonization technique can give a tremendous intuition in to physics of isotropic strongly correlated two-dimensional electron and boson systems.

Having mentioned that the edges of quantum Hall system are one-dimensional and well known to be described by a TL liquid, we continue next with the introduction to the quantum Hall effect. We then describe effects of spin-orbit coupling in condensed matter systems. And finally, give an introduction to a spin-liquid state on the kagome lattice antiferromagnet.

1.2 Integer and fractional quantum Hall effects

A unique quantum state of matter appears when a two-dimensional electron system is cooled down to small temperatures and is subjected to a strong perpendicular magnetic field. Let us describe this state of matter by its responses to external electric fields via the longitudinal and Hall conductivities. Let us focus only on the latter. From the classical mechanics we know that the Hall conductivity behaves linearly with the magnetic field. And that what is partially seen in the experiment. However, a special regime was found where the conductivity takes integer values of e^2/h, where e is the electron charge and h is Planck's constant, and stays constant for a wide range of the magnetic field strengths[77]. This effect is known as the integer quantum Hall effect (IQHE) signifying that the origin of this effect is quantum mechanical.

In quantum mechanics, the magnetic field quenches the kinetic energy of two-dimensional electrons and forms the dispersionless Landau energy levels [80]. These energy levels are equidistant from each other by a quanta of cyclotron energy, and are massively degenerate. Basics semiconductor physics predicts macroscopically that the properties of the system will depend on the position of the Fermi energy, which determines the density of electrons in the system. Insulators are materials with filled energy bands, while metals are the materials with partially filled energy bands. Therefore, whenever the Fermi energy lies in the Landau level, the system behaves as a metal with both non-zero longitudinal and the Hall conductivities. But when the Fermi energy is between the Landau levels, the system becomes a bulk insulator with a zero

longitudinal conductivity. What is new about the later case is the quantization of the Hall conductivity. This opens a new chapter in the physics of band insulators, which is deals with the topological properties. The state at the integer quantum Hall regime is called the Chern insulator [44].

There is another counterintuitive effect which occurs when the Fermi energy is inside of one of the Landau levels, for example zeroth Landau level. In this case the filling factor is less than one. One would assume that the system is a metal having both non-zero longitudinal and Hall conductivities. However at some special filling factors the quantized plateaus of the Hall conductivity reappear again [20, 138]. This happens at filling factors equal to $\nu = \frac{m}{2n+1}$, where $m,\ n$ are non-zero integers. Laughlin gave a theoretical explanation for a state at filling factor $\nu = 1/3$ by constructing a variational many-body wave-function [81]. It turned out that it correctly describes the ground state of the system, namely a incompressible electron liquid. The excitations above the ground state are collective fermion excitations carrying a fractional charge of $\frac{1}{3}$ of electron's charge and obeying the non-Abelian statistics [65].

One of the works presented in the dissertation is an analytical model of the fractional quantum Hall effect based on the one-dimensional bosonization.

1.3 Spintronics and topological insulators

In past couple of decades, spin-orbit coupling (SOC) has become a central theme in condensed matter physics.[61, 102] It is the coupling of the electron motion with spin that makes the spin-orbit coupling attractive to

think about when devising novel mechanisms of the electron spin manipulation. The research field emerged from the studies of SOC is called the spintronics[61].

The SOC is a relativistic in origin and in the context of condensed matter it appears in crystals which lack one of the spatial inversion symmetry. For example, in two-dimensional electron system the application of the gate voltage breaks inversion symmetry and allows for a Rashba type SOC [14]. Another type of the SOC is the absence of the center inversion symmetry in the crystal structure of the material. This is so-called Dresselhaus [23] type SOC. Also, any type of impurity locally acts as a source of SOC for the crystal electrons. Here are some important examples of the effect of the SOC on the properties of the materials.

One of the important discoveries in the field of spintronics is the observation of spin helix waves [10, 79]. Both of the spin-orbit coupling types, Rashba and Dresselhaus, break the $SU(2)$ spin rotation symmetry. However, there is a special point of competition of these two types of spin-orbit coupling. Namely, when their strengths match each other, the $SU(2)$ spin-rotation symmetry gets restored at the spin-orbit coupling dependent wave vector. This corresponds to a spin wave excitation with diverging life-time.

Another important discovery is the accumulation of opposite spins at the boundaries of a a two-dimensional electron system when the external electric field is applied [25, 26, 57, 73, 101, 154]. This effect has a resemblance with the Hall effect and gained its name after it - the spin-Hall effect. There are several causes of the spin-Hall effect. One of them is extrinsic, due to spin-orbit

scattering of electrons by impurities. Second type is called intrinsic, which is driven by either Dresselhaus type or Rashba type spin-orbit couplings [61].

The anomalous Hall effect in magnetized two-dimensional electron gas with Rashba or Dresselhaus spin-orbit coupling is another manifestation of the spin-orbit coupling. The Zeeman magnetic field splits the spin bands. Due to breaking of time-reversal and inversion symmetry, the Chern number is non-zero in this case, resulting in quantized Hall conductivity whenever the Fermi energy lies between the magnetic field split bands [102].

The latter two advantages of the spintronics made physicists to think about the possibility of spin-orbit coupled analogue of the integer quantum Hall effect. It eventually lead to a discovery of new materials which are now called topological insulators [53, 115]. In topological insulators the intrinsic spin-orbit coupling can be seen as an effective spin and momentum dependent magnetic field , which does not break the time-reversal symmetry. The scenario is the same as in the quantum Hall effect. Namely, the spin-orbit coupling opens up a bulk gap leaving gapless edge states.

Two-dimensional TI were first theoretically predicted to exist in graphene with an intrinsic spin-orbit coupling [68, 69]. A new topological theory was then developed to characterize the time-reversal symmetry preserving insulators. They are classified by a Z_2 number [36], which counts number of Kramer's pairs on the edge. The topological insulators are described by an odd number, while the trivial insulators are by even number of Kramer's pairs. The reason for the name topological is the protection of the edge states with an odd num-

ber of Kramer's pairs from electron-electron interaction and weak disorder at the edge, due to prohibited electron backscattering.

Experimentally two-dimensional insulators were observed in band-inverting contacts based on Hg(Cd)/Te quantum wells [9, 11, 78, 108]. To mention, there exist three-dimensional topological insulators [37, 38].

One of the works presented in this dissertation studies properties of edges of quantum spin-Hall system. Another work is devoted to effects of spin-orbit coupling on the magnetic phase diagram of kagome antiferromagnet. Let us now review a spin liquid phase on the kagome lattice antiferromagnet.

1.4 Spin liquid phase on a kagome lattice

A spin liquid is a charge insulator which does not have any magnetic order down to zero temperature[8]. A requirement put on a spin liquid state is not to break any of the symmetries of the system. Theoretically, there is a number of Heisenberg antiferromagnetic lattice models which support the spin liquid as a ground state. Common ingredients of all these models are the geometrical frustration which works against an ordered state, and the small size of the spin which enhances quantum fluctuations. The most important examples of such models are the square lattice with next nearest neighbor interaction (so-called $J_1 - J_2$ model), triangular and kagome lattices.

Let us focus from now on the kagome lattice. Among the experimentally studied spin-1/2 kagome antiferromagnet materials, an absence of long-range

magnetic order down to small temperatures (compared to the characteristic exchange energy) is common. Important examples of spin-1/2 kagome antiferromagnets include herbertsmithite, $ZnCu_3(OH)_6Cl_2$,[94] vesignieite $BaCu_3V_2O_8(OH)_2$,[163] volborthite $Cu_3V_2O_7(OH)_2 \cdot 2H_2O$,[166] $MgCu_3(OH)_6Cl_2$ (a cousin of herbertsmithite),[74] and $Rb_2Cu_3SnF_{12}$.[92]

Herbertsmithite has isotropic exchange interactions and has received perhaps the largest amount of theoretical and experimental attention among the materials listed above. No magnetic order appears in this system down to temperatures of 40 mK (nearest-neighbor exchange $J \sim 180$K) making it a leading quantum spin liquid candidate.[94] Vesignieite also possesses an isotropic kagome lattice and exhibits similar behavior to herbertsmithite over a wide temperature range ($J \sim 53$K).[163] However, it was recently observed that vesignieite exhibits an exotic phase at very low temperatures which appears to be described by the coexistence of dynamical and small frozen moments.[19] The Dzyaloshinski-Moriya interaction, with an energy scale set by D, may play an important role in understanding the low temperature phase in vesignieite ($D/J \approx 0.14$).[19] Volborthite is characterized by a small spatial anisotropy in the exchange interactions between spins, and no magnetic order has been reported down to temperatures of order $2K$ (with $J \sim 77$K).[166] However, a signature of frozen magnetic moments appears below this temperature scale.[166] The low-temperature magnetic order may be a consequence of spatial anisotropy in the exchange interactions.[126, 139] One of the main advantages in studying volborthite over herbertsmithite and vesignieite is that

it can be prepared with fewer impurities.[166] In another deformed kagome compound, $Rb_2Cu_3SnF_{12}$,[92] a valence bond state of a pinwheel type was experimentally observed at low temperatures $1.7K$, and again no magnetic order was seen over a wide range of higher temperatures ($J \sim$ 180K with $D/J \approx 0.2$).[92] Finally, the material $Cs_2Cu_3CeF_{12}$ is a buckled kagome lattice with a quasi-one-dimensional structure in the exchange constants (similar to that shown in Fig. 4.1) which shows clear signs of order at low temperature.[4] Taken together, these data indicate that while these systems may appear to be heading towards quantum spin liquid states over a wide temperature range, weak interactions, such as spin-orbit coupling, can eventually select an ordered phase.[137]

1.5 Outline of the presented results

1.5.1 Coulomb drag between helical edge states.

In this part of the dissertation correlation between the helical edges in eternal magnetic field is studied. First of all, the magnetic field breaks a time-reversal symmetry. If the magnetic field is parallel to the spin quantization axis which is determined by the bulk properties, it will result in imbalance in spin-up and spin-down occupation, without opening a gap. However, whenever the magnetic field is perpendicular to the spin quantization, the gap will be opened in the spectrum of the edge states. We show that the opening of the gap, or a mass term, results in magnetic field dependent backscattering between electrons. We use this fact as a mean to experimentally test the helical

edge states.

We propose to use this theoretical result to study the Coulomb drag between two helical edge states. In the drag experiment the current is driven through one wire (active wire) while the voltage is measured in the second one (passive wire). Due to Coulomb interactions between electrons in wires there will be a momentum transfer from active to passive wires. It will build up a voltage drop in the passive wire which is then measured. Let us now focus on the system which consists of two one-dimensional wires. There are two processes that contribute to the Coulomb drag resistivity in this case. Forward scattering and backscattering of electrons. Forward scattering is a measure of non-linearity of the spectrum, while the backscattering is a measure of linearity. For example, in case of Luttinger liquids, when the spectrum is approximated to be linear, the backscattering processes govern the Coulomb drag.

Coming back to helical edge states, we notice that their low-energy description is a spinless Luttinger liquid without backscattering. Therefore, the Coulomb drag vanishes between two helical edge states when the time-reversal symmetry is conserved. In the presented work we show that application of the magnetic field perpendicular to the spin quantization axis opens up a gap in the spectrum and allows for the backscattering processes between the electrons. The backscattering strength is shown to be proportional to the second power of the magnetic field. Therefore, the Coulomb drag scales as a fourth power of the magnetic field. In the physics of the Coulomb drag such a strong mag-

netic field dependence is unusual for conventional quantum wires. Therefore the prediction of the presented work can be used as an experimental verification of helical nature of electrons on the edges of two dimensional topological insulators, for example HgTe/CdTe hetero-structure.

1.5.2 Spatially anisotropic kagome antiferromagnet with Dzyaloshinskii-Moriya interaction.

As it was discussed, a major motivation for the experimental and theoretical study of spin-1/2 kagome antiferromagnets is the possibility of spin liquid and other highly fluctuating phases.[8, 159] The spin liquid on the kagome lattice received perhaps the most attention. However, small deviations from the isotropic spin-1/2 kagome antiferromagnet, such as Dzyaloshinskii-Moriya (DM) [16, 60] interaction or spatial exchange interaction, experimentally result in signatures of low temperature magnetic order. Large anisotropic exchange interaction, such as in material $Cs_2Cu_3CeF_{12}$, are responsible for the high temperature magnetic order. Therefore, it is obvious that there is a tendency of anisotropy driven phase transition at small temperatures.

One can draw analogies with Fermi liquid in two or three dimensions. Being described by free quasi-particles excitations, Fermi liquid undergoes phase transitions once the conditions, for example, for superconductivity or magnetic phase instabilities are met. This suggests that in spin liquids any anisotropies are analogous to conditions for the Fermi liquid instabilities. We would like to point out that an analytical theory which would describe a spin

liquid in isotropic kagome antiferromagnet (or any other frustrated magnetic lattice), and in analogy with Fermi liquid predict anisotropy driven phase transitions to magnetically ordered phases is still lacking.

In this chapter we study a spin-1/2 kagome antiferromagnet with spatial exchange anisotropy and the DM interaction. By spatial anisotropy it is meant that the exchange energy between spins along one selected direction is larger than one in different direction. In case of kagome geometry the exchange along every horizontal line (spin chain from now on) is assumed to be larger than along the diagonals. The DM interaction that is considered in this work is an intrinsic property of the kagome lattice.

The spatial anisotropy allows to apply a one-dimensional bosonization approach to describe the physics of spin chains. All the diagonal exchange interactions are then treat perturbatively. The results of this work are the following. First of all, we do not find any spin liquid state, which is due to the anisotropic exchange interactions. However, we find a DM interaction driven phase transition, which is a novel theoretical prediction in the physics of spatially anisotropic kagome lattice antiferromagnet. First of all, we obtain that when the DM interaction is weak, the overall magnetic order is ferrimagnetic with a small Neel component. As the DM interaction strength is increased this small Neel component undergoes a phase transition to a phase with both Neel and dimer states coexisting.

1.5.3 Fractional quantum Hall effect from phenomenological bosonization.

In this chapter a model of fractional quantum Hall effect based on the phenomenological bosonization [48] is given. Previously, there was an approach to describe the fractional quantum Hall effect from one-dimensional bosonization in an array of one-dimensional quantum wires in magnetic field [70, 143]. The novelty of present work is in its application to a two-dimensional electron system in a quantizing magnetic field.

The construction of the model is based on two assumptions. First of all, the electron-electron interactions tend to mix electron states with different Landau momentum. Second, a wave function of an electron in magnetic field chosen in Landau gauge consists of a plane wave in one direction and a decaying part in other. The decaying nature of the wave function makes possible to bosonize electron states with different Landau momentum. Based on these assumptions, a trial fermion operator is constructed using the approach of phenomenological one-dimensional bosonization [48].

The effective Hamiltonian describing density fluctuations is then derived. It is shown that the fractional states are described by a sine-Gordon action. In which case the kinks carry the fractional charge. The nature of the emerging sine-Gordon action term is the coupling of high harmonics of the density fluctuations of states with different Landau momentum. Importantly, this coupling originate not from the Coulomb interaction but from the kinetic term of the Hamiltonian. This is consistent with the Chern-Simons flux attachment

procedure. The condition on the relevancy of the fractional quantum state is given. Presented theory describes the hierarchy of the fractional states, which is consistent with previous theories and experiments [48, 49, 64, 118].

Chapter 2

Introduction to one-dimensional bosonization

2.1 Introduction to bosonization

The main theme of the dissertation is the application of the one-dimensional bosonization to study two-dimensional structures. In this chapter we are going to cover the basics of the bosonization formalism which is a basis for further chapters. We advise to consult books [43, 46, 124] and reviews [127, 128, 146] for more detailed description of the model. Let us start with a spinless electrons described by a quadratic spectrum with a finite Fermi energy. The first, and as we will see later, crucial approximation that we will make is linearize the spectrum near the Fermi momentums. It is well justified since all of the properties of the systems are defined by the correlations of electrons near the Fermi surface. And the linearization of the spectrum is a standard trick to make. In one-dimensional world, electrons have only two spatial degrees of freedom, namely they either move to the right or left. See figure (2.1). With all that in mind, we write down the kinetic part of the Hamiltonian

$$H_0 = \sum_{k,r} v_F \left(\epsilon_r k - k_F\right) c^\dagger_{r,k} c_{r,k}, \tag{2.1}$$

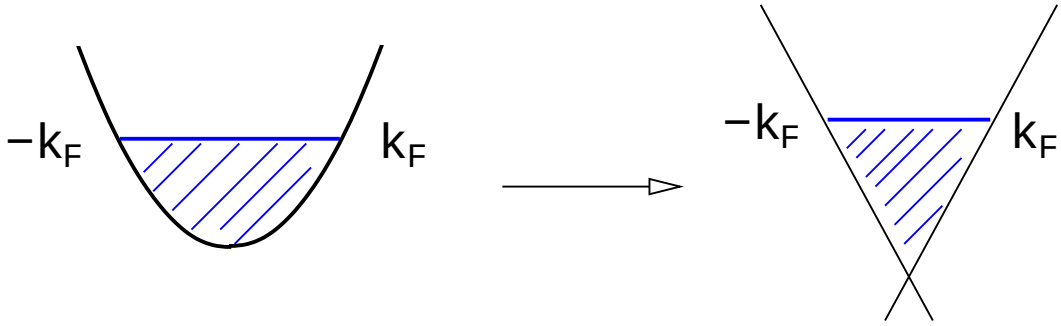

Figure 2.1: Linearization of the spectrum. Two Fermi points corresponding to right and left movers.

where $\epsilon_R = +1$ denoting a right mover in the one-dimensional system, and $\epsilon_L = -1$ is denoting a left mover. The $c^\dagger_{r,k}$ is a fermion creation operator with a momentum k and a $r = R(L)$ direction of motion, $c_{r,k}$ is fermion annihilation operator. For a electron-hole excitation take an electron below the Fermi surface and put it above. The energy of this excitation is

$$E(q) = v_F(k+q) - v_F k = v_F q. \tag{2.2}$$

the energy of an electron-hole excitation depends only on the momentum of the pair, which is a property of a linearized spectrum of a one-dimensional system. Let us now write down the expression for the density operator of electron-hole pair

$$\rho(q) = \sum_{k,r} c^\dagger_{k+q,r} c_{k,r}. \tag{2.3}$$

As described above, this new operator has a well defined energy and a momentum, therefore there is a desire to quantize the electron-hole excitation. And since the operator is quadratic in fermion operators, it has a bosonic statistics. A possible usefulness of this operator will be clear after observing that

the Coulomb interaction between electrons

$$H_{int} = \frac{1}{2V}\sum_{q} V(q)\rho(q)\rho(-q). \tag{2.4}$$

has four fermions operators. And therefore, diagonalization of the total Hamiltonian of interacting electrons is quite a challenge. In higher dimensions, the Coulomb interaction is normally treated perturbatively or within the mean field (Hartree-Fock approximation). However, in one dimensions standard perturbation theory fails due to strong quantum fluctuations. It turns out that in one-dimensions it is possible to reexpress the kinetic energy to be quadratic in bosonic operator. And the Coulomb interaction, which is also quadratic in density operators, can then be easily managed. To show that, let us study different commutation relationships of these bosonic operators. To derive correct commutation relationship, we have to recall that the original spectrum of electrons was quadratic. After it's linearization, an infinite amount of states are introduced by hand in to the Hilbert space. One has to take that in to account by defining normal ordering of the operators in the system. The normal ordering is defined as

$$: AB := AB - <0|AB|0>, \tag{2.5}$$

where the expectation value on the ground state of the system is taken in the second term of the right hand side expression. Let us now use the normal ordering procedure in the commutation relationship between the densities

$$[\rho_r^\dagger(p), \rho_{r'}^\dagger(-p')] = \delta_{p,p'}\frac{rpL}{2\pi} \tag{2.6}$$

Where we assumed the system to be of the length L with periodic boundary conditions imposed, which makes momentum to be discrete $k_n = \frac{2\pi n}{L}$. We also used the normal ordering procedure. These commutation relationship imply that the electron-hole excitation density indeed behave as bosonic particles and can be treated as creation and annihilation operators of density fluctuations. Introduce renormalized creation and annihilation operators as

$$b_p^\dagger = \left(\frac{2\pi}{L|p|}\right)^{1/2} \sum_r \Theta(rp)\rho_r^\dagger(p), \tag{2.7}$$

$$b_p = \left(\frac{2\pi}{L|p|}\right)^{1/2} \sum_r \Theta(rp)\rho_r^\dagger(-p) \tag{2.8}$$

Most importantly, we can show that the commutation relations of the operator above with the Hamiltonian is

$$[b_{p_0}, H] = v_F p_0 b_{p_0}. \tag{2.9}$$

This implies that the kinetic part of the Hamiltonian can be presented as quadratic in these bosonic operators

$$H = \sum_p v_F |p| b_p^\dagger b_p \tag{2.10}$$

And we were able to show that Hamiltonian instead of being quadratic in fermion operators is now quadratic in bosonic operators. Before studying the complete Hamiltonian of the interacting fermions, let us learn how to present a fermion operator in terms of bosonic ones. For that consider commutation relationship of the density with the fermion operator

$$[\rho_r^\dagger(p), \psi_r(x)] = -e^{ipx}\psi_r(x) \tag{2.11}$$

Therefore, the most general expression of the fermion operator that commutes with the density operator, can be written in the following form

$$\psi_r(x) = \eta_r e^{\sum_p e^{ipx}\rho_r^\dagger(-p)\left(\frac{2\pi r}{pL}\right)} \tag{2.12}$$

where η_r is a Klein's factor ensuring the fermionic commutation relationships. It is more convenient to introduce different bosonic operators

$$\phi(x),\ \theta(x) = \mp(N_R \pm N_L)\frac{\pi x}{L} \mp \frac{i\pi}{L}\sum_{p\neq 0}\frac{1}{p}e^{-\alpha|p|/2-ipx}(\rho_R^\dagger(p) \pm \rho_L^\dagger(p)), \tag{2.13}$$

where the upper sign is for ϕ and the lower for θ. It can be shown that the commutation relationship ϕ and θ satisfy is

$$[\phi(x_1), \nabla\theta(x_2)] = i\pi\delta(x_1 - x_2), \tag{2.14}$$

Therefore, the conjugate momentum to the field ϕ is given by $\Pi(x) = \frac{1}{\pi}\nabla\theta(x)$. Physical meaning of the bosonic fields can be understood from the following identities

$$\begin{aligned}\nabla\phi(x) &= -\pi\left(\rho_R(x) + \rho_L(x)\right),\\ \nabla\theta(x) &= \pi\left(\rho_R(x) - \rho_L(x)\right),\end{aligned} \tag{2.15}$$

which states that $\nabla\phi$ is the zero momentum of the total electron density, while $\nabla\theta$ corresponds to a current in the one-dimensional system. Hamiltonian corresponding to fermion density fluctuations of non-interacting fermions written in terms of bosonic fields can now be written in the form

$$H_0 = \frac{1}{2\pi}\int dx\ v_F\left[(\nabla\theta(x))^2 + (\nabla\phi(x))^2\right] \tag{2.16}$$

And the fermion operator written in new bosonic fields is

$$\psi_r(x) = \frac{\eta_r}{\sqrt{2\pi\alpha}} e^{irk_F x} e^{-i[r\phi(x)-\theta(x)]}. \tag{2.17}$$

Let us now consider a Coulomb interaction between electrons. The most general form of interactions of spinless electrons is

$$H_{int} = \int dx dx' \; U(x-x')\rho(x)\rho(x') \tag{2.18}$$

To remind, the density is a sum of a zero and a $2k_F$ momentum terms

$$\rho(x) = -\frac{1}{\pi}\nabla\phi(x) - \frac{1}{\pi a}\sin(2k_F x + 2\phi(x)) \tag{2.19}$$

We now plug in the expression for the density above in to Coulomb interaction. One has to then make a change in variables, introducing $x = x - x'$ and $X = (x_1 + x_2)/2$. Using the correlation function

$$H_{int} = \int dx \; \left(\frac{U(0) - U(2k_F)}{2\pi^2}\right) (\nabla\phi(x))^2 \tag{2.20}$$

where $U(0),\ U(2k_F)$ are zero (forward scattering) and $2k_F$ momentum (backscattering) contributions of the Coulomb interaction. See figure (2.1) for an example of scattering types.

Combining all of the terms we get that the total Hamiltonian of the system is

$$H = H_0 + H_{int} = \frac{1}{2\pi}\int dx \; \left[v_F(\nabla\theta(x))^2 + \left(v_F + \frac{U(0) - U(2k_F)}{\pi}\right)(\nabla\phi(x))^2\right] \tag{2.21}$$

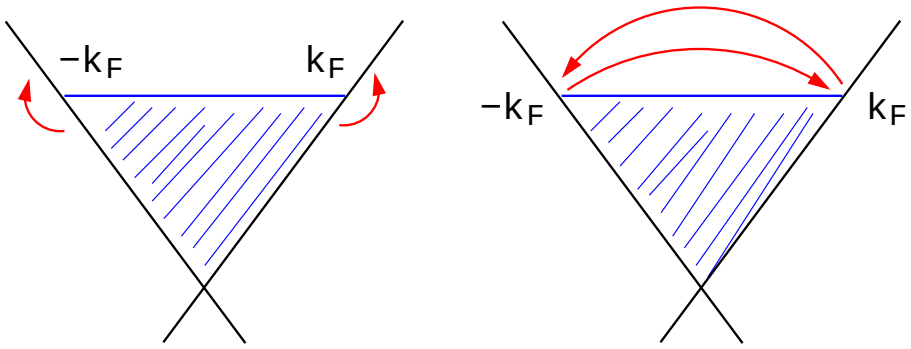

Figure 2.2: Examples of scattering processes. Left figure shows the forward scattering while the right is the backscattering.

And let us present it in the standard Luttinger liquid form, introducing the following parameters $uK = v_F$ and $\frac{u}{K} = \left(v_F + \frac{U(0)-U(2k_F)}{\pi}\right)$. With this new notation the Hamiltonian is now

$$H = \frac{1}{2\pi}\int dx \ \left[uK(\nabla\theta(x))^2 + \frac{u}{K}(\nabla\phi(x))^2\right] \tag{2.22}$$

The rest of the bosonization, such as phenomenological bosonization (which is an alternative derivation of the technique), a model of electrons with spin and corresponding sine-Gordon model, application of the bosonization to one-dimensional spin chains will be covered in next sections.

2.2 Correlation functions

The most important correlation functions in the theory of one-dimensional bosonization are $\langle(\phi(x,t)-\phi(0,0))^2\rangle$ and $\langle\phi(x,t)\theta(0,0)\rangle$. Here they are given without the derivation. At non-zero temperature

$$\langle(\phi(x,\tau)-\phi(0,0))^2\rangle = \frac{K}{2}\ln\left[\frac{u^2\beta^2}{\pi^2 a^2}\left(\sin^2\left(\frac{\pi\tau}{\beta}\right)+\sinh^2\left(\frac{\pi x}{u\beta}\right)\right)\right], \tag{2.23}$$

and the expression for the second one is

$$\langle\phi(x,\tau)\theta(0,0)\rangle = -iArg\left(\tan(\frac{\pi\tau}{\beta}) + \tanh(\frac{\pi x}{\beta u})\right). \tag{2.24}$$

Here $\beta = 1/T$, where T is temperature and $\tau = it$ is an imaginary time. For the zero temperature correlation functions, one can take a limit of $T \to 0$ in the expressions above. One then gets

$$\langle(\phi(x,\tau) - \phi(0,0))^2\rangle = \frac{K}{2}\ln\left(\frac{u^2\tau^2+x^2}{a^2}\right) = KF_1(r), \tag{2.25}$$
$$\langle\phi(x,\tau)\theta(0,0)\rangle = -iArg\,(u\tau + ix) = F_2(r).$$

We now can use these correlation functions, for example, to show the breakdown of the Fermi liquid in one-dimension.

2.3 Green's function and occupation number of Tomonaga-Luttinger liquid

Let us now show that the Fermi liquid breaks down in interacting one-dimensional electron system. In non-interacting electron gas the occupation number behaves as $n(\epsilon_k) = \frac{1}{e^{(\epsilon_k-\mu)/T}+1}$, where ϵ_k is the energy spectrum, E_F is the Fermi energy, and T is temperature. At zero temperature there is a discontinuous jump at the Fermi energy, which is a important feature of an electron gas. In dimensions higher than one, electron-electron interactions simply renormalize the mass and velocity of electrons, keeping the discontinuous jump at the Fermi energy. The excitations of the Fermi liquid behave as free electrons. Here we would like to show that the Fermi liquid does not

exist in interacting one-dimensional electron system. For that let us calculate the occupation number, which is related to a retarded Greens function. The Green's function is defined as

$$G_R(r) = - < \Psi_R(r)\Psi_R^\dagger(0,0) >= -\frac{e^{-ik_F x}}{2\pi a} < e^{i(\phi(r)-\theta(r))}e^{-i(\phi(0)-\theta(0))} > \\ = -\frac{e^{ik_F x}}{2\pi a}e^{-\left(\frac{K+K^{-1}}{2}F_1(r)+F_2(r)\right)} \tag{2.26}$$

Then, the occupation number is given by

$$n(k) = \int dx\ e^{-ikx}G_R(x, \tau = 0) \tag{2.27}$$

At zero temperature the occupation number behaves as

$$n(k) \propto |k - k_F|^{\frac{K+K^{-1}}{2}-1} \tag{2.28}$$

And there is no discontinuity jump at the Fermi energy, which signals a break down of a Fermi liquid. See figure (2.3) for a schematics of the behavior of the occupation number.

2.4 Incorporating spin

Here we are going to include spin in to the description of electrons [43]. For that we need to update the definition of the fermion operator

$$\Psi_{r,\sigma} = \frac{U_{r,\sigma}}{\sqrt{2\pi a}}e^{irk_F x}e^{-\frac{i}{\sqrt{2}}[r\phi_\rho(x)-\theta_\rho(x)+\sigma(r\phi_\sigma(x)-\theta_\sigma(x))]}, \tag{2.29}$$

where $r = R(L)$ denotes the mover, ρ and $\sigma =\uparrow,\ \downarrow$ are denoting the charge and spin bosonic fields. It is also useful to define charge and spin density as

$$\rho(x) = \frac{1}{\sqrt{2}}\left[\rho_\uparrow(x) + \rho_\downarrow(x)\right], \\ \sigma(x) = \frac{1}{\sqrt{2}}\left[\rho_\uparrow(x) - \rho_\downarrow(x)\right]. \tag{2.30}$$

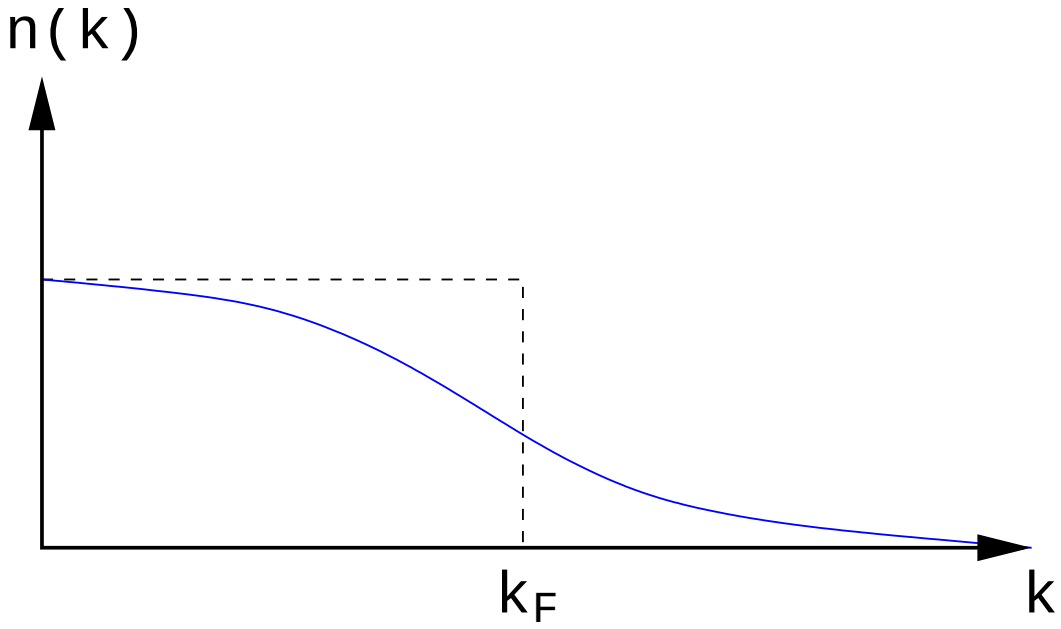

Figure 2.3: Solid line schematically describes occupation number of a Tomonaga-Luttinger liquid. Dashed line represents occupation number of a Fermi gas. There is no discontinuous jump in the former case.

The Coulomb interaction written in the most general form is

$$H_{int} = \int dx dx' \; V(x - x')\rho(x)\rho(x'), \tag{2.31}$$

will now have extra contributions due to spin. For derivations of the interaction types see book **??**. Here we just give a final Hamiltonian of interacting fermions with spin

$$\begin{aligned} H = \tfrac{1}{2\pi} \int dx \;\; \left[\tfrac{u_\rho}{K_\rho} (\nabla \phi_\rho)^2 + u_\rho K_\rho (\nabla \theta_\rho)^2 \right] \\ + \tfrac{1}{2\pi} \int dx \;\; \left[\tfrac{u_\sigma}{K_\sigma} (\nabla \phi_\sigma)^2 + u_\sigma K_\sigma (\nabla \theta_\sigma)^2 \right] + \tfrac{2 g_{1\perp}}{(2\pi\alpha)^2} \int dx \;\; \cos\left(\sqrt{8}\phi_\sigma\right), \end{aligned} \tag{2.32}$$

where $u_{\rho/\sigma}$ and $K_{\rho/\sigma}$ are defined in a same fashion as for spinless TL liquid. For more details see book [43], we just would like to notice that the cosine term in the expression above originates from the backscattering processes. One can see that the charge sector (ρ) and the spin sector (σ) are independent of each other. This is one of the important results of the bosonization, namely the charge-spin separation.

2.5 Umklapp scattering

There is another important interaction which we have omitted. Two right movers can be scattered in to two left movers. Therefore, it can be seen that the total momentum is not conserved. For the most of the times, this interaction process is not allowed in the description of the one-dimensional system. However, at special point of half-filling, when the $k_F = \pi/2a$, the change of the total momentum equals to a reciprocal lattice vector, $2\pi/a$, and

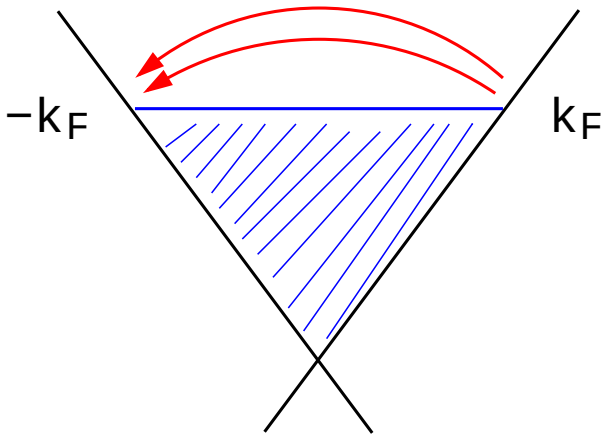

Figure 2.4: An example of umklapp scattering event. Two right movers scatter to become left movers

therefore, such processes are allowed. Schematically the umklapp process is shown on the figure (2.5). The expression for the umklapp process in terms of bosonic fields reads

$$H_u = g_u \int dx \ \cos(\sqrt{8}\phi_\rho). \tag{2.33}$$

Whenever this term is relevant, the charge sector becomes gapped, signaling an interaction driven metal-insulator transition (Mott transition). The relevancy of the cosine term will be discussed in next section.

2.6 Renormalization group analysis of a sine-Gordon model

Here we give a simple argument on the analysis of the sine term in the action [124]. The term that we are going to analyze is given by

$$H_s = g \int dx \ \cos(\sqrt{8}\phi), \tag{2.34}$$

which appears as a backscattering term in the spinfull Tomonaga Luttinger liquid, or as an umklapp scattering process. To understand whether this term is important, one has to obtain its scaling dimension. The scaling dimension of an operator describes behavior of this operator once the time and length scales of the field theory are increased. One says that if the operator is exponentially increases with the rescaling, then it is relevant. The operator is irrelevant if it decreases exponentially with rescaling. And it is marginally irrelevant in the case when it does not change with the rescaling. To obtain the scaling of a given above cosine operator, let us consider the following correlation function

$$< e^{ip\phi(x)} e^{-ip'\phi(0)} > \sim \frac{\delta_{pp'}}{x^{p^2 K/2}}, \tag{2.35}$$

therefore, the scaling dimension of the cosine operator is

$$dim\left[e^{ip\phi}\right] = \frac{p^2 K}{4}. \tag{2.36}$$

For the operator of interest, (2.34) the $p = \sqrt{8}$ and the scaling dimension of the operator is $2K$. This can be written in the renormalization group equation way under the rescaling of the coordinate $x \to x e^{d\ell}$ and time $\tau \to \tau e^{d\ell}$

$$\frac{dg}{d\ell} = (2 - 2K)g. \tag{2.37}$$

Another part to the renormalization group equation will come from the second order perturbation theory in the operator (2.34). In this case the cosine term will contribute to the TL interaction constant

$$\frac{dK}{d\ell} = -\delta v^2, \tag{2.38}$$

where δ is a positive model dependent constant. Equations (2.36) and (2.38) form a well-known Kosterlitz-Thouless equations. We are going to meet such equations later in the dissertation. We suggest to consult books [43, 124] for details on the solution of these equations.

2.7 One dimensional spin chain

Here we are going to show the application of bosonization to understand the physical properties of one-dimensional spin chains. Consider a one-dimensional spin chain described by the following Heisenberg exchange Hamiltonian

$$H = J \sum_i \left[S_i^x S_{i+1}^x + S_i^y S_{i+1}^y + \lambda S_i^z S_{i+1}^z \right], \tag{2.39}$$

where $J > 0$ is Heisenberg antiferromagnetic exchange, λ is an anisotropy parameter and it will be important later, and $\mathbf{S}_i$ denotes a spin on a site i. The question is how to understand the ground state of this system. There are two equivalent approaches to answer this question. One of them is a one-dimensional Jordan-Wigner transformation, another is the spin-current formalism. Both of the approaches are equivalent to each other. However, the second one has an advantage of keeping the original $SU(2)$ symmetry of the spins, while after the Jordan-Wigner transformation this symmetry is hidden. Let us first introduce the Jordan-Wigner transformation.

2.7.1 Jordan-Wigner transformation

There is an exact mapping between a space of spin-1/2 degree of freedom per site and that of spinless fermions occupying each site [124]. For that we can associate a spin-up state with an empty fermion state, while a spin-down with an occupied fermion state. Present the fermion creation operator on a site i as $c_i^\dagger$, and annihilation operator as c_i. Then the fermion density on a site i is connected to a S_i^z as

$$S_i^z = 1 - 2c_i^\dagger c_i. \tag{2.40}$$

Also, the spin operator $\hat{S}_i^+ = (S_i^x + iS_i^y)/2$ responsible for flipping the spin from down to up, corresponds to a fermion annihilation operator c_i. So as $\hat{S}_i^- = (S_i^x + iS_i^y)/2$ corresponds to $c_i^\dagger$. The final mapping that obeys correct commutation relationships is given by

$$\begin{aligned} \hat{S}_i^z &= 1 - 2c_i^\dagger c_i, \\ \hat{S}_i^+ &= \textstyle\prod_{j<i} \left(1 - 2c_j^\dagger c_j\right) c_i, \\ \hat{S}_i^- &= \textstyle\prod_{j<i} \left(1 - 2c_j^\dagger c_j\right) c_i^\dagger. \end{aligned} \tag{2.41}$$

To every spin site we connect a string operator which has a value of 0 or 1. The inverse mapping is given by

$$\begin{aligned} c_i &= \left(\prod_{j<i} \hat{S}_j^z\right) \hat{S}_i^+, \\ c_i^\dagger &= \left(\prod_{j<i} \hat{S}_j^z\right) \hat{S}_i^-. \end{aligned} \tag{2.42}$$

It can be easily checked that these fermion operators obey anti-commutation relationship

$$\{c_i, c_j^\dagger\} = \delta_{i,j}, \quad \{c_i, c_j\} = \{c_i^\dagger, c_j^\dagger\} = 0. \tag{2.43}$$

Let us now apply the Jordan-Wigner transformation to spin chain Hamiltonian (2.39). After careful calculations (some of the terms cancel due to Pauli exclusion principle), one gets

$$H = -J \sum_i \left[c_i^\dagger c_{i+1} + c_{i+1}^\dagger c_i - \lambda(1 - 2c_i^\dagger c_i)(1 - 2c_{i+1}^\dagger c_{i+1}) \right]. \tag{2.44}$$

First two terms here describe hopping of spinless fermions between neighboring sites of a one-dimensional chains. Last, four-fermion, term represents interaction between fermions. Let us first consider the hopping term alone (put $\lambda = 0$), which will define the energy spectrum of fermions. Performing a Fourier transformation, one gets for the energy spectrum a $E = -2J\cos(ka)$, where a is a distance between the sites, with the Fermi momentum being $k_F = \frac{\pi}{2a}$. Since the system is one dimensional, and the spectrum can be approximated to be linear near the Fermi energy, we can immediately apply the bosonization technique to study the properties of the system. As it was discussed before, the fermion operator can be presented in terms of bosonic operators as

$$\Psi_F(x) = \sum_{m \ odd} A_m e^{imk_F x + im\phi(x) - i\theta(x)}, \tag{2.45}$$

where the higher harmonics are attached due to a Jordan-Wigner transformation, and A_m constants are model dependent. The most important harmonics

in the representation above are those with $m = \pm 1$. The non-interacting Hamiltonian then takes a standard Gaussian form

$$H = \frac{v}{2\pi} \int dx \ \left[(\nabla\phi(x))^2 + (\nabla\theta(x))^2 \right]. \tag{2.46}$$

The interactions between fermions are included in the last, four-fermion, term. Upon bosonization, it renormalizes the velocity v as usual, and also introduces an umklapp process, which is given by

$$H_{int} = g_u \int dx \ \cos(4\phi(x)). \tag{2.47}$$

So that, the overall interacting Hamiltonian is

$$H = \frac{u}{2\pi} \int dx \ \left[\frac{1}{K} (\nabla\phi(x))^2 + K(\nabla\theta(x))^2 \right] + g_u \int dx \ \cos(4\phi(x)). \tag{2.48}$$

This term, whenever it is relevant will drive the spin system in to one of the ordered states. Either a Neel state or a spin-Peierls state (depending on the sign of the coupling constant g_u).

Let us now express the spin operators in terms of the bosonic fields

$$\hat{\sigma}_i^z = -\frac{2}{\pi} \nabla\phi(x_i) + \sum_{m \neq 0, even} C_m e^{imk_F x + im\phi(x_i)}. \tag{2.49}$$

Here, C_m are again model dependent constants.

$$\hat{\sigma}_i^+ = (-1)^i \sum_{m \ even} B_m e^{imk_F x_i + im\phi(x_i) - i\theta(x_i)}. \tag{2.50}$$

See the book [124] for more descriptions and discussions on the treatment of the spin chains within the Jordan-Wigner transformation.

2.7.2 Spin-current formalism

Another, mathematically equivalent approach can be applied to study the physics of one-dimensional spin chain [46]. Instead of performing the Jordan-Wigner transformation, we can present spins as a sum of uniform and staggered magnetization

$$\mathbf{S}_i \to a_0 \left[\mathbf{M}(x) + (-1)^{x/a_0}\mathbf{N}(x)\right], \tag{2.51}$$

where a_0 is distance between the spins on a one-dimensional chain, $x = ia_0$. There are two direction of motion in one-dimensional system, namely, right and left. Therefore, the uniform magnetization is presented as

$$\mathbf{M}(x) = \mathbf{J}_R(x) + \mathbf{J}_L(x), \tag{2.52}$$

where $\mathbf{J}_{R/L}(x) = \frac{1}{2}\Psi^{\dagger}_{R/L,\alpha}(x)\boldsymbol{\sigma}_{\alpha,\beta}\Psi_{R/L,\beta}(x)$. And it can be easily seen that it corresponds to a zero momentum spin density. The staggered magnetization is $2k_F$ density of the spin density

$$\mathbf{N}(x) = \Psi^{\dagger}_{R,\alpha}(x)\boldsymbol{\sigma}_{\alpha,\beta}\Psi_{L,\beta}(x) + h.c. \tag{2.53}$$

In these notations the Heisenberg exchange Hamiltonian takes the next form

$$H = \int dx\ \left[\mathbf{J}_R(x)\mathbf{J}_R(x) + \mathbf{J}_L(x)\mathbf{J}_L(x)\right] + g_{bs}\int dx\ \mathbf{J}_R(x)\mathbf{J}_L(x) \tag{2.54}$$

which has a name of Sugawara Hamiltonian. This form of bosonization will be used in the study of a spatially anisotropic spin - 1/2 kagome antiferromagnet.

2.8 Phenomenological bosonization

Let us introduce another, alternative, bosonization approach to one-dimensional bosonic or fermionic system [15, 47]. Let us study a one-dimensional system of particles. That can be, for example, bosons confined in a harmonic well potential in one selected dimension and free to move in another. This is, in fact, a model for a one-dimensional optical lattice [15]. The density of particles can be described by zero of some smooth function which takes values of $2\pi n$ at the positions of the particles

$$\rho(x) = \sum_i \delta(x - x_i) = \sum_n |\nabla\Phi(x)|\delta(\Phi(x) - 2\pi n). \tag{2.55}$$

The labeling function can always be chosen to be increasing, so that its derivative is always positive. The Poisson summation formula is then applied to rewrite the sum above as

$$\rho(x) = \frac{\nabla\Phi(x)}{2\pi} \sum_{p=-\infty}^{\infty} e^{ip\Phi(x)}. \tag{2.56}$$

It is convenient to redefine the labeling field as $\Phi(x) = 2\pi\rho_0 x - 2\phi(x)$, where $\rho_0 = 1/d$ is the particle density at equilibrium with the distance between the particles being d, and $\phi(x)$ is a deviation from it. The density then takes the form

$$\rho(x) = \left[\rho_0 - \frac{1}{\pi}\nabla\phi(x)\right] \sum_{p=-\infty}^{\infty} e^{i2p(\pi\rho_0 x - \phi(x))} \tag{2.57}$$

With the knowledge of the density we can construct a general form of the particle creation operator

$$\Psi^\dagger(x) = \sqrt{\rho(x)}e^{-i\theta(x)}, \tag{2.58}$$

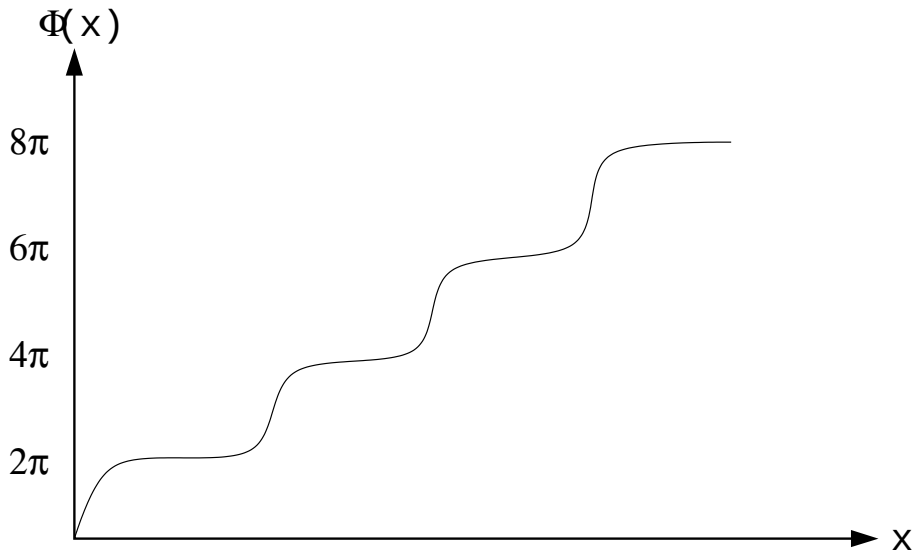

Figure 2.5: An example of the labeling function $\Phi(x)$. It has a smooth coordinate dependence and it takes integer values of 2π at the positions of the particles.

where $\theta(x)$ is an arbitrary operator. It will gain its meaning after the bosonic commutation relationships will be imposed on the introduced above particle operator

$$[\Psi(x), \Psi^{\dagger}(x')] = \delta(x - x') \tag{2.59}$$

From this we get the commutation relationship between the $\rho(x)$ and $\theta(x)$ fields

$$[\rho(x), e^{-i\theta(x')}] = \delta(x - x')e^{-i\theta(x')} \tag{2.60}$$

For the smeared density $\rho(x) \approx \rho_0 - \frac{1}{\pi}\nabla\phi(x)$, this relationship reads

$$[\frac{1}{\pi}\nabla\phi(x), \theta(x')] = -i\delta(x - x') \tag{2.61}$$

from here it is evident that the $\phi(x)$ and $\theta(x)$ are canonically conjugate operators.

To conclude, let us write a general form of the bosonic creation operator

$$\Psi_B^\dagger(x) = \left[\rho_0 - \frac{1}{\pi}\nabla\phi(x)\right]^{1/2} \sum_p e^{i2p(\pi\rho_0 x - \phi(x))} e^{-i\theta(x)} \tag{2.62}$$

Based on the bosonic creation operator it is straightforward to write an expression for the fermion creation operator

$$\Psi_F^\dagger(x) = \Psi_B^\dagger(x) e^{i\frac{1}{2}\Phi(x)} \tag{2.63}$$

So that its full expression is

$$\Psi_F^\dagger(x) = \left[\rho_0 - \frac{1}{\pi}\nabla\phi(x)\right]^{1/2} \sum_p e^{i(2p+1)(\pi\rho_0 x - \phi(x))} e^{-i\theta(x)} \tag{2.64}$$

With the knowledge of the particle (either boson or fermion) creation operator, we can construct the Hamiltonian that describes the density fluctuations. The kinetic part will come from taking the matrix element of $\frac{\hat{p}^2}{2m}$, which for fermions results in

$$H = \frac{v_F}{2\pi} \int dx \ \left[(\nabla\phi)^2 + (\nabla\theta)^2\right] \tag{2.65}$$

where $v_F = \pi\hbar^2\rho_0/m$. Another contribution to the Hamiltonian comes from the electron-electron interaction, for that we just have to plug in the smooth part of the density in to the expression of the Coulomb interaction. Overall, we get the following familiar Hamiltonian

$$H = \frac{1}{2\pi} \int dx \ \left[(v_F + g)(\nabla\phi)^2 + v_F(\nabla\theta)^2\right] \tag{2.66}$$

Which is then transformed by redefining the velocity and introducing the Luttinger liquid parameter K, to a standard TL liquid Hamiltonian. We will be using this particular phenomenological bosonization when discussing a model of the fractional quantum Hall effect based on the bosonization.

Chapter 3

Coulomb drag between helical edge states

3.1 Coulomb drag between one-dimensional quantum wires

This chapter is devoted to a study of the Coulomb drag between two QSH systems, each having one Kramer's pair as shown schematically in Fig.5.1. The drag experiment we discuss should be carried out at energy (temperature) scales above which the inter-edge correlated state forms,[142] but below the bulk energy gap of the QSH system. In a Coulomb drag experiment current is driven in an "active" wire/edge and voltage is measured in a "passive" wire/edge. The Coulomb interaction between electrons in different system results in a momentum transfer between the two systems and produces a voltage drop in the "passive" system. The drag is characterized by the drag resistivity,

$$r_D = -\lim_{I_1 \to 0} \frac{e^2}{h} \frac{1}{L} \frac{dV_2}{dI_1}, \tag{3.1}$$

where V_2 is voltage induced in the "passive" system by the current I_1 driven in "active" system. Here e is the electron charge, h is a Planck's constant, and L is the length of the edge along which momentum is transferred.

[2]This chapter is based on a published paper by V.A. Zyuzin and G.A. Fiete, "Coulomb drag between helical edge states", Phys. Rev. B **82**, 113305 (2010)

Coulomb drag in non-HL one-dimensional systems has been studied both theoretically[6, 35, 39, 76, 110, 112] and experimentally.[21, 22, 158] First of all, for the Coulomb drag effect to be observable, the electron densities in both wires should match. Otherwise the drag exponentially decays with the density mismatch. When there is a match of electron densities, the Coulomb drag between one-dimensional electron systems has two important contributions. In the case of linear regime of the spectrum (Tomonaga-Luttinger liquid), the drag is governed only by the inter-wire backscattering processes [39, 76, 110]. Any non-linear corrections to the spectrum result in inter-wire forward-scattering interaction contributions to the drag resistivity. The main signature of the Coulomb drag is its temperature and possibly magnetic field behaviors. In case of linear regime, theory predicts T^{4K-3} temperature behavior of the drag resistivity. Here K is a Tomonaga-Luttinger liquid interaction parameter. The forward-scattering in case of quadratic non-linear corrections to the spectrum gives a standard T^2, Fermi liquid, dependence of the Coulomb drag resistivity [112]. The magnetic field dependence of the drag resistivity is minimal, namely magnetic field only enters the interaction parameter K, and not changing the overall amplitude of the drag resistivity. There is another interesting proposal of the magnetic field driven spin Coulomb drag. The system is composed of two wires with different electron densities. Applied magnetic field shifts the energy bands for spin-up and spin-down by a Zeeman energy. At some particular value of magnetic field the electron density mismatch for opposite spins of two wires will be zero, resulting in the Coulomb drag of only

a certain spin in the passive wire [113].

3.2 Helical edge states

In this chapter a unique signature of an edge of the two-dimensional topological insulator (quantum spin Hall (QSH) state) is obtained. To remind, the QSH state has an insulating bulk and metallic edge states composed of an odd number of Kramer's pairs of electrons. A Z_2 invariant distinguishes the topological insulators with time-reversal symmetry from their "trivial" counterparts.[11, 68, 69] The simplest topologically non-trivial case is a single Kramer's pair on the edge. Due to the spin-orbit coupling that drives the QSH state, the spin of an electron on the edge is correlated with its momentum. This property leads to an absence of back-scattering from weak non-magnetic impurities and therefore prevents Anderson localization on the edge of the QSH system.[151, 156]

The gapless edge modes of the QSH system are commonly referred to as a helical liquid (HL).[151] The stability of the HL to interactions,[151, 156] and magnetic disorder[89, 151] has been investigated, as has its response to "pinching" the sample into a point contact[82, 140, 144] or related geometries.[59] Properties of superconducting-QSH hybrid structures were investigated as well.[155] When two HL (of different QSH systems) are allowed to interact with each other, a novel one-dimensional correlated state is formed at the lowest energies.[142]

The HL can be viewed as a spinless Tomonaga-Luttinger liquid (because

it has the same number of degrees of freedom) without backscattering; since it is known that the backscattering governs the drag between systems with linear dispersions,[35, 76, 112] one can not expect drag between helical liquids. However, in this chapter we show that an applied Zeeman field $\vec{h}$ opens up a backscattering process in the HL, and results in $r_D \propto h^4$ for a linear spectrum. We also compute the temperature dependence of the drag over a range of temperature and field values.

3.3 The model

A general form of the expression for the Coulomb drag resistivity comes from the second order perturbation theory in the interwire Coulomb interaction, it is given by the following expression [112]

$$r_D = \int_0^\infty dq \int_0^\infty d\omega \, \frac{q^2 U_{12}^2(q)}{4\pi^3 n_1 n_2 T} \frac{\Im\Pi_1(q,\omega)\Im\Pi_2(q,\omega)}{\sinh^2(\frac{\omega}{2T})}, \tag{3.2}$$

where $\Im\Pi_i(\omega, q)$ is the imaginary part of the retarded density-density correlation function of wire $i = 1(2)$ [1], n_i is electron density of wire i, T is the temperature, and $U_{12}(q)$ is the Fourier transform of the interwire Coulomb interaction which is cut off at short distances by the interwire separation d.

The system we study consists of two identical QSH systems, each with one Kramer's pair on its edge (helical liquid), as shown in Fig.5.1. As it was already discussed, in case of linear spectrum of the helical edge liquid there is no contribution to the drag from forward scattering, and back scattering is forbidden by time-reversal symmetry. Therefore, one must break time-reversal

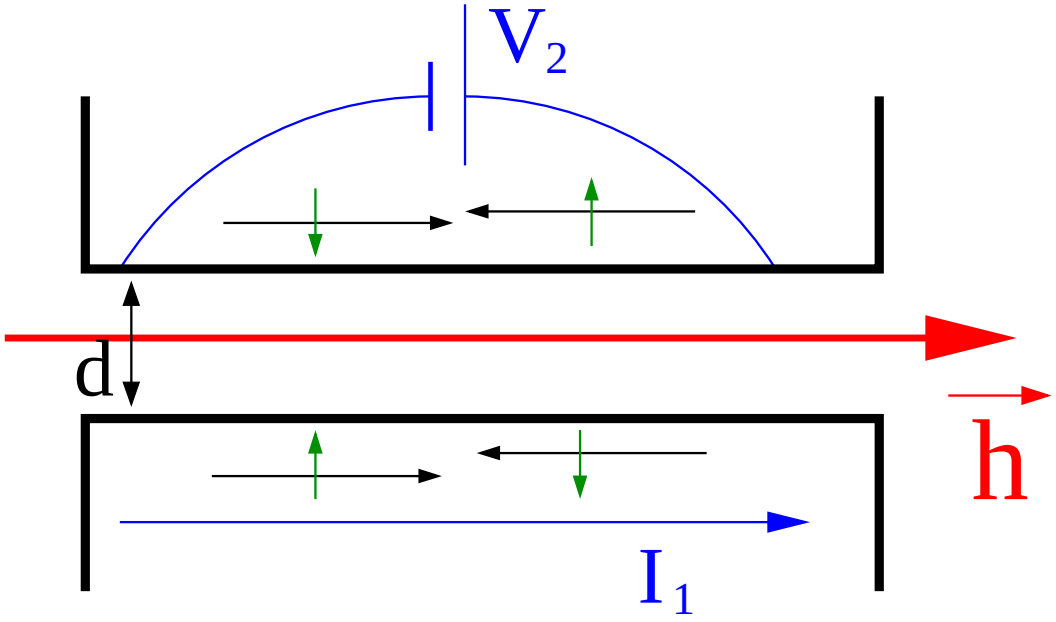

Figure 3.1: Schematic of a drag measurement between two QSH systems. A current I_1 is driven along the upper edge of the lower QSH system and through electron-electron interactions a voltage V_2 is induced in the lower edge of the upper QSH system. A magnetic field $\vec{h}$ is applied in the plane of wires, perpendicular to the spin quantization axis (assumed perpendicular to the plane of QSH systems). Time-reversed Kramer's pairs are indicated for the two edges. A QSH on top of QSH geometry could also be used.

symmetry in order to open up a backward scattering channel (unless there are magnetic impurities present) for a generic Dirac edge mode. Our Hamiltonian for a single HL in the presence of a Zeeman field is

$$H_0 = \int dx \hat{\psi}^\dagger(x) \left(v\hat{p}_x\hat{\sigma}_z + h\hat{\sigma}_x - \mu \right) \hat{\psi}(x), \tag{3.3}$$

where v is the edge velocity, $\hat{p}_x = -i\partial_x$, μ is the Fermi energy (which can be adjusted by gating the system), and $\hat{\sigma}_{z,x}$ are Pauli spin matricies describing the spin degree of freedom. A Zeeman field $\vec{h}$ pointing in the x-direction opens

up a gap in Dirac spectrum and tilts the spins away from the z-axis. The edge dispersion is $\epsilon_{\pm} = \pm\sqrt{v^2p^2 + h^2} - \mu$. We assume that Fermi energy is in the upper band ($\mu > 0$) so that the properties of system are determined by the ϵ_+ band over the energy scales of interest. The wavefunction of electrons in the ϵ_+ band is

$$\hat{\psi}_+(x) = \frac{e^{ipx}}{\sqrt{2}} \begin{pmatrix} \cos(\gamma_p/2) + \sin(\gamma_p/2) \\ \frac{\cos(\gamma_p)}{(\cos(\gamma_p/2)+\sin(\gamma_p/2))} \end{pmatrix} = e^{ipx}\hat{U}_p, \tag{3.4}$$

where $\gamma_p = \arctan(\frac{vp}{h})$. Next, we consider two different scenarios of the spectrum. When the Fermi energy μ is large comparing to $2h$ (small magnetic field h), the spectrum can be approximated as linear and the Tomonaga-Luttinger liquid formalism is used to derive an expression for the Coulomb drag resistivity. In this limit the backscattering events govern the drag. In the opposite limit of small Fermi energy, the spectrum can only be approximated as quadratic and we show that the forward scattering events contribute the most to the Coulomb drag resistivity. See Figs. 3.2 and 3.3.

3.4 Regime of linear spectrum

We first consider the case $\mu - h > h$, and linearize the spectrum near the Fermi energy, $\epsilon_+ = v|p_x| - \mu$ (see Fig. 3.2). We can now bosonize the electron states on the edge.[43] The standard procedure begins with expressing the electron operator as a sum of left- and right- moving states: $\hat{\psi}_+ = \hat{\psi}_R(x) + \hat{\psi}_L(x)$, where $R(L)$ stands for right (left) movers. The non-interacting Hamiltonian

can then be written:

$$H_0 = \int dx \Big[\hat{\psi}_R^\dagger(x)\hat{p}_+\hat{\psi}_R(x) + \hat{\psi}_L^\dagger(x)\hat{p}_-\hat{\psi}_L(x)\Big]. \tag{3.5}$$

where $\hat{p}_\pm = \pm v\hat{p}_x - \mu$. Let us now study the intrawire electron-electron interactions, which have the form

$$H_{int} = \frac{1}{2}\int dx dx'\ U(x-x')\rho(x)\rho(x'), \tag{3.6}$$

where $U(x-x')$ is the intrawire Coulomb interaction. The electron density $\rho(x)$ is given by

$$\rho(x) = \hat{\psi}_R^\dagger\hat{\psi}_R + \hat{\psi}_L^\dagger\hat{\psi}_L + \cos(\gamma_p)\left(\hat{\psi}_R^\dagger\hat{\psi}_L + \hat{\psi}_L^\dagger\hat{\psi}_R\right), \tag{3.7}$$

which contains cross terms due to the presence of the magnetic field. In terms of bosonic fields $\phi(x)$ and $\theta(x)$, $\hat{\psi}_R$ and $\hat{\psi}_L$ are expressed as[43]

$$\hat{\psi}_R(x) = e^{ipx}\tfrac{\eta_R}{\sqrt{2\pi a}}e^{-i(\phi(x)-\theta(x))}, \tag{3.8}$$

$$\hat{\psi}_L(x) = e^{-ipx}\tfrac{\eta_L}{\sqrt{2\pi a}}e^{-i(-\phi(x)-\theta(x))}, \tag{3.9}$$

where $\eta_{R(L)}$ are Klein factors, and a is a short-distance cut-off. The electron density in terms of bosonic fields takes the form

$$\rho(x) = -\frac{1}{\pi}\partial_x\phi(x) - \frac{\cos(\gamma_{p_F})}{\pi a}\sin(2p_F x - 2\phi(x)). \tag{3.10}$$

The electron density has a zero momentum part (first term). The second term is a magnetic field dependent $2k_F$ contribution to the electron density. Substituting this expression into (3.6), we find the interacting Hamiltonian to be

$$H_{int} = \frac{U(0) - \cos^2(\gamma_{p_F})U(2p_F)}{2\pi^2}\int dx\ (\partial_x\phi(x))^2, \tag{3.11}$$

where $U(0)$ and $U(2p_F)$ are the zero and $2p_F$ momentum parts of the interaction, respectively. Note that the $2p_F$ part has a $\cos^2(\gamma_{p_F})$ factor, which is proportional to h^2 for small h. The full Hamiltonian then becomes

$$H = \frac{1}{2\pi}\int dx \ \left[v(\partial_x\theta(x))^2 + (v+g)\left(\partial_x\phi(x)\right)^2\right], \tag{3.12}$$

where $g = (U(0) - \cos^2(\gamma_{p_F})U(2p_F))/\pi$. We observe that the Hamiltonian of an interacting HL in a Zeeman field is equivalent to a spinless Luttinger liquid where the strength of backscattering depends on the Zeeman field. Similar results for the interacting Hamiltonian above were obtained in studies of Luttinger liquids with Rashba spin-orbit coupling and a Zeeman magnetic field.[40, 141]

The Coulomb drag resistivity is defined by a retarded density-density correlation function. It is known that the only contribution to the drag resistivity comes from the $2k_F$ parts of the electron density. We have already made all necessary calculations regarding this correlation function in the introduction to the bosonization. We give its result

$$\Pi_R^{2p_F}(q,\omega) = \frac{1}{2}\left[\tilde{\Pi}(q+2p_F,\omega) + \tilde{\Pi}(q-2p_F,\omega)\right], \tag{3.13}$$

with $\tilde{\Pi}(q,\omega)$ given by

$$\tilde{\Pi}(q,\omega) = \frac{2^{2K}D}{u}\left(\frac{\beta u}{2\pi}\right)^2 F(q,\omega), \tag{3.14}$$

where $F(q,\omega) = B(-i\frac{\beta}{4\pi}(\omega - uq) + \frac{K}{2}, 1-K)B(-i\frac{\beta}{4\pi}(\omega + uq) + \frac{K}{2}, 1-K)$, $\beta = 1/T$, $u = \sqrt{v(v+g)}$, $K = v/u$, and $B(x,y)$ is the Beta function. The

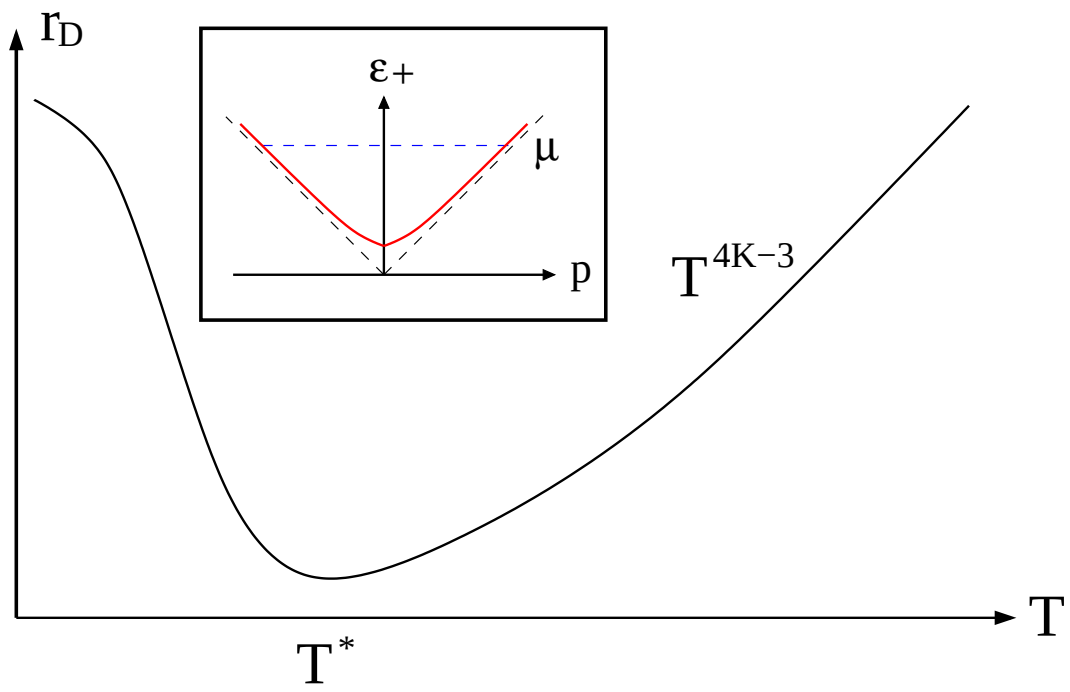

Figure 3.2: Temperature dependence of the drag in the regime of small h where the spectrum may be approximated as linear, as shown in the inset. T^* is the temperature at which the wires begin to "lock" to each other.[76] For $T > T^*$, we find $r_D \propto h^4 T^{4K-3}$ where K is the Luttinger parameter in the charge sector.

parameter D is

$$D = \cos^2(\gamma_{p_F}) \sin(\pi K) \frac{(\pi a)^{2K-2}}{(u\beta)^{2K}}. \tag{3.15}$$

dependent on the magnetic field and the Luttinger liquid interaction constants. With (3.14) in hand, the drag resistivity is readily computed from (3.2): $\Im F(q \pm 2p_F, \omega)$ is sharply peaked about $q = \mp 2p_F$ with peak widths proportional to temperature. Since the momentum integration in (3.2) runs from 0 to ∞, we neglect the $\tilde{\Pi}(q + 2p_F, \omega)$ contribution. Taking the imaginary part of the retarded density-density correlation function and assuming identical helical liquids we obtain

$$r_D \simeq \frac{2^{4K} u^2 D^2}{16^2 \pi^7} (2p_F)^2 U_{12}^2 (2p_F) \frac{I}{n^2 T^3}, \tag{3.16}$$

where $I \equiv \int_0^\infty d\Omega \, \frac{(\Im F(0,\Omega))^2}{\sinh^2(\Omega/2)}$, with $\Omega = \omega/T$. The density of states, $n = 1/\pi v$. Extracting the temperature and magnetic field dependence using (3.15), we find

$$r_D \propto h^4 T^{4K-3}. \tag{3.17}$$

Eq.(4.51) is one of the central results of the present chapter. This result is valid at temperatures larger than T^*, below which the drag begins to exhibit an exponential dependence on temperature.[76, 110] Since $T^* \sim \mu e^{-\frac{p_F d}{1-K}}$ depends[76] on the backscattering via K, it will also depend on the Zeeman field via the dependence of K on h.

By contrast, in a spinful Luttinger liquid the magnetic field only enters the interaction constant in the spin channel and therefore the drag is only

(weakly) dependent on magnetic field through the interaction parameter appearing in an exponent to the temperature. Therefore, Coulomb drag can be used as a method for experimental verification of the HL, complementing the earlier studies.[59, 82, 89, 140, 142, 144, 151, 155] We note that a spin-Coulomb drag effect in which two density mismatched Luttinger liquids can be brought into more favorable kinematic conditions for enhanced drag effects has also been studied.[113] To complete our analysis of drag between two HL, we turn to the case when the spectrum is approximately quadratic.

3.5 Regime of quadratic spectrum

When $0 < \mu - h < h$, the spectrum of upper band is approximately $\epsilon_+ = \frac{1}{2}\frac{(vp)^2}{h} - (\mu - h)$ (see an inset in Fig. 3.3). In this section, we simplify the problem by assuming no intrawire electron interactions. The neglect of weak interactions in the regime of a quadratic dispersion has been shown to have no effect on the temperature dependence of the drag.[112] The imaginary part of the retarded density-density correlation function is

$$\Im\Pi_R(q,\omega) = -\frac{h}{4v^2 q} f_+^2(p_0,q) \frac{\sinh(\frac{\omega}{2T})}{\cosh(\frac{\epsilon_+(p_0)}{2T})\cosh(\frac{\epsilon_+(p_0+q)}{2T})}, \tag{3.18}$$

where $p_0 = -\frac{1}{2}q + \frac{h\omega}{v^2 q}$, and $f_+(p,q) = \hat{U}_p^\dagger \hat{U}_{p+q}$, which we assume to be approximately equal to one. One also needs to take into account restrictions on ω defined by $\epsilon_+(p_0) < 0$ and $\epsilon_+(p_0+q) > 0$ which will give

$$\frac{1}{2}vq + \sqrt{2h(\mu-h)} > \frac{h\omega}{vq} > -\frac{1}{2}vq + \sqrt{2h(\mu-h)}. \tag{3.19}$$

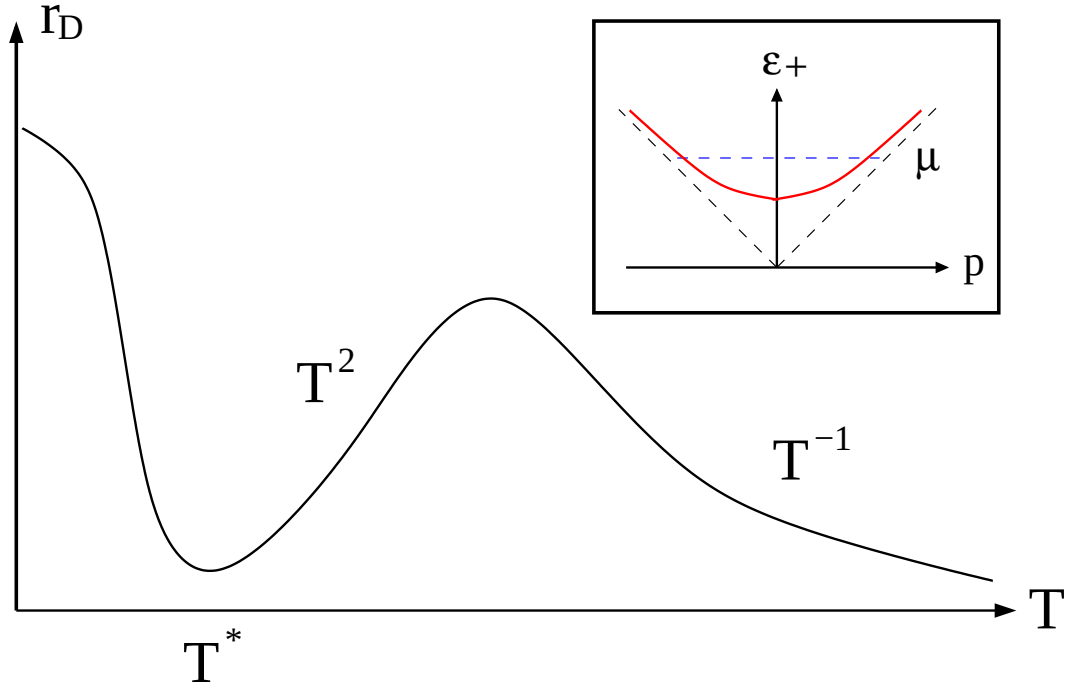

Figure 3.3: Temperature dependence of the drag in the regime of small μ where the spectrum is approximately quadratic, as shown in the inset, and $0 < \mu - h < \frac{v^2}{2d^2h}$. Note the non-monotonic temperature dependence[35] above T^*. For the dependence of r_D on the Zeeman field h in each region of temperature, see the text. The second crossover from T^2 to T^{-1} occurs for $T \sim \frac{v}{4d}\sqrt{\frac{\mu-h}{2h}}$ where d is the distance between wires.

Plugging (3.18) into (3.2) and evaluating the integrals we obtain the following results. When $\mu - h > \frac{v^2}{2d^2h}$ [here d is the inter-edge separation distance and $1/d$ serves as high momentum cut-off to $U_{12}(q)$ in the q integration in (3.2)] and for small temperatures $T < \frac{v}{4d}\sqrt{\frac{\mu-h}{2h}}$,

$$r_D \simeq \frac{1}{2^5\pi^2 n^2}\frac{g_\gamma^2}{v^4}\sqrt{\frac{h^5}{(\mu-h)^3}}T^2, \tag{3.20}$$

while at large temperatures $T > \frac{v}{4d}\sqrt{\frac{\mu-h}{2h}}$,

$$r_D \simeq \frac{1}{2^8\pi^3 n^2}\frac{hg_\gamma^2}{vd^3}\frac{1}{T}. \tag{3.21}$$

When $\mu - h < \frac{v^2}{2d^2h}$ and for small temperatures $T < \frac{v}{d}\sqrt{\frac{\mu-h}{2h}}$,

$$r_D \simeq \frac{2^{7/2}}{\pi^2 n^2}\frac{g_\gamma^2}{v^4}h^{5/2}\sqrt{T}, \tag{3.22}$$

while at large temperatures $T > \frac{v}{d}\sqrt{\frac{\mu-h}{2h}}$

$$r_D \simeq \frac{2^{15/2}}{3\pi^3 n^2}\frac{g_\gamma^2}{v}\frac{h(\mu-h)^{3/2}}{d^3}\frac{1}{T^{5/2}}. \tag{3.23}$$

Here $g_\gamma = -\gamma + \ln(2)$ ($\gamma \approx 0.5772$ is Euler's constant) is an estimate of interwire Coulomb interaction at small momentum. The density of states, $n = \frac{1}{\pi}\frac{1}{\sqrt{\mu-h}}$. The results are summarized in Fig. 3.3. We emphasize that in obtaining these results we have not considered effects of interband (intra-edge) particle-hole excitations. These excitations will result in Fermi edge singularity physics.[34, 111]

3.6 Conclusions

We studied the Coulomb drag between identical one dimensional helical liquids. We showed that the helical liquid can be mapped to a spinless Luttinger liquid where backscattering is prohibited. Since backscattering governs the drag between one-dimensional liquids with linear dispersion, there is no Coulomb drag unless there is a nonlinearity in the spectrum. Nonlinearity in the spectrum gives rise to a small momentum scattering contribution to the drag which has a T^2 temperature dependence.[112] Our calculations confirm these results for a nonlinear spectrum.

For a linear spectrum, the application of a Zeeman field opens up backscattering processes which are proportional to the square of the magnetic field at small fields, see (5.4) and (4.12). We also showed that when the magnetic field is small (μ large) and the spectrum can be approximated as linear, the Hamiltonian of a helical liquid with a magnetic field is identical to that of a spinless Luttinger liquid with a magnetic field dependent backscattering term (3.12). In this case, the Coulomb drag becomes proportional to the fourth power of magnetic field (4.51) which is distinct from the case of Luttinger liquids where the magnetic field enters only via the interaction constant in the spin channel.

For completeness we studied the case when the spectrum of a helical liquid in a magnetic field can not be approximated as linear, but is rather approximately quadratic (valid for a strong magnetic field). Expressions for the Coulomb drag in this case are given by (3.20)-(3.23). Finally, we note that

the presence of a few magnetic impurities on the edge of a QSH system would allow a finite drag contribution even in the absence of applied magnetic fields since they would allow backscattering. Inclusion of Rashba coupling would not affect our results, provided the zero-field case is still adiabatically connected to the topologically non-trivial state.

Chapter 4

Spatially anisotropic kagome antiferromagnet with Dzyaloshinskii - Moriya interaction

4.1 Introduction

In this chapter, we study a highly frustrated spin model - the spin-1/2 kagome antiferromagnet with spatially anisotropic exchange interaction constants and spin-orbit coupling. We investigate the physics of this system as the spin-orbit coupling, realized in the form of Dzyaloshinskii-Moriya (DM) interaction,[27, 99] is increased. The ground state of the spatially isotropic spin-1/2 Heisenberg antiferromagnet in the absence of DM interaction has been studied for some time.[29, 31, 83, 85, 90, 96, 117, 125, 130–132, 165] Its large classical ground state degeneracy was thought to make it an excellent candidate for a quantum spin liquid, and the most recent density matrix renormalization group results seem to indicate this is indeed the case.[159] Exactly solvable spin-3/2 spin liquids have also been studied on the isotropic kagome lattice.[18]

However, some kagome antiferromagnets, such as volborthite, $Cu_3V_2O_7(OH)_2 \cdot 2H_2O$, are spatially anisotropic which allows a quasi-one dimensional approach

[3]This chapter is based on a published paper by V.A. Zyuzin and G.A. Fiete, "Spatially anisotropic kagome antiferromagnet with Dzyaloshinskii-Moriya interaction", Phys. Rev. B **85**, 104417 (2012).

to be used in their study.[126, 134–137] This approach is especially powerful because one-dimensional methods are adept at describing strongly correlated physics.[43, 46] In this work, we extend earlier studies of the DM interaction on the spatially isotropic kagome lattice[16, 28, 52, 56, 60, 91, 95, 119, 120, 122, 145, 153, 167] to the spatially *anisotropic* case by using a quasi-one dimensional approach. Our main result is that we find a transition from a spiral ordered state with weak Neel order perpendicular to the spiral[126] to a spiral state with weak in-plane Neel order coexisting with dimer order as the strength of the DM interaction is tuned up. (See Fig.4.2.) We argue this transition may be in an experimentally accessible parameter range and could possibly be tuned by pressure.

4.2 Overview of theoretical approach and summary of results

The quasi one-dimensional approach to spin systems was mainly developed in works [126, 134–136] for various anitferromagnetic lattices. In this approach one constructs a two-dimensional spin system by weakly coupling one-dimensional spin chains together. Thus, the exchange interaction between spin chains is assumed smaller than the exchange interaction between spins on a given spin chain. (See Fig.4.1.) In a one-dimensional spin-1/2 chain, the spin degrees of freedom are then represented in the spin-current formalism (non-Abelian bosonization) and the low-energy theory of the spin chains is described by a $SU(2)_1$ Wess-Zumino-Novikov-Witten (WZNW) theory.[46]

The inter-chain interactions can then be analyzed by perturbation theory using a scaling and a renormalization group approach. The advantage of such an approach is that the quantum fluctuations are already included in the field theoretical description of the spin chains. Even though there are not that many magnetic materials with spatially anisotropic exchange interactions, the theoretical predictions from the bosonization approach can shed a light and give intuition on the possible phases of isotropic two-dimensional systems.

In this chapter the quasi-one dimensional approach is applied to a spatially anisotropic kagome antiferromagnet. For that we assume that the exchange interaction along the horizontal lines is assumed to be larger than the interaction across the diagonals. Previous studies in this limit have neglected the DM interaction.[5, 103, 126, 148, 160] And the present work is devoted to understanding of the effect of Dzyaloshinskii-Moriya interaction.

The basic structure that emerges from the quasi one-dimensional analysis is the following:[126] there are two temperature scales that enter into the magnetic ordering. First, the middle spins order in either a spiral state with small wave vector or a ferromagnetic state (spiral state with vanishing ordering vector) on a temperature scale $T_m \sim (J')^2/J$. As the temperature decreases further the spin chains also begin to order on a scale $T_{ch} \sim (J')^4/J^3$, with an order dictated by the magnetic state of the middle spins.[126] Because of this separation of energy scales, the middle spins produce an effective exchange field on the spins of the spin chains which ultimately plays an important role in the magnetic order at the lowest temperatures. We note that we do not

find a spin-liquid ground state in any regime we study. Which is reasonable since two of the lattice geometries are broken by the exchange anisotropy and the Dzyaloshinskii-Moriya interaction.

Our main results are the following. For weak spin-orbit coupling, the DM interaction selects the plane of the kagome lattice in which the middle spins take on a spiral order (the plane of the kagome lattice itself). Our analysis of the spin chains shows that the spins along a chain are predominantly anti-parallel to the direction of the middle spins. However, there is small a component which is perpendicular to the main order, and this component undergoes a phase transition as the DM interaction is increased. For small values of the DM interaction the perpendicular component orders antiferromagnetically perpendicular to the plane of the spiral, while for larger values this component becomes a mixture of coexisting antiferromagnetic and dimerized states and rotates into the plane of the spiral. We estimate the value of the critical DM interaction [see Eq.(4.50)] to be $D/J \sim (J'/J)^{5/2}$.

The remainder of this chapter is organized as follows. In Sec 4.3 we begin with a tight-binding model with spin-orbit coupling on the kagome lattice. We then derive the effective spin Hamiltonian in the limit of a large on-site repulsion potential at half-filling. Thus, the parameters of a spatially anisotropic kagome antiferromagnet are determined. In this section, a non-Abelian bosonization mapping is introduced that we will use throughout the remainder of the chapter. In Sec. 4.4 we perform perturbation theory in the exchange interaction J' between spin chains and middle spins. Our approach

closely follows that of the work [126]. In Sec. 4.5 the order of the spin chains and the two dimensional system is analyzed from the point-of-view of perturbative renormalization group equations. Finally, we present our main conclusions in Sec. 4.6. Some technical formulas are given in Appendix .1.

4.3 Model Hamiltonian

In order to remind the reader of the microscopic origin of the DM interaction, and to establish some relationship with other phases where spin-orbit coupling plays a role (such as topological band insulators[53, 98, 115]), we first consider a tight-binding model on the spatially isotropic kagome lattice with intrinsic spin-orbit coupling. We study a model with only on-site interactions, and assuming half-filling we derive an effective spin Hamiltonian. The spin-orbit coupling translates into a DM interaction which induces an anisotropy in the exchange interaction. With insight from the spatially isotropic case, we then describe the case of a spatially anisotropic kagome lattice, which is the main focus of this paper.

4.3.1 Tight-binding model on the kagome lattice with spin-orbit coupling

In this section we give a derivation of the nearest-neighbor spin Hamiltonian in the presence of spin orbit-coupling on the kagome lattice. The calculation is standard,[7, 129] but clearly illustrates how the DM interaction is obtained and gives the precise form we will use in this work.

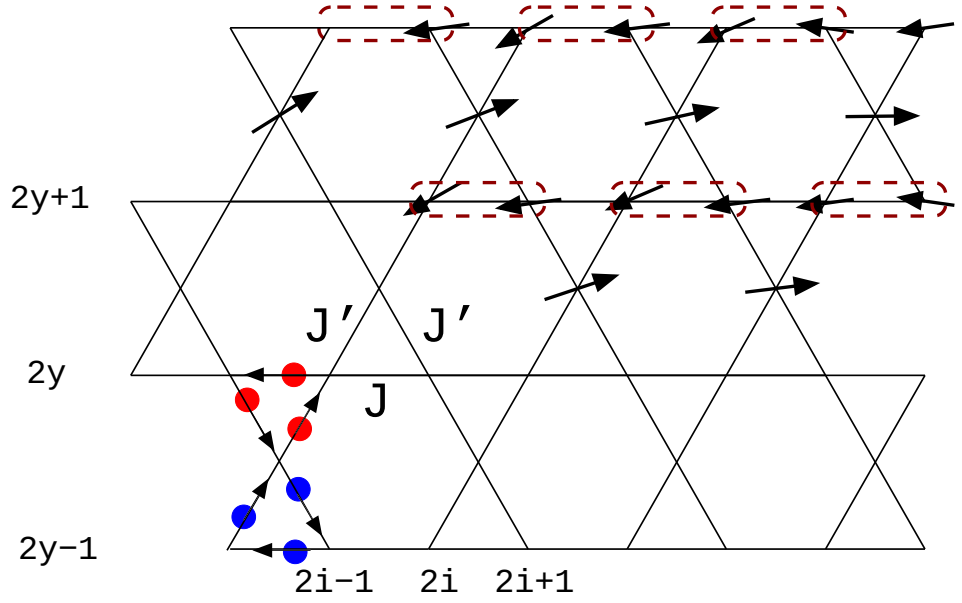

Figure 4.1: The kagome lattice with spatially anisotropic exchange couplings. Sites along the one-dimensional spin chains (running horizontally) are labeled by i as indicated, and different horizontal chains are labeled by y. The scale of the antiferromagnetic nearest neighbor spin exchange along the chains is J, and the scale of the corresponding exchange between spins on a chain and the "middle spins" (between chains) is J' as shown. We consider the anisotropic limit $J' \ll J$ in this paper. Our convention for the staggered Dzyaloshinskii-Moriya (DM) interaction is indicated by the different colors on the "up" and "down" triangles of the kagome lattice, with the up triangles having a DM vector pointing out of the kagome plane and a down triangle having a DM vector pointing into the plane of the kagome. The arrows indicated the direction going from site $i \to j$. The strength of the DM interaction is given by (4.7), and shares the same anisotropy as J and J' (*i.e.* $D^{z'} \ll D^{z}$) due to the spatial anisotropy of the lattice. Black arrows and brown dashed rectangles correspond to a DM interaction driven spin ordering we found in this paper and described by expression (4.51). Arrows stand for the spin direction while brown dashed rectangles describe dimers.

For a one-electron tight-binding model on the kagome lattice the nearest neighbor hopping Hamiltonian is given by

$$H_t = -t \sum_{\langle ij \rangle \alpha} c^\dagger_{i\alpha} c_{j\alpha}, \tag{4.1}$$

where t is the hopping, and $c_{i\alpha}$ is a operator that annihilates a fermion on a site i with spin α. Likewise, $c^\dagger_{i\alpha}$ is the analogous fermion creation operator. The notation $\langle .. \rangle$ denotes nearest neighbor sites, and will be used throughout the paper.

The symmetry of the kagome lattice allows a nearest-neighbor spin-orbit hopping term of the form

$$H_{so} = i\lambda_{so} \sum_{\langle ij \rangle \alpha\beta} \nu_{ij} c^\dagger_{i\alpha} \sigma^z_{\alpha\beta} c_{j\beta}, \tag{4.2}$$

where λ_{so} parameterized the spin-orbit coupling strength, and $\nu_{ij} = \pm$ depending on the direction of hopping–"+" when the third site in a triangle is "to the left" and "-" when the third site in a triangle is "to the right" (see Fig. 4.1).[68, 69] Here σ^z is the Pauli spin matrix representing the z-component of the spin.

We are interested in the strongly interacting limit at half-filling. We model the interactions by a Hubbard on-site repulsive potential

$$H_U = U \sum_i n_{i\uparrow} n_{i\downarrow}, \tag{4.3}$$

where $n_{i\alpha} = c^\dagger_{i\alpha} c_{i\alpha}$ is the on-site density of electrons with spin α. At half-filling and in the limit of large electron interaction $t \ll U$ we anticipate the Mott

metal-insulator transition. There is finite and large energy U for electrons to overcome when hopping from one site to the other. A hopping of an electron to a neighboring occupied site and back will then result in the exchange interaction between spins of neighboring electrons. The exchange Hamiltonian is obtained by performing second-order perturbation theory in t, we get

$$H_M = J \sum_{\langle ij \rangle} \left[\cos(2\theta)(S_i^x S_j^x + S_i^y S_j^y) + S_i^z S_j^z \right. \\ \left. -\nu_{ij} \sin(2\theta)[\mathbf{S}_i \times \mathbf{S}_j]_z \right], \tag{4.4}$$

where

$$J = \frac{4(t^2 + \lambda_{so}^2)}{U}, \tag{4.5}$$

and

$$\theta = \arctan(\lambda_{so}/t). \tag{4.6}$$

The first line in Eq.(4.4) is the weakly anisotropic (when $\lambda_{so} \ll t$) exchange coupling between nearest-neighbor spins, and the second line is a staggered DM interaction with a strength

$$D_{ij}^z = -J\nu_{ij} \sin(2\theta). \tag{4.7}$$

In this chapter we are going to focus only on this particular DM interaction, which is an intrinsic property of the two-dimensional kagome lattice. We would like to notice that the more elegant way to obtain results described above is by noticing that the spin-orbit coupling can be absorbed in to a definition of the first-nearest neighbor hopping matric element t, making it spin-dependent.[129] The equations (4.4-4.6) describe the spin Hamiltonian of

the *spatially isotropic* kagome lattice. When the lattice is anisotropic, the form is slightly modified as we describe below.

4.3.2 Spatially anisotropic case

In the previous section we derived the Hamiltonian of spins on the isotropic kagome lattice, and found the DM conventions are of the same form earlier studied in the literature.[16, 60, 95] Let us now describe how the interactions are modified in the spatially anisotropic case which will be studied in the remainder of the paper.

In a spatially anisotropic lattice such as that shown in Fig. 4.1, the bonds between horizontal chains are "stretched" leading to a modified hopping $t' < t$ (and spin-orbit coupling) along the diagonals. (In fact, the spin-orbit coupling will also be modified along the chains as well because its value is dependent on the position of the "middle spins".) The modified hopping parameters and spin-orbit coupling will change the exchange constants in (4.5) and (4.7) along the diagonal bonds. We take the exchange between spins on diagonals to be J' and on horizontal lines to be J, as before. The DM interaction also takes on a similar anisotropy with an angle θ described as in (4.6) (slightly modified from the isotropic case since the spin-orbit coupling is modified, but this will not play a crucial role in our study) along the chains, and a similarly defined θ' (in terms of t' and λ'_{so}) along diagonals, giving

$$D_{ij}^{z'} = -J'\nu_{ij}\sin(2\theta'). \tag{4.8}$$

Thus, in the spatially anisotropic case the Hamiltonian has the same form

as (4.4), only with different exchange and DM interactions along chains and between spins on the chains and the middle spins.

4.3.2.1 Hamiltonian of spin chains

Since we are interested in the limit $J' \ll J$, we will first focus on the Hamiltonian of the spin chains and later treat the interaction with middle spins perturbatively. The spin chain Hamiltonian is thus

$$\begin{aligned} H_0 = J \textstyle\sum_{\langle ij\rangle,y} \left[\cos(2\theta)(S^x_{i,y}S^x_{j,y} + S^y_{i,y}S^y_{j,y}) + S^z_{i,y}S^z_{j,y}\right] \\ + J\sin(2\theta) \textstyle\sum_{\langle ij\rangle,y} \nu^y_{ij}[\mathbf{S}_{i,y} \times \mathbf{S}_{j,y}]_z, \end{aligned} \tag{4.9}$$

with $J > 0$ given by (4.5) as before, the index y labels the different spin chains, and $\nu^y_{ij} = \pm 1$ which alternates from bond to bond. For even and odd spin chains the ν^y_{ij} differs by a sign for the same $\langle ij\rangle$ bond. These features are evident from Fig. 4.1.

We now absorb the DM term into the exchange interaction of (4.9) by rotating spins with a local spin rotation [2] given by a matrix

$$\hat{R}_{DM}(\theta) = \begin{pmatrix} \cos(\theta) & -\sin(\theta) & 0 \\ \sin(\theta) & \cos(\theta) & 0 \\ 0 & 0 & 1 \end{pmatrix}, \tag{4.10}$$

which rotates the spin on site i on chain y as $\mathbf{S}_{i,y} \to \hat{R}_{DM}\left((-1)^{i+y+1}\theta\right)\mathbf{S}_{i,y}$. After the rotation, the Hamiltonian (4.9) becomes an isotropic Heisenberg model

$$H_0 = J \sum_{\langle ij\rangle,y} \mathbf{S}_{i,y} \cdot \mathbf{S}_{j,y}, \tag{4.11}$$

which is very convenient for performing perturbation theory in the interactions with middle spins. For a purely one dimensional system, this result of absorbing staggered DM interaction was obtained in works [2, 129]. They claimed that the frustration of the lattice is necessary for the DM interaction to play an essential role in spin ordering. And the kagome meets this requirement being a geometrically frustrated lattice.

4.3.2.2 Diagonal interactions between spins

We start with the interactions between the spin chains with middle spins (those lying along the diagonals in Fig. 4.1 between the spin chains). These terms consist of XXZ-type terms and the DM interaction. Performing the rotation (4.10) on the spin chains as described above, we arrive at the following form of the interaction

$$\begin{aligned} V = J'\cos(\chi)\sum_{i,y} s^{x(y)}_{2i\pm 1/2,2y\mp 1/2}\left[S^{x(y)}_{2i,2y\mp 1}+S^{x(y)}_{2i\pm 1,2y\mp 1}+S^{x(y)}_{2i,2y}+S^{x(y)}_{2i\pm 1,2y}\right] \\ +J'\sum_{i,y} s^{z}_{2i\pm 1/2,2y\mp 1/2}\left[S^{z}_{2i,2y\mp 1}+S^{z}_{2i\pm 1,2y\mp 1}+S^{z}_{2i,2y}+S^{z}_{2i\pm 1,2y}\right] \\ +J'\sin(\chi)\sum_{i,y}\left[-[\mathbf{s}_{2i\pm 1/2,2y\mp 1/2}\times\mathbf{S}_{2i,2y\mp 1}]_z+[\mathbf{s}_{2i\pm 1/2,2y\mp 1/2}\times\mathbf{S}_{2i\pm 1,2y\mp 1}]_z\right. \\ \left.+[\mathbf{s}_{2i\pm 1/2,2y\mp 1/2}\times\mathbf{S}_{2i,2y}]_z-[\mathbf{s}_{2i\pm 1/2,2y\mp 1/2}\times\mathbf{S}_{2i\pm 1,2y}]_z\right], \end{aligned} \tag{4.12}$$

where $\chi = 2\theta' + \theta$ and the small "s" describes the spin degrees of freedom of the middle spins. Note that the first two terms describe the nearly isotropic exchange interaction (for weak spin-orbit coupling), while the last two terms describe the DM interaction between middle spins and the spins on the spin

chains.

4.3.2.3 Non-Abelian bosonization

Focusing on the case, $J' \ll J$, we can apply powerful bosonization methods to describe the low-energy physics of spin chains and construct perturbation theory in the interaction inter-chain interactions. The basic approach has been successfully applied to large variety of lattice [126, 134–136] with one of them being the spatially anisotropic kagome antiferromagnet without the DM interaction.[126] We take the continuum limit of local spin degrees of freedom and present them in terms of a uniform and staggered magnetization,[126]

$$\mathbf{S}_i \to a_0 \left[\mathbf{M}(x) + (-1)^x \mathbf{N}(x)\right], \tag{4.13}$$

where $x = ia_0$, with a_0 being the lattice spacing, and i labels sites along the chains. The definitions of these operators and the fusion rules which they obey are heavily discussed in the literature.[126, 134–136] For completeness, we provide the necessary details in Appendix .1.

The low-energy form of the spin chain Hamiltonian (4.11) can be written using non-Abelian bosonization (spin current operators)[126] as a Sugawara Hamiltonian with a backscattering term[46]

$$H_0 = \frac{2\pi u}{3} \int dx \left[\mathbf{J}_R \cdot \mathbf{J}_R + \mathbf{J}_L \cdot \mathbf{J}_L\right] + g_{bs} \int dx \; \mathbf{J}_R \cdot \mathbf{J}_L, \tag{4.14}$$

where $u = \pi J a_0/2$, and the second term in this expression is the backscattering with strength $g_{bs} < 0$.

Let us now derive the diagonal exchange interaction between spins. Substituting the low-energy form (4.13) into (4.12) we find,

$$\begin{aligned}
V_1 &= \tilde{\gamma}_1 \textstyle\sum_{x,y} s^{x(y)}_{2x\pm 1/2, 2y\mp 1/2} \left(M^{x(y)}_{2y\mp 1}(2x) + M^{x(y)}_{2y}(2x) \right) \\
&+\gamma_1 \textstyle\sum_{x,y} s^{z}_{2x\pm 1/2, 2y\mp 1/2} \left(M^{z}_{2y\mp 1}(2x) + M^{z}_{2y}(2x) \right), \\
V_2 &= \gamma_2 \textstyle\sum_{x,y} \Big[-s^{x}_{2x\pm 1/2, 2y\mp 1/2} (N^{y}_{2y}(2x) - N^{y}_{2y\mp 1}(2x)) \\
&+s^{y}_{2x\pm 1/2, 2y\mp 1/2} (N^{x}_{2y}(2x) - N^{x}_{2y\mp 1}(2x)) \Big], \\
V_3 &= \tilde{\gamma}_3 \textstyle\sum_{x,y} (\pm) s^{x(y)}_{2x\pm 1/2, 2y\mp 1/2} \partial_x (N^{x(y)}_{2y}(2x) + N^{x(y)}_{2y\mp 1}(2x)) \\
&+\gamma_3 \textstyle\sum_{x,y} (\pm) s^{z}_{2x\pm 1/2, 2y\mp 1/2} \partial_x (N^{z}_{2y}(2x) + N^{z}_{2y\mp 1}(2x)),
\end{aligned} \tag{4.15}$$

where the last interaction, V_3, is important as it will generate relevant interchain couplings in the renormalization group analysis to follow.[126]

In (4.15) we have used the approximations $M(2x + a_0) \approx M(2x)$ and $N(2x + a_0) \approx N(2x) + \frac{a_0}{2}\partial_x N(2x)$. The coupling constants in (4.15), $\gamma_1 = 2a_0 J'$, $\tilde{\gamma}_1 = 2a_0 J' \cos(\chi)$, $\gamma_2 = 2a_0 J' \sin(\chi)$, $\gamma_3 = -\frac{a_0^2}{2} J'$, and $\tilde{\gamma}_3 = -\frac{a_0^2}{2} J' \cos(\chi)$ will flow under the renormalization group. Since $\chi = 2\theta' + \theta$, the strength of the spin-orbit coupling terms partially set the scale of the initial coupling constants. We now proceed to treat the interaction $V = V_1 + V_2 + V_3$ in perturbation theory.

Note that $V_2 \equiv 0$ if the DM interaction vanishes. The term V_2 will turn out to give rise to dimer correlations for sufficiently large DM interaction, and therefore may potentially drive a quantum phase transition.

4.4 Perturbation theory and the ordering of the middle spins

The remainder of the chapter is devoted to an analysis of the phase diagram of the anisotropic kagome antiferromagnet with spin-orbit coupling based on the perturbative interactions in (4.15). The basic elements of our approach closely follow that of a work [126]. The new element in the present study is the presence of a DM interaction.

The operators **M** and **N** [from Eq.(4.13)] that enter expression (4.15) have scaling dimension 1 and 1/2, respectively. That is, under rescaling of coordinate $x_\ell = xe^{-l}$ and time $\tau_\ell = \tau e^{-l}$, where $b = e^{d\ell}$ they change as

$$M_y(x,\tau) = b^{-1} M_y(x/b, \tau/b), \tag{4.16}$$

$$N_y(x,\tau) = b^{-1/2} N_y(x/b, \tau/b). \tag{4.17}$$

There is another important operator $\epsilon_y(x,\tau)$, the dimerization operator, related to the continuum limit of the scalar product of two neighboring spins, $\mathbf{S}_{i,y} \cdot \mathbf{S}_{i+1,y} \to (-1)^x \epsilon_y(x)$, which does not appear in the interactions (4.15) but will be generated under the renormalization group flow.[126] It has scaling dimension 1/2, so changes as $\epsilon_y(x,\tau) = b^{-1/2}\epsilon_y(x/b, \tau/b)$ under a rescaling of space and time. All of these operators obey fusion rules (see Appendix .1) which will be used in perturbation theory beyond leading order.

4.4.1 Inter-chain interactions

A symmetry analysis yields the form of all the possible terms that are expected to be generated through the renormalization group (RG) transfor-

mations.[126] The most relevant ones, with lowest scaling dimension, are[126]

$$H_N = \sum_y \left[\gamma_{N1} \int dx N_y^z N_{y+1}^z + \gamma_{N2} \int dx N_y^{x(y)} N_{y+1}^{x(y)} \right],$$
$$H_\epsilon = \sum_y \gamma_\epsilon \int dx \epsilon_y \epsilon_{y+1}. \tag{4.18}$$

There are also irrelevant interactions between spin chains which are important because they will *generate relevant terms* of the form (4.18)

$$\begin{aligned} H_{\partial N} &= \sum_y \gamma_{\partial N1} \int dx \partial_x N_y^z \partial_x N_{y+1}^z \\ &\quad + \sum_y \gamma_{\partial N2} \int dx \partial_x N_y^{x(y)} \partial_x N_{y+1}^{x(y)}, \\ H_M &= \sum_y \gamma_{M1} \int dx M_y^z M_{y+1}^z \\ &\quad + \sum_y \gamma_{M2} \int dx M_y^{x(y)} M_{y+1}^{x(y)}. \end{aligned} \tag{4.19}$$

Next, we need to perform perturbation expansion in all of the interactions.

4.4.2 Perturbation theory and the renormalization group equations

We now proceed to apply perturbation theory to second order in interaction between the spin chains and middle spins. The second order perturbation expansion is given by

$$Z = \int e^{-S_0} \left[1 - \int d\tau V(\tau) + \frac{1}{2} T \int d\tau_1 d\tau_2 V(\tau_1) V(\tau_2) \right], \tag{4.20}$$

where $V = V_1 + V_2 + V_3$ is given by (4.15). In (4.20) S_0 is the fixed-point action of spin chains, and T is the time ordering operator.

At second order in the interaction, the following combinations of middle spins will occur $Ts^a_{i,y}s^b_{j,y'}$. For the same site ($i = j$, $y = y'$) the relationship $Ts^a(\tau_1)s^b(\tau_2) = \frac{1}{4}\delta^{ab} + \frac{i}{2}[\theta(\tau_1 - \tau_2) - \theta(\tau_2 - \tau_1)]\epsilon^{abc}s^c((\tau_1 + \tau_2)/2)$ is obeyed, where ϵ^{abc} is the fully antisymmetric tensor, and $\theta(\tau)$ is the heaviside function: $\theta(\tau) = 1$ for $\tau > 0$ and $\theta(\tau) = 0$ for $\tau < 0$. To derive the inter-chain operators one has to pick middle spins on the same sites with the same components (so that the middle spin degree of freedom "drops out"). Integration over the relative time is performed over the interval $\alpha < |\tau_1 - \tau_2| < b\alpha$ with $\alpha = a_0/u$.

To obtain contributions to the interaction V in (4.15) one must select middle spins on the same site but with different components. After straightforward but somewhat tedious calculations, we obtain the RG equations

$$\begin{gathered}
\frac{d\tilde{\gamma}_1}{d\ell} = \frac{\tilde{\gamma}_1\gamma_1}{2\pi u}, \quad \frac{d\gamma_1}{d\ell} = \frac{\tilde{\gamma}_1^2}{2\pi u}, \quad \frac{d\gamma_2}{d\ell} = \frac{1}{2}\gamma_2 + \frac{\gamma_1\gamma_2}{4\pi u}, \\
\frac{d\tilde{\gamma}_3}{d\ell} = -\frac{1}{2}\tilde{\gamma}_3 + \frac{\gamma_1\tilde{\gamma}_3}{\pi u}, \quad \frac{d\gamma_3}{d\ell} = -\frac{1}{2}\gamma_3 + \frac{\tilde{\gamma}_1\tilde{\gamma}_3}{\pi u}, \\
\frac{d\gamma_\epsilon}{d\ell} = \gamma_\epsilon - \frac{(\gamma_{\partial N1}\gamma_{M1} + 2\gamma_{\partial N2}\gamma_{M2})}{8\pi u^3\alpha^2}, \\
\frac{d\gamma_{N2}}{d\ell} = \gamma_{N2} + \frac{\gamma_2^2}{4u} + \frac{\gamma_{M1}\gamma_{\partial N2}}{8\pi u^3\alpha^2}, \\
\frac{d\gamma_{N1}}{d\ell} = \gamma_{N1} + \frac{\gamma_{M2}\gamma_{\partial N1}}{8\pi u^3\alpha^2}, \\
\frac{d\gamma_{M2}}{d\ell} = \frac{\gamma_{M1}\gamma_{M2}}{4\pi u} - \frac{\tilde{\gamma}_1^2}{4u}, \quad \frac{d\gamma_{M1}}{d\ell} = \frac{\gamma_{M2}^2}{4\pi u} - \frac{\gamma_1^2}{4u}, \\
\frac{d\gamma_{\partial N2}}{d\ell} = -\gamma_{\partial N2} - \frac{\tilde{\gamma}_3^2}{4u}, \quad \frac{d\gamma_{\partial N1}}{d\ell} = -\gamma_{\partial N1} - \frac{\gamma_3^2}{4u},
\end{gathered} \tag{4.21}$$

which are the generalization of the corresponding results in Eq.(14) of work [126]. We also obtained RG equations for exchange coupling constants of interaction between middle spins. The derived exchange interaction constants between the middle spins can be shown to be of the order of $(J')^2/J$, which is

consistent with work [126]. We are not showing them here since they resemble those given in work [126]. The only modification due to DM interaction is the parametric enhancement of exchange in $x-y$ plane.

4.4.3 Estimate of energy scales

While the equations (4.21) are somewhat more involved than the case of vanishing DM interaction, they may be analyzed in a similar fashion. Because the DM interaction is expected to be small compared to J', J (or at most of the same order), the hierarchy of energy scales at higher energies is not expected to change. Namely, there an ordering temperature for the middle spins $T_m \propto (J')^2/J$, which should be relatively insensitive to the DM interactions. The spin chains will start to order only at a lower temperature $T_{ch} \propto (J')^4/J^3$.[126] The procedure for determining the low-temperature magnetic order (that is, below T_{ch}) is to first find the order of the middle spins. These middle spins will then produce an average exchange field that acts on the spin chains. Thus, the final ordering of the anisotropic kagome lattice will be obtained by analyzing the spin chains in the presence of a (potentially) spatially varying exchange field.

At the energy scale for which the middle spins interactions become non-perturbative, corresponding to $\ell \sim 1$, one can estimate the values of the relevant coupling constants of inter-chain interactions,

$$\gamma_\epsilon \sim -\tfrac{a_0(J')^4}{16\pi^4 J^3}(1+2\cos^4(\chi)), \quad \gamma_{N1} \sim \tfrac{a_0(J')^4}{16\pi^4 J^3}\cos^2(\chi)$$
$$\gamma_{N2} \sim \tfrac{a_0(J')^4}{16\pi^4 J^3}\cos^2(\chi) + \tfrac{2a_0(J')^2}{\pi J}\sin^2(\chi), \tag{4.22}$$

where we have used that $\gamma_{\partial N1} \sim -\frac{\gamma_3^2}{4u}$, $\gamma_{\partial N1} \sim -\frac{\tilde{\gamma}_3^2}{4u}$, $\gamma_{M1} \sim -\frac{\tilde{\gamma}_1^2}{4u}$, $\gamma_{M2} \sim -\frac{\gamma_1^2}{4u}$, and substituted in the corresponding "initial" values of $\gamma_1, \tilde{\gamma}_1, \gamma_2, \gamma_3, \tilde{\gamma}_3$ given below Eq.(4.15).

4.4.4 Order of middle spins

In order to determine the order of the middle spins (which form a triangular lattice) we follow arguments of work [126] which uses perturbation theory to derive the effective Hamiltonian of interactions between middle spins. Before we proceed, however, one comment is in order. A full solution of the effect of the DM interactions on the middle spins is involved. As we have argued earlier, the DM interaction is not expected to have a significant effect on the ordering temperature, T_m. However, it still plays a role: It selects the plane of the spiral order found in work [126] to be the $x-y$ plane. (Without the DM interaction, the plane of the spiral order is arbitrary.) With the plane of the spiral order determined, we then follow the work [126] and write the Hamiltonian of the middle spins as

$$\begin{aligned} H_{\triangle} = 2(J')^2 \left(A(1) - B(1)\right) \textstyle\sum_{\langle ij \rangle} s_i^{x(y)} s_j^{x(y)} \\ +4(J')^2 \left(A(2) - B(2)\right) \textstyle\sum_{[ij]} s_i^{x(y)} s_j^{x(y)}, \end{aligned} \tag{4.23}$$

where notation $\langle .. \rangle$ denotes first nearest neighbor, and $[..]$ second nearest neighbor pairs of spins. The coefficients of these terms involve

$$\begin{aligned} A(r) &= \cos^2(\chi) \left(2G_M(r) + G_M(r+1) + G_M(r-1)\right), \\ B(r) &= \sin^2(\chi) \left(2G_M(r) - G_M(r+1) - G_M(r-1)\right), \end{aligned}$$

where

$$G_M(r) = \frac{2}{\pi}\int_0^\infty d\omega' \int_0^\pi dq\ S(q,\omega')\frac{\cos(qr)}{\omega'}, \tag{4.24}$$

and $S(q,\omega')$ is the dynamical structure factor. With the definition (4.24), we find

$$\begin{aligned} A(r) - B(r) = \tfrac{8}{\pi}\textstyle\int_0^\infty d\omega' \int_0^\pi dq\ \cos^2(q/2)\cos(qr)\frac{S(q,\omega')}{\omega'} \\ -\tfrac{8\sin^2(\chi)}{\pi}\textstyle\int_0^\infty d\omega' \int_0^\pi dq\ \cos(qr)\frac{S(q,\omega')}{\omega'}. \end{aligned} \tag{4.25}$$

The first integral in (4.25) was numerically estimated in the work [126], and it scales as $1/J$. At zero temperature, the second integral in (4.25) diverges, but for finite temperatures small compared to J, this integral scales as $1/T$.[71, 133] Thus, overall one has that the exchange coupling in (4.23), $J_{eff} = (J'^2)\left[\frac{c_1}{J} + \frac{c_2\sin^2(\chi)}{T}\right]$, where c_1, c_2 are order one constants. Because the middle spins order at a finite temperature given approximately by $T_m \sim (J')^2/J$, the ratio of the second integral to the first integral in (4.25) can be estimated as $J\sin^2(\chi)/T_m \sim (J\sin(\chi)/J')^2$, which we assume to be smaller than one.

The result of this analysis is that for temperatures of order $T_{crit} \sim J\sin^2(\chi)$ and larger, we may use the results of a work [126] for the ordering of middle spins as a good approximation. Classical considerations and an analysis of the two-spinon dynamical structure factor suggest that spiral order is a leading candidate,[126]

$$\langle \mathbf{s}_x \rangle = s_0[\mathbf{e}_x\cos(qx) + \mathbf{e}_y\sin(qx)], \tag{4.26}$$

where $\mathbf{e}_{x(y)}$ is a unit vector along the $x(y)$ coordinate, and with $q \ll 1$, and $q = 0$ (ferromagnetic) a distinct possibility. Here $s_0 < 1/2$ is the local static

moment of the middle spins. Below we study the effect of these two possible middle spin orders on the ordering of the spin chains: (i) spiral order in $x-y$ plane, and (ii) ferromagnetic order along x direction.

We also showed that for small temperatures, when the second term in J_{eff} dominates, the results of work [126] still hold. Namely, the two-spinon dynamical structure factor approximation still predicts the spiral order of middle spins.

4.5 Ordering of the spin chains in response to the ordering of the middle spins

We discuss how the spin chains order for q finite and small, and $q = 0$ in the middle spin ordering described in Eq.(4.26). At small Dzyaloshinskii-Moriya interaction strength we expect a spiral order (4.26) with $q \ll 1$, since the results of work [126] remain unchanged above T_{crit}, and our estimates suggest that they hold below the T_{crit}. The ordered middle spins then produce an effective exchange field (which can be treated in mean-field theory) that acts on the spin chains and causes them to order. We now determine the order of the spin chains on various temperature scales as a function of the Dzyaloshinskii-Moriya interaction.

To do so, we plug (4.26) back into (4.12) and obtain the result that the order of the middle spins appears as an effective magnetic field for the spins

on the chain,

$$V^{odd/even} = J'h\cos(\chi)\sum_i \left[\cos(qx)S_i^x + \sin(qx)S_i^y\right]$$
$$\pm J'h\sin(\chi)\sum_i(-1)^i\left[\cos(qx)S_i^y - \sin(qx)S_i^x\right], \tag{4.27}$$

where $h = 2s_0\cos(q/2)$ and the x in the argument of the sin and cos is $x = ia_0$, with a_0 the spacing of the spins along the chains. The first line of (4.27) describes a uniform spiral magnetic field while the second line describes a staggered, slowly rotating (in space) magnetic field. Performing a local rotation of spins as $\mathbf{S}_i \to \hat{R}_x(x)\mathbf{S}_i$, where

$$\hat{R}_x(x) = \begin{pmatrix} \cos(qx) & \sin(qx) & 0 \\ -\sin(qx) & \cos(qx) & 0 \\ 0 & 0 & 1 \end{pmatrix}, \tag{4.28}$$

the Hamiltonian $H^{odd} = H_0 + V^{odd}$ of the odd spin chains becomes,

$$H^{odd} = J\cos(q)\sum_i \mathbf{S}_i\cdot\mathbf{S}_{i+1} + J(1-\cos(q))\sum_i S_i^z S_{i+1}^z$$
$$+J\sin(q)\sum_i\left(S_i^y S_{i+1}^x - S_i^x S_{i+1}^y\right)$$
$$+J'h\sum_i\left(\cos(\chi)S_i^x + (-1)^i\sin(\chi)S_i^y\right), \tag{4.29}$$

where the first line describes anisotropic exchange between spins, the second line describes an effective *uniform* Dzyaloshinskii-Moriya interaction, and the third line are uniform and staggered magnetic fields resulting from exchange interactions with the middle spins. For even chains, one may take $\chi \to -\chi$. *Note that since the effect of the spin-orbit coupling is included in $\chi = 2\theta + \theta'$, the main role of the DM interaction is to give rise to the staggered magnetic field in the last line of* (4.29).

For the convenience of the following analysis we make a $\pi/2$ rotation about the y-axis which transforms $S_i^x \to S_i^z$ and $S_i^z \to -S_i^x$. We further assume that $q \ll 1$ which allows us to neglect anisotropy $J(1-\cos(q))$ up to corrections of order q^2.

We now bosonize the spin chain spins in the non-Abelian spin-current representation. The Hamiltonian (4.14) of spin chains under the rotation (4.28) has the same form but with updated constants: $u \to \cos(q)u$, and $g_{bs} \to \cos(q)g_{bs}$. We note that the backscattering coupling constant is negative, $g_{bs} < 0$. The effective (uniform) Dzyaloshinskii-Moriya interaction (after the rotation about the y-axis) in (4.29) takes the form[40]

$$H' = J\sin(q)\sum_i \left(S_i^y S_{i+1}^z - S_i^z S_{i+1}^y\right) = \tilde{d}\int dx(J_R^x - J_L^x), \tag{4.30}$$

where $\tilde{d} = J\sin(q)\frac{4}{\pi}$. The uniform magnetic field (after the rotation about the y-axis) in (4.29) becomes

$$H'' = J'h\cos(\chi)\sum_i S_i^z = \tilde{h}\int dx(J_R^z + J_L^z), \tag{4.31}$$

where $\tilde{h} = J'h\cos(\chi)$, and the staggered magnetic field takes the form

$$H_{st} = J'h\sin(\chi)\sum_i (-1)^i S_i^y = \gamma_n \int dx N^y, \tag{4.32}$$

where $\gamma_n = J'h\sin(\chi)$. The corresponding Hamiltonian for the even spin chains is obtained by simply putting $\chi \to -\chi$ in expressions (4.31) and (4.32) above.

We now perform a chiral rotation of the spin currents to absorb the Dzyaloshinskii-Moriya term (4.30) into the uniform magnetic field term, (4.31).

The right and left spin currents can be rotated independently while keeping the WZNW field theory invariant. We make the rotation $\mathbf{J}_R \to \hat{R}_R \mathbf{J}_R$ and $\mathbf{J}_L \to \hat{R}_L \mathbf{J}_L$ using

$$\hat{R}_{R/L} = \begin{pmatrix} \cos(\phi) & 0 & \mp\sin(\phi) \\ 0 & 1 & 0 \\ \pm\sin(\phi) & 0 & \cos(\phi) \end{pmatrix}, \tag{4.33}$$

where $\phi = \arctan(\tilde{d}/\tilde{h})$. Under this transformation the uniform Dzyaloshinksii-Moriya interaction and uniform magnetic field combine to take the form

$$H' + H'' = \sqrt{\tilde{h}^2 + \tilde{d}^2} \int dx (J_R^z + J_L^z), \tag{4.34}$$

and let us define $h^z = \sqrt{\tilde{h}^2 + \tilde{d}^2}$. The backscattering term transforms as

$$\begin{aligned} H_{bs} = g_{bs} \int dx \, \big(& \tfrac{1}{4}(\cos(2\phi) - 1)(J_R^+ J_L^+ + J_R^- J_L^-) \\ & + \tfrac{1}{4}(\cos(2\phi) + 1)(J_R^- J_L^+ + J_R^+ J_L^-) \\ & + \tfrac{1}{2}(J_R^z J_L^+ + J_R^z J_L^- - J_R^+ J_L^z - J_R^- J_L^z) \\ & + \cos(2\phi) J_R^z J_L^z \big), \end{aligned} \tag{4.35}$$

where $J^{\pm} = J^x \pm i J^y$, and we define

$$g_1 = \frac{1}{2}(\cos(2\phi) - 1) g_{bs}, \tag{4.36}$$

$$g_2 = \cos(2\phi) g_{bs}, \tag{4.37}$$

whose flow under the renormalization group will turn out to be important in the eventual analysis of the low-temperature phase of the spin chains. The

fields with scaling dimension 1/2 transform as[126]

$$\begin{aligned} N^{x(z)} &\rightarrow N^{x(z)}, && (4.38)\\ N^{y} &\rightarrow \cos(\phi)N^{y} + \sin(\phi)\epsilon, && (4.39)\\ \epsilon &\rightarrow \cos(\phi)\epsilon - \sin(\phi)N^{y}, && (4.40) \end{aligned}$$

so that the staggered magnetic field becomes

$$H_{st} = \gamma_n \int dx \left(\cos(\phi)N^{y} + \sin(\phi)\epsilon\right). \tag{4.41}$$

The inter-chain interactions transform as

$$\begin{aligned} H_N + H_\epsilon = \int dx \ \big(&\gamma_{N1} N^z_y N^z_{y+1} + \gamma_{N2} N^x_y N^x_{y+1}\\ &+(\gamma_{N2}\cos^2(\phi) + \gamma_\epsilon \sin^2(\phi)) N^y_y N^y_{y+1}\\ &+(\gamma_{N2}\sin^2(\phi) + \gamma_\epsilon \cos^2(\phi))\epsilon_y \epsilon_{y+1}\\ &+\cos(\phi)\sin(\phi)(\gamma_{N2} - \gamma_\epsilon)(N^y_y \epsilon_{y+1} + \epsilon_y N^y_{y+1})\big). \end{aligned} \tag{4.42}$$

The total Hamiltonian, which is a subject for the further analysis, is a sum (4.34), (4.35), (4.41), (4.42), together with the free part expressed through spin-currents (4.14). We now absorb the effective magnetic field (4.34) into the spin-currents by a shift of the bosonic field[126] $\varphi_s \rightarrow \varphi_s + \frac{x h^z}{\sqrt{2\pi}u}$. The spin currents are then transformed as

$$\begin{aligned} J^{\pm}_R &= J^{\pm}_R e^{\mp i x h^z/u},\\ J^{\pm}_L &= J^{\pm}_L e^{\pm i x h^z/u},\\ J^{z}_{R/L} &= J^{z}_{R/L} + \frac{h^z}{4\pi u}. \end{aligned} \tag{4.43}$$

The fields with scaling dimension 1/2 transform as[126]

$$N^z = \cos\left(xh^z/u\right) N^z - \sin\left(xh^z/u\right) \epsilon,$$
$$\epsilon = \cos\left(xh^z/u\right) \epsilon + \sin\left(xh^z/u\right) N^z, \tag{4.44}$$

and $N^{x,y}$ remain unchanged. This shift renders the first and third terms in (4.35) oscillatory on scales $x > u/h^z$ so that they will not contribute to the long distance, low-energy flows of the coupling constants.

4.5.1 Analysis of the low-energy physics of the spin chains

We will now use perturbation theory to study the coupling of the spin chains to the middle spins. We first note that there are two scales in the problem. At small length scales $\ell < \ell^*$, where $\ell^* \sim ln(J/J')$ which is obtained as $a_0 e^{\ell^*} h^z/u \sim 1$, oscillating factors do not play a role. One may assume that $h^z = 0$ in the relations given immediately above. The coupling constants under renormalization in this case are given by

$$\frac{dg_{bs}}{d\ell} = \frac{g_{bs}^2}{2\pi u}, \quad \frac{d\gamma_n}{d\ell} = \left(\frac{3}{2} - \frac{g_{bs}}{4\pi u}\right)\gamma_n,$$
$$\frac{d\gamma_{N1(2)}}{d\ell} = \left(1 - \frac{g_{bs}}{4\pi u}\right)\gamma_{N1(2)},$$
$$\frac{d\gamma_\epsilon}{d\ell} = (1 + \frac{3g_{bs}}{4\pi u})\gamma_\epsilon, \tag{4.45}$$

and should be stopped at $\ell \sim \ell^*$. Solving for the backscattering we get

$$g_{bs}(l) = \frac{g_{bs}^0}{1 - \frac{\ell g_{bs}^0}{2\pi u}}, \tag{4.46}$$

which is a decreasing function of ℓ since $g^0_{bs} < 0$.[126] The solutions for the coupling constants at $l \sim l^*$ are

$$\begin{aligned}
\gamma_{N1(2)} &= \gamma^0_{N1(2)} e^{\ell^*} \left(1 - \tfrac{\ell^* g^0_{bs}}{2\pi u}\right)^{1/2}, \\
\gamma_\epsilon &= \gamma^0_\epsilon e^{\ell^*} \left(1 - \tfrac{\ell^* g^0_{bs}}{2\pi u}\right)^{-3/2}, \\
\gamma_n &= \gamma^0_n e^{3\ell^*/2} \left(1 - \tfrac{\ell^* g^0_{bs}}{2\pi u}\right)^{1/2}.
\end{aligned} \tag{4.47}$$

The coupling constant γ_n has the largest scaling dimension 3/2 [from (4.32)]. We thus expect that it will grow at long length scales and compete with the inter-chain coupling constants, $\gamma_{N1(2)}$ (which have scaling dimension 1), and result in a phase transition.

To study the phase transition as a function of the Dzyaloshinskii-Moriya coupling we analyze renormalization group flows at large scales. At large scales $\ell > \ell^*$ rapid oscillations of various terms in the Hamiltonian [the first and third terms in (4.35)] causes them to average to zero and we neglect them. The inter-chain interaction (4.42) after the rotation (4.44) becomes

$$\begin{aligned}
H_N + H_\epsilon = \int dx \ \big(&\gamma_x N^x_y N^x_{y+1} + \gamma_y N^y_y N^y_{y+1} \\
&+ \gamma_+ (\epsilon_y \epsilon_{y+1} + N^z_y N^z_{y+1})\big),
\end{aligned} \tag{4.48}$$

where we have defined the coupling constants as $\gamma_x = \gamma_{N2}$, $\gamma_y = \gamma_{N2}\cos^2(\phi) + \gamma_\epsilon \sin^2(\phi)$, $\gamma_+ = \frac{1}{2}(\gamma_{N2}\sin^2(\phi) + \gamma_\epsilon \cos^2(\phi) + \gamma_{N1})$. We only keep g_1 and g_2 terms in the backscattering (4.35), and only the first term, with N^y, in staggered magnetic field (4.41) and label its coupling constant $\tilde{\gamma}_n = \cos(\phi)\gamma_n$. The remaining terms are oscillatory and therefore ignored for this long-distance

analysis. The resulting renormalization group equations describing the coupling constants of the non-oscillatory terms are

$$\frac{dg_1}{d\ell} = -\frac{g_1 g_2}{2\pi u}, \quad \frac{dg_2}{d\ell} = -\frac{g_1^2}{2\pi u}, \tag{4.49}$$
$$\frac{d\gamma_x}{d\ell} = \left(1 + \frac{g_1}{2\pi u} - \frac{g_2}{4\pi u}\right)\gamma_x, \quad \frac{d\gamma_y}{d\ell} = \left(1 - \frac{g_1}{2\pi u} - \frac{g_2}{4\pi u}\right)\gamma_y,$$
$$\frac{d\gamma_+}{d\ell} = \left(1 + \frac{g_2}{4\pi u}\right)\gamma_+, \quad \frac{d\tilde{\gamma}_n}{d\ell} = \left(\frac{3}{2} - \frac{g_1}{2\pi u} - \frac{g_2}{4\pi u}\right)\tilde{\gamma}_n.$$

The analysis[126] of these equations show that there are two competing operators: γ_x and $\tilde{\gamma}_n$. The latter is due to the Dzyaloshinkii-Moriya interaction (recall $\tilde{\gamma}_n = \cos(\phi)\gamma_n = \cos(\phi)J'2s_0\cos(q/2)\sin(\chi)$ and $\gamma_x = \gamma_{N2} \sim (J')^4/J^3$ are the bare couplings before the short-scale renormalization).

From the short-scale renormalization, new "bare" couplings emerge from which the long-scale renormalization flows begin. These are determined from (4.47). We give a rough estimate of the value of Dzyaloshinskii-Moriya interaction constant at which the phase transition between γ_x and $\tilde{\gamma}_n$ dominated states occurs. Comparing lengths at which $\tilde{\gamma}_n e^{3\ell/2} \sim 1$ where $\tilde{\gamma}_n \sim \sin(\chi)\left(\frac{J}{J'}\right)^{1/2}$ from (4.47), and $\gamma_x e^{\ell} \sim 1$ where $\gamma_x \sim \left(\frac{J'}{J}\right)^3$ we get the critical value of the angle θ which defines the critical strength of Dzyaloshinkii-Moriya interaction in our model:

$$\sin(\chi_c) = \left(\frac{J'}{J}\right)^{5/2}, \tag{4.50}$$

where for simplicity one may assume that $\theta \sim \theta'$ since they are parametrically of similar order of magnitude, giving $\chi_c \approx 3\theta_c$. The condition (4.50) is one of the central results of this work. For $\theta < \theta_c$ coupling constant γ_x dominates, while for $\theta > \theta_c$ staggered magnetic field $\tilde{\gamma}_n$ dominates.

A rough numerical estimate of θ_c can be made since $\sin(2\theta) \approx D/J$ [from (4.7)], which gives $\sin(3\theta_c) \approx 3D/(2J) \approx (J'/J)^{5/2}$. For $D/J \approx 0.2$ (possible in the class of materials described in the introduction), one finds the critical point would be reached for lattice sufficiently anisotropic that $J'/J < 0.7$. It is possible that the application of pressure could further distort an anisotropic lattice to reach these values and possibly drive a phase transition.

4.5.2 Resulting order of the spin chains at low temperatures

For $\theta > \theta_c$, one finds from (4.41), $\langle N_y^y \rangle = \cos(\phi)(-1)^y M_1$, where $M_1 \sim \frac{J'}{J}\sin(3\theta)$. Tracing back all the transformations performed (4.43), (4.33), (4.28), and (4.10), we obtain the final order of the spin chains,

$$\begin{aligned}
\langle S^x_{x,y} \rangle &= -\frac{h^z}{2\pi u}\cos(\phi)\cos(qx - (-1)^{x+y}\theta) \\
&\quad -(-1)^{x+y} M_1 \cos(\phi)\sin(qx - (-1)^{x+y}\theta), \\
\langle S^y_{x,y} \rangle &= -\frac{h^z}{2\pi u}\cos(\phi)\sin(qx - (-1)^{x+y}\theta) \\
&\quad +(-1)^{x+y} M_1 \cos(\phi)\cos(qx - (-1)^{x+y}\theta), \\
\langle S^z_{x,y} \rangle &= 0, \\
\langle \epsilon_y \rangle &= -\sin(\phi)(-1)^y M_1. \qquad (4.51)
\end{aligned}$$

This spin-orbit coupling dominated phase is characterized by a non-zero value of dimerization operator and staggered magnetization (Neel order) in the plane of the spiral (as opposed to Neel order in the plane perpendicular to the plane of the spiral as occurs for $\theta < \theta_c$–see below). The presence of a non-vanishing dimer correlation in (4.51) implies spin-Peierls-like physics occurs simultane-

ously with Neel order. This Neel + dimer phase is a consequence of the completely broken spin rotational symmetry realized by a uniform Dzyaloshinkii-Moriya interaction, and uniform plus staggered magnetic fields. Schematically, obtained phase (4.51) is depicted in the Fig. 4.1. The same phase, namely Neel + dimer, was obtained in double-frequency sine-Gordon model,[32] and in the work by Garate and Affleck on spin chains with uniform Dzyaloshinkii-Moriya interaction, uniform Zeeman magnetic field and exchange anisotropy,[41] both strictly one-dimensional systems. Perhaps, a latter's work Hamiltonian can be mapped via a gauge transformation on to the one discussed, expression (4.29), in the present chapter.

On the other hand, when coupling constant γ_x dominates for $\theta < \theta_c$, we find that the order is given by

$$\begin{aligned} \langle S^x_{x,y} \rangle &= -\frac{h^z}{2\pi u} \cos(\phi) \cos(qx + (-1)^{x+y}\theta), \\ \langle S^y_{x,y} \rangle &= -\frac{h^z}{2\pi u} \cos(\phi) \sin(qx + (-1)^{x+y}\theta), \\ \langle S^z_{x,y} \rangle &= -(-1)^{x+y} M_2, \end{aligned} \tag{4.52}$$

where $M_2 \sim \left(\frac{J'}{J}\right)^2$. In addition to the predominant spiral order in the xy-plane, this phase is characterized by a Neel order along the z-direction with moment M_2. The result (4.52) is consistent with the prediction of work [126], which does not include the Dzyaloshinskii-Moriya interaction (vanishes in the limit $\theta \to 0$). These results are summarized in Fig.4.2. The main role of the Dzyaloshinskii-Moriya interaction in the Neel phase is to choose the direction of Neel order parameter. However, it also enters the spiral configuration (4.52)

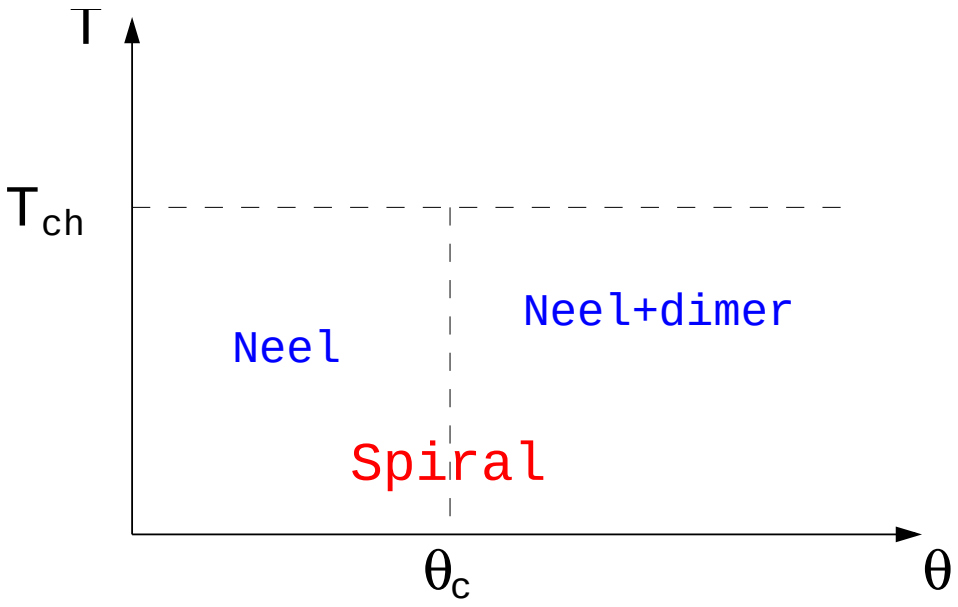

Figure 4.2: Schematic phase diagram below the spin-chain ordering temperature, T_{ch}, as a function of the Dzyaloshinskii-Moriya interaction parameterized by the angle θ, as given in (4.6) with $\chi_c = 3\theta_c$. "Spiral" refers to the order of the middle spins which is established at a temperature scale of $T_m \sim (J')^2/J \gg T_{ch}$, while "Neel" and "Neel+dimer" refers to the dominant order (on top of the spiral) along the spin chains below a temperature $T_{ch} \sim (J')^4/J^3$. The "Neel" phase is described by (4.52), while the "Neel + dimer" phase is described by (4.51).

of spin chains via the argument of the *sin* and *cos*.

4.6 Conclusions

In summary, we have studied the spatially anisotropic spin-1/2 kagome antiferromagnet with a staggered Dzyaloshinskii-Moriya (DM) interaction as shown in Fig.4.1. As a function of increasing DM interaction, there is a phase transition from a spiral phase in the plane of the kagome lattice with an out-of-

plane Neel order to a phase with with spiral order and an in-plane Neel order coexisting with dimer order. Our results are summarized in Fig. 4.2. A rough numerical estimate the the DM interaction need to enter the "Neel+dimer" phase suggest that it may be in an experimentally accessible range ($J'/J \approx 0.7$), and could possibly be tuned through the application of pressure to a spatially anisotropic system. We hope this work will help inspire further experimental studies of spatially anisotropic kagome lattices.

It might also be interesting to realize a phase where both Neel and spin-Peierls orders coexist for an anisotropic two-dimensional lattice. It would seem that necessary conditions for such phase is a fully broken $SU(2)$ spin rotational symmetry (possibly obtained by the application of an external magnetic field) as well as spin anisotropy-inducing terms such as DM interaction. We leave that possibility as a topic for future study.

Chapter 5

Fractional Quantum Hall Effect from 2+1 Bosonization

5.1 Introduction

The fractional quantum Hall effect (FQHE) is the most striking effect in condensed matter physics. Since the discovery of FQHE [20, 138] there were a number of theories explaining the fractional states. Laughlin [81] constructed variational many-body wave-function and showed that it describes the ground state of interacting two-dimensional electron gas in a quantizing magnetic field. The ground state is an incompressible fermionic liquid with fractional excitations. The Chern-Simons effective field theory was then shown to describe the edges of the Hall system [45, 67]. Also, the conformal field theory approach was developed to describe many-body wave-function [97]. Hierarchy of fractional numbers that correspond to the Hall plateaux was developed in the series of works [48, 49, 64, 118]. In another work [70, 143], an attempt to understand the FQHE was made by using sliding Luttinger liquid. Present paper generalizes [70, 143] for the case of two-dimensional electron gas in quantizing magnetic field. A possible justification to use the bosonization approach to a problem

[4]This chapter is based on unpublished paper by V.A. Zyuzin, "Fractional quantum Hall effect from 2+1 bosonization", arXiv:1111.6931 (2011)

of FQHE is the existence of one-dimensional presentation of Laughlin wave function [24, 107].

5.2 A two-dimensional electron gas in a magnetic field

Let us study a two-dimensional electron gas in a perpendicular magnetic field and choose Landau gauge for vector potential, $A_x = -Hy,\ A_y = A_z = 0$, where H is a magnetic field. The Hamiltonian is [80]

$$H = \frac{1}{2m_e}\left(\hat{p}_x + \frac{eH}{c}y\right)^2 + \frac{\hat{p}_y^2}{2m_e}, \tag{5.1}$$

eigenfunctions corresponding to this Hamiltonian are Landau wave-functions:

$$\Psi_{n,y_0} = e^{ip_x x/\hbar}\chi_n(y - y_0), \tag{5.2}$$

where $\chi_n(y) = \frac{1}{\pi^{1/4}a_H^{1/2}\sqrt{2^n n!}}\exp\left(-\frac{y^2}{2a_H^2}\right)H_n\left(\frac{y}{a_H}\right)$. The eigenfunctions (5.2) correspond to the energy values $E_n = \hbar\omega_H(n + \frac{1}{2})$, where $a_H = \sqrt{\frac{\hbar}{m_e\omega_H}}$, $\omega_H = \frac{|e|H}{m_e c}$, $y_0 = \frac{cp_x}{|e|H}$ is a position, H_n are Hermite polynomials, m_e is an electron mass, e is charge, and c is a speed of light. The energy levels take discrete values and are degenerate [80]. Throughout the paper, we will be working with zeroth Landau level ($n = 0$), set $|e| = e$, and assume spinless electrons.

Let us assume that the positions y_j are discrete, and let us set the distance between two neighboring positions as d_y. Throughout the paper, we are going to label momenta as p_j and mean that they correspond to the positions $y_j = jd_y$, where j is an integer. Let us now dope the system with

electrons. Due to the presence of Coulomb interactions

$$H_C = \int d\mathbf{r} d\mathbf{r}' \; V(\mathbf{r} - \mathbf{r}')\rho(\mathbf{r})\rho(\mathbf{r}'), \tag{5.3}$$

where $\rho(\mathbf{r})$ is the electron density, the electron states can no longer be described by free wave-function given by (5.2). Instead of solving for the new eigenfunctions of interacting Hamiltonian (5.1) and (5.3), we are going to construct a trial wave-function based on the following two analogies.

It is known that the tunneling current between two perfect two-dimensional gases is non zero due to the Coulomb interactions [66, 168]. Coulomb interaction lifts the orthogonality between the electron states in two gases, allowing for them to mix. And we notice that in our problem, the non-interacting electron states with different momentum, which are defined by (5.2), are orthogonal to each other. Therefore, one should expect that, due to the Coulomb interaction, there will be a mixing of states with different momentum.

We then notice that a wave-function (5.2) with a given momentum p_j has a sharp peak at y_j . Therefore, an electron corresponding to this state can be seen as one-dimensional. That allows one to use phenomenological bosonization, motivated by the knowledge that the effect of electron interactions can be treated non-perturbatively within this approach [15, 43, 47]. Let us show that the bosonization in quantizing magnetic field is effectively two-dimensional.

5.3 Fermion operator within phenomenological bosonization

In the approach of phenomenological bosonization, the one-dimensional electron density is described by the harmonics of density fluctuations

$$\rho(x) = \left(\rho_0 - \frac{1}{\pi}\nabla\phi(x)\right) \sum_{n=-\infty}^{+\infty} e^{i2n(\pi\rho_0 x - \phi(x))}, \tag{5.4}$$

where $\phi(x)$ is a smooth function describing the deviation from the homogeneous density distribution given by ρ_0. Following the lines of [15, 43, 47], we can present a fermion operator as

$$\Psi^\dagger(x) = \left(\rho_0 - \frac{1}{\pi}\nabla\phi(x)\right)^{1/2} \sum_{n=-\infty}^{+\infty} e^{i(2n+1)(\pi\rho_0 x - \phi(x))} e^{-i\theta(x)}, \tag{5.5}$$

where $\theta(x)$ is a conjugate to $\phi(x)$ bosonic field. This fermion operator describes one-dimensional electrons without a magnetic field.

Let us now adopt phenomenological bosonization to construct a fermion operator for two-dimensional electrons in a quantizing magnetic field. We have to bosonize electrons with a fixed momentum $\exp(ip_j x/\hbar)$. Fixing the momentum dictates choosing a fermion operator as

$$\Psi^\dagger_{b,j} \propto e^{-ieHy_j x/c\hbar}. \tag{5.6}$$

The bosonized fermion operator should have a similar form to the expression (5.5). If we just multiply (5.5) with (5.6), the harmonics will shift the phase $(-ieHy_j/c\hbar)$ by a factor of $i(2n+1)\pi\rho_0$. Therefore, we write the bosonized

fermion operator as

$$\Psi^{\dagger}_{b,j}(x,y) = \eta_j e^{-ieHy_j x/c\hbar} \left(\rho_0 - \tfrac{1}{\pi}\nabla\phi_j(x)\right)^{1/2}$$
$$\times \sum_{n=-\infty}^{+\infty} \chi_0(y - \tilde{y}_{j,n}) e^{i(2n+1)(\pi\rho_0 x - \phi_j(x))} e^{-i\theta_j(x)}, \tag{5.7}$$

where η_j is a Klein factor which assures the fermionic anti-commutation relationship between the states with different momentum, we define them as $\{\eta_j, \eta_{j'}\} = 2\delta_{jj'}$, and $\eta_j\eta_{j'} = i$. The

$$\tilde{y}_{j,n} = y_j - (2n+1)\nu d_y/2 \tag{5.8}$$

is a position (guiding center) of electron state which contributes the $(2n+1)$ harmonic (composite fermion) to the fermion operator with a fixed momentum p_j (see Fig. 5.1). Here $\nu = \frac{\rho_{2d}hc}{eH}$ is a filling factor of a two-dimensional electron gas in a magnetic field, where $h = 2\pi\hbar$, ρ_0 is an effective one-dimensional electron density and $\rho_{2d} = \rho_0/d_y$ is a two-dimensional electron density.

Being borrowed from one-dimensional electron picture, this fermion operator describes electron density fluctuations of a state with a fixed momentum at different y coordinates. This makes the (5.7) effectively two-dimensional. The dynamics of the mixing of states with different momentum will be described by the Hamiltonian of density fluctuations, which we are going to construct next.

5.4 Hamiltonian of density fluctuations

Let us first build a Hamiltonian describing fluctuations of the electron density of a state with a fixed momentum p_j. The diagonal matrix element of

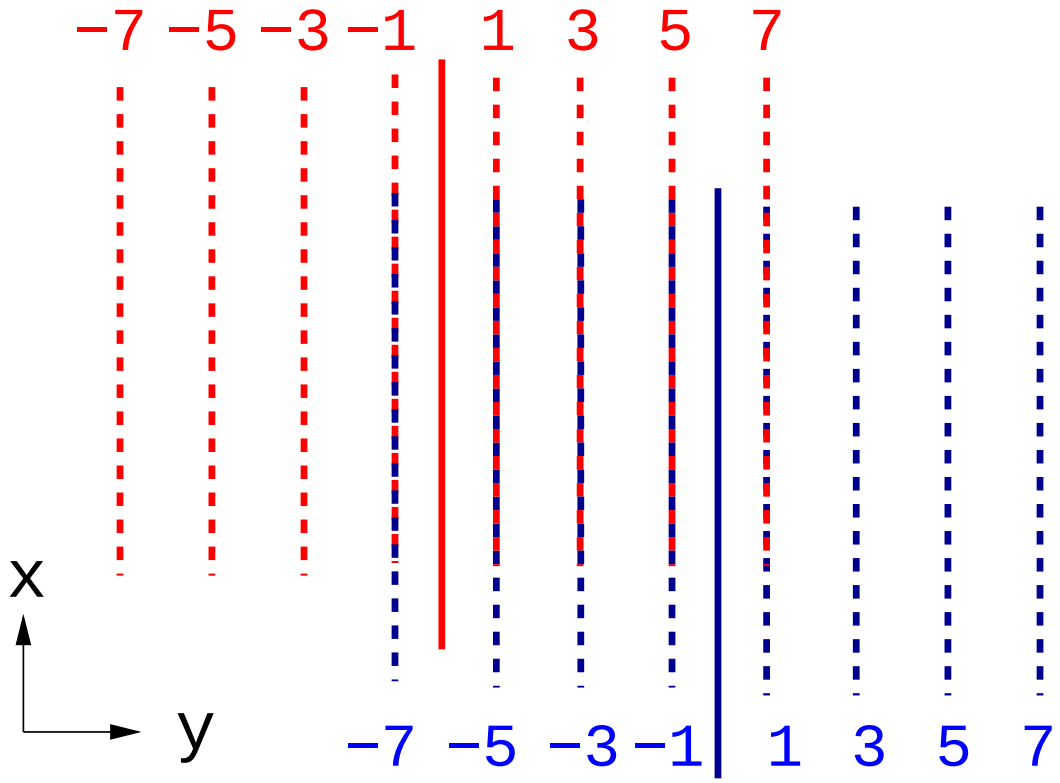

Figure 5.1: Solid lines represent positions of two Landau wave-function (5.2) with two different momentum, red corresponds p_j, while blue - to p_{j+1}. Dashed lines represent positions of harmonics corresponding to the $(2n+1)$- harmonic of the density fluctuations of the two bosonized fermion operator (5.7). Again, red dashed line corresponds to the momentum p_j, while blue to p_{j+1}. Any bosonized fermion operator covers the entire plane with its harmonics. This figure describes $\nu = 1/3$ filling factor, and the Laughlin state is shown: match of the (3,-3) harmonics.

Hamiltonian (5.1) on the fermion operator (5.7) with a given momentum p_j, taken with $(n = 0, \ -1)$, is

$$H_j^{kin} = \frac{\hbar^2 \rho_0}{m_e} \int dx \ \left[(\nabla \phi_j(x))^2 + (\nabla \theta_j(x))^2 \right]. \tag{5.9}$$

Another part of the Hamiltonian is due to the Coulomb interaction (5.3) between electrons with momentum p_j. Forward scattering between electrons is obtained if one plugs (5.7) with $n = 0$ into the expression of Coulomb interaction (5.3)

$$H_j^{fs} = \frac{g_1}{2\pi} \int dx \ (\nabla \phi_j(x))^2, \tag{5.10}$$

where $g_1 \cong 2e^2/\pi\epsilon_0$ and ϵ_0 is the dielectric constant. The total Hamiltonian of electron density fluctuations then takes a form

$$H_j = \frac{1}{2\pi} \int dx \ \left[v(\nabla \theta_j(x))^2 + (v + g_1)(\nabla \phi_j(x))^2 \right], \tag{5.11}$$

here $v = 2\pi\hbar^2\rho_0/m_e$. Now let us include the Coulomb interaction between electron states with different momentum. The forward-scattering reads

$$H_{j,m}^{fs} = \frac{g_2}{2\pi} \int dx \ (\nabla \phi_j(x))(\nabla \phi_{j+m}(x)), \tag{5.12}$$

where m is a non-zero integer denoting the number of a neighbor. Backscattering between the states with different momentum gives

$$H_{j,m}^{bs} = 2g_3\rho_0^2 \int dx \ \cos\left(2\phi_j(x) - 2\phi_{j+m}(x)\right). \tag{5.13}$$

Here the interaction constants are $g_{3,4} \cong 2e^2/\pi\epsilon_0$. To complete the description of the Hamiltonian of density fluctuations, we need to include non-diagonal matrix elements of the Hamiltonian (5.1).

5.5 Derivation of fractional states

The non-diagonal matrix elements are obtained by acting with $\frac{\hat{p}_y^2}{2m_e}$ of the Hamiltonian (5.1) on the (5.7) of a momentum p_{j+m}, and taking the overlap with the neighboring p_j momentum

$$\frac{-\hbar^2}{2m_e}\int dxdy\ \Psi^{\dagger}_{b,j}(x,y)\partial_y^2\Psi_{b,j+m}(x,y). \tag{5.14}$$

Let us show how fractional charges appear at $\nu = 1/3$ filling. In this case, we need to set $m = 1$ and pick the harmonics of (5.7) in the expression above as $(3,\ -3)$ (see Fig. 5.1 for explanation of the latter notation)

$$\begin{aligned} t_1\rho_0 \int dx\ (\Psi^{(n=1)}_{b,j})^{\dagger}\Psi^{(n=-2)}_{b,j+1} + h.c. = t_1\rho_0\eta_j\eta_{j+1} \\ \times \int dx\ e^{-i(6\pi\rho_0 - \frac{eH}{c\hbar}d_y)x}e^{-i3(\phi_j+\phi_{j+1})}e^{i(\theta_{j+1}-\theta_j)} + h.c. \end{aligned} \tag{5.15}$$

The constant t_1 is defined as $t_1 = \frac{-\hbar^2}{2m_e}\int dy\ \chi_0(y-\tilde{y}_{j,1})\partial_y^2\chi_0(y-\tilde{y}_{j+1,-2})$. Another, equal, contribution to this matrix element will come from the $\propto (y-\tilde{y}_{j,1})^2$ term of the Hamiltonian (5.1), and we are going to double the t_1 due to that. For this term to be relevant, the oscillating part $\exp\left[-i\left(6\pi\rho_0 - \frac{eH}{c\hbar}d_y\right)x\right]$ has to be zero. This sets a condition on the filling factor

$$\nu = \frac{\rho_{2d}hc}{eH} = \frac{1}{3}. \tag{5.16}$$

Notice that the $\nu = 1/3$ makes the $y-$coordinates of selected in (5.15) harmonics, $(3,\ -3)$, to match (see Fig. 5.1). The estimate of the overlap is $t_1 = \hbar\omega_H/2$. Let us rewrite the expression (5.15) in the form

$$H_{j,L} = \hbar\omega_H\rho_0\int dx\ \cos(3(\phi_j+\phi_{j+1}))\sin(\theta_j-\theta_{j-1}). \tag{5.17}$$

One can show that all matchings of harmonics to the left, such as $(-1,\ -7)$ and $(1,\ -5)$ on Fig. 5.1, vanish because the oscillating part in the overlap between them can not be put to zero. However, the matchings of the harmonics to the right, such as $(5,\ -1)$ and $(7,\ 1)$, do not have an oscillating part. We are going to argue that they vanish due to the effect of interactions. This reason will be clear from the following analysis. Let us study the following Hamiltonian, which is a sum of (5.11), (5.12), (5.13) and (5.17) taken with $m = 1$

$$\mathcal{H} = \sum_j \left[H_j + H^{fs}_{j,1} + H^{bs}_{j,1} + H_{j,L} \right]. \tag{5.18}$$

It can be shown that the Hamiltonian (5.18) decomposes into a sum of coupled symmetric and anti-symmetric sectors of neighboring momentum, with corresponding bosonic fields $\phi_{j+1/2,\pm} = (\phi_j \pm \phi_{j+1})/\sqrt{2}$ and $\theta_{j+1/2,\pm} = (\theta_j \pm \theta_{j+1})/\sqrt{2}$. We can then describe the whole system by focusing on just one pair of neighboring momentum (below we omit $j + 1/2$ index for simplicity)

$$\begin{aligned} H_{pair} &= H_+ + H_- + H_L, \\ H_+ &= \tfrac{1}{2\pi} \textstyle\int dx\ \left[u_+ K_+ (\nabla\theta_+)^2 + \tfrac{u_+}{K_+} (\nabla\phi_+)^2 \right], \\ H_- &= \tfrac{1}{2\pi} \textstyle\int dx\ \left[u_- K_- (\nabla\theta_-)^2 + \tfrac{u_-}{K_-} (\nabla\phi_-)^2 \right] \\ &\quad + \tfrac{2\rho_0^2}{(2\pi)^2} g_3 \textstyle\int dx\ \cos(\sqrt{8}\phi_-), \\ H_L &= \tfrac{2\rho_0^2}{(2\pi)^2} g_L \textstyle\int dx\ \cos(3\sqrt{2}\phi_+) \sin(\sqrt{2}\theta_-), \end{aligned} \tag{5.19}$$

where $K_\pm = \sqrt{v/(v + g_1 \pm g_2)}$ are Luttinger liquid interaction parameters, $u_\pm = \sqrt{v(v + g_1 \pm g_2)}/2$ are renormalized velocities, and we have defined $g_L = \hbar\omega_H \frac{(2\pi)^2}{2\rho_0}$. The scaling dimension of the g_3 operator is $(2 - 2K_-)$, and it

corresponds to an anti-symmetric charge density wave. The scaling dimension of the g_L is $(2 - 1/(2K_-) - 9K_+/2)$. The renormalization equations defining the fate of the two operators are (see for example [43])

$$\frac{dg_L}{d\ell} = \left(2 - \frac{1}{2K_-} - \frac{9K_+}{2}\right) g_L, \quad \frac{dg_3}{d\ell} = (2 - 2K_-)\, g_3$$
$$\frac{dK_+}{d\ell} = -\frac{K_+^2 g_L^2}{2}, \quad \frac{dK_-}{d\ell} = -\frac{K_-^2 g_3^2}{2} + \frac{g_L^2}{2}. \tag{5.20}$$

Let us notice that $v\rho_0 = \nu\hbar\omega_H$ depends linearly on the magnetic field, while $g_i\rho_0 \propto \frac{e^2}{\epsilon_0}\rho_0 = \sqrt{\frac{\nu}{2\pi}}\frac{e^2}{\epsilon_0 a_H}$ scales as a square-root of the magnetic field. In the limit of large cyclotron energy, the g_L term is always relevant. The energy of the kink excitation [17] is

$$\Delta_{1/3} = \frac{1}{48\sqrt{3\pi}}\hbar\omega_H, \tag{5.21}$$

which might be what is seen in the recent experiments [42, 75].

In the case of, for example, $(5, -1)$ harmonic matchings, the corresponding term is $\propto \sin(3(\phi_j + \phi_{j+1}) + 2(\phi_j - \phi_{j+1}) + (\theta_j - \theta_{j-1}))$. In terms of definitions of expression (5.19) and (5.20), its scaling dimension is $(2 - 1/(2K_-) - 9K_+/2 - 2K_-)$. This term is always irrelevant because of K_-, or, in other words, both ϕ_- and θ_- fields can not order simultaneously. From the analysis above we can conclude that the only relevant operators derived from (5.14) are those *with a match of the opposite in sign and equal in magnitude harmonics* (for example $(3, -3)$ in the Fig. 5.1).

When the g_L dominates, all neighboring momentum states strongly couple via $(3, -3)$. In this case, ϕ_+ field is three fold degenerate. The kink

connecting two ground states carries a charge of $e/3$ [127]. There are only two remaining decoupled harmonics which are located at the edges [70, 143]. If the kink is excited, it will set a condition on the bosonic fields on the right and left edges $\phi_R - \phi_L = \pi/3$. Therefore, the edges carry a fractional charge of $e/3$. This is a $\nu = 1/3$ Laughlin state [81]. The same scenario was proposed in [70, 143] within the sliding Luttinger liquid formalism.

For the case of $\nu = 2/3$ filling factor, one has to consider the same harmonics as in (5.15), but with $m = 2$. And the same analysis of relevancy of operators applies. There will be two states on every edge each carrying a charge of $e/3$ so that the overall charge on the edge is $2e/3$. When the filling factor is $\nu = 1/2$, the expression for non-diagonal matrix element (5.15) has to be taken as $\int dx\ (\Psi_{b,j}^{(n=1)})^\dagger \Psi_{b,j+1}^{(n=-1)}$. It is a coupling of $(3,\ -1)$ harmonics. And from the discussions above, the interactions smear out this fractional state. The symmetric sector, $(+)$ in the definitions of the expression (5.19), is gapless, corresponding to a Fermi liquid. This is consistent with previous theories (for example [50]). From the above discussions we can conclude that the allowed fractional states are

$$\nu = \frac{m}{2n+1}, \tag{5.22}$$

where m and n are integers, which is consistent with [48, 49, 64, 118].

5.6 Conclusions

To conclude, this paper proposes an approach to understand the fractional quantum Hall effect. The approach is based on the phenomenological bosonization generalized for the case of two-dimensional electron gas in a strong quantizing magnetic field. The constructed bosonized fermion operator (5.7) of a electron state with a given Landau gauge momentum is represented by its harmonics of the density fluctuation, and it covers the entire $x-y$ plane. This fermion operator was used to understand the problem of the fractional quantum Hall effect. It was shown that the $\nu = 1/3$ Laughlin state is a mixing of high harmonics of the two wave-functions (5.7) with different momentum. A small value of interaction stabilizes the Laughlin state, resulting in the gapped bulk. When the kink is excited, the edge states are gapless carrying a fractional charge of $e/3$. Based on the calculations, a hierarchy of fractional states is established, (5.22), this result is consistent with [48, 49, 64, 118].

Chapter 6

Conclusions

The original work presented in this dissertation extended the one-dimensional bosonization approach to describe properties and phase diagrams of strongly interacting electron systems in higher dimensions. The dimension of the studied systems increased as the chapters progressed.

First, we studied correlations between two one-dimensional edges of the quantum spin-Hall states. We predicted a signature of the edge states that can be revealed in the Coulomb drag experiment. Namely, application of the magnetic field opens up the backscattering events in the system. And it is known that the Coulomb drag between one-dimensional electron systems is mainly governed by the backscattering processes. We predicted that the Coulomb drag resistivity between helical edge states scales as a fourth power of the applied magnetic field.

In the second part we studied a magnetic phase diagram of spatially anisotropic spin-1/2 kagome lattice antiferromagnet with Dzyaloshinskii-Moriya interaction. The dimension of such a system is quasi one-dimensional, meaning that the exchange interaction between spins makes it possible to decompose the kagome lattice in to an array of spin chains coupled weakly with

each other through the middle spins. The low-energy description of every spin chain is a Tomonaga-Luttinger liquid and all the rest of exchange interactions are then treated perturbatively. From the analysis, we predicted a Dzyaloshinskii-Moriya interaction driven phase transition in the magnetic order of the system. Namely, a transition from a phase characterized by a Neel component to a phase with both Neel and dimer states coexisting as the strength of the Dzyaloshinskii-Moriya interaction increases.

In the third work we presented a study of a two-dimensional electron system in a strong perpendicular magnetic field. Based on the one-dimensional phenomenological bosonization we presented a novel approach to understand the fractional quantum Hall effect. Signatures of the composite fermions such as the guiding centers and the composite charge are naturally present in the presented bosonized theory. The hierarchy of the fractional states predicted in this chapter is consistent with previous theories. An advantage of the presented approach is in its ability to study the effect of electron interaction in the physics of the integer and fractional quantum Hall states. This question is a subject for future research.

Appendices

Appendix

.1 Non-Abelian bosonization and Fusion rules

The operators used in the chapter are defined by

$$\begin{aligned}
\mathbf{J}_R &= \tfrac{1}{2} R^\dagger_\alpha \boldsymbol{\sigma}_{\alpha,\beta} R_\beta, \\
\mathbf{J}_L &= \tfrac{1}{2} L^\dagger_\alpha \boldsymbol{\sigma}_{\alpha,\beta} L_\beta, \\
\mathbf{M} &= \mathbf{J}_R + \mathbf{J}_L, \\
\mathbf{N} &= \tfrac{1}{2} R^\dagger_\alpha \boldsymbol{\sigma}_{\alpha,\beta} L_\beta + h.c., \\
\epsilon &= \tfrac{i}{2}(R^\dagger_\alpha L_\alpha - h.c.),
\end{aligned} \tag{1}$$

where R and L denote fields of right- and left-moving fermions in one dimension. See the book [46] for their definition in terms of bosonic fields. All of the operators defined above are functions of position and time (x, τ), which we have not explicitly indicated. Correlation functions of these fields are given by the following expressions

$$\begin{aligned}
F_R &= -\langle T R_\alpha(x,\tau) R^\dagger_\alpha(0,0)\rangle = -\tfrac{1}{2\pi u(\tau - ix/u + \alpha\sigma_\tau)} \\
F_L &= -\langle T L_\alpha(x,\tau) L^\dagger_\alpha(0,0)\rangle = -\tfrac{1}{2\pi u(\tau + ix/u + \alpha\sigma_\tau)}
\end{aligned}$$

where $\alpha = a_0/u$ is short time cut-off, a_0 is a short distance cut-off (distance between neighboring spins on a lattice), $\sigma_\tau = \mathrm{sgn}(\tau)$, and $u = \pi J a_0/2$. Below we set $y = (x, \tau)$ for further convenience. The operators obey the fusion rules

$$\begin{aligned}
J^a_{R/L}(y_1) J^b_{R/L}(y_2) &= -F_{R/L}(y) i\epsilon^{abc} J^c_{R/L}(Y) + \tfrac{1}{2}\delta^{ab} F^2_{R/L}(y), \\
J^a_{R/L}(y_1) N^b(y_2) &= -\tfrac{i}{2} F_{R/L}(y)[\epsilon^{abc} N^c(Y) \mp \delta^{ab}\epsilon(Y)], \\
J^a_{R/L}(y_1)\epsilon(y_2) &= \mp\tfrac{i}{2} F_{R/L}(y) N^a(Y),
\end{aligned} \tag{2}$$

from which the one-loop renormalization group flows are obtained. Above, $y = y_1 - y_2$ and $Y = (y_1 + y_2)/2$.

.2 Derivation of renormalization group equations

Here we are going to show one example of a derivation of the renormalization group equations of a relevant inter-chain interaction. One has to plug in (4.19) in to (4.20). For our example we pick the next term

$$2\frac{1}{2}\gamma_{M1}\gamma_{\partial N1}\int dx_1 dx_2 d\tau_1 d\tau_2 \; M^z_y(y_1)M^z_{y+1}(y_1)\partial_{x_2}N^z_y(y_2)\partial_{x_2}N^z_{y+1}(y_2), \qquad (3)$$

where, as in the previous appendix, the coordinates $y_{1(2)}$ stand for $y_{1,2} = (x_1, \tau_1)$. Using the fusion rules of current operators one gets

$$\begin{aligned} M^z_y(y_1)\partial_{x_2}N^z_y(y_2) &= \tfrac{i}{2}\epsilon(X,t)\partial_{x_2}\left(F_R(y_1-y_2) - F_L(y_1-y_2)\right) \\ &= \tfrac{1}{4\pi}\epsilon(X,t)\left(\tfrac{1}{(x+iu\tau)^2} + \tfrac{1}{(x-iu\tau)^2}\right). \end{aligned} \qquad (4)$$

Resulting integral is then

$$\begin{aligned} &\gamma_{M1}\gamma_{\partial N1}\tfrac{1}{(4\pi)^2}\int dX dt \; \epsilon_y(X,t)\epsilon_{y+1}(X,t)\int_{-\infty}^{\infty} dx \int d\tau \; \left(\tfrac{1}{(x+iu\tau)^2} + \tfrac{1}{(x-iu\tau)^2}\right)^2 \\ &\qquad = \gamma_{M1}\gamma_{\partial N1}\tfrac{d\ell}{8\pi u^3\alpha^2}\int dX dt \; \epsilon_y(X,t)\epsilon_{y+1}(X,t), \end{aligned} \qquad (5)$$

here $X = (x_1 + x_2)/2$, $x = x_1 - x_2$, $t = (\tau_1 + \tau_2)/2$, and $\tau = \tau_1 - \tau_2$. Integration over τ is $\alpha < |\tau| < b\alpha$. One has this term in the renormalization group equation for γ_ϵ in the third line of (4.21).

Bibliography

[1] A.A. Abrikosov, L.P. Gorkov, and I.E. Dzyaloshinski. *Methods of Quantum Field Theory in Statistical Physics*. Dover Publications, 1963.

[2] Ian Affleck and Masaki Oshikawa. Field-induced gap in cu benzoate and other $s = \frac{1}{2}$ antiferromagnetic chains. *Phys. Rev. B*, 60:1038–1056, Jul 1999.

[3] A. Altland and B. Simons. *Condensed Matter Field Theory*. Cambridge University Press, 2006.

[4] T. Amemiya, M. Yano, K. Morita, I. Umegaki, T. Ono, H. Tanaka, K. Fujii, and H. Uekusa. Partial ferromagnetic ordering and indirect exchange interaction in the spatially anisotropic kagome antiferromagnet $cs_2cu_3cef_{12}$. *Phys. Rev. B*, 80:100406, Sep 2009.

[5] W Apel, T Yavorskii, and H-U Everts. Spatially anisotropic heisenberg kagome antiferromagnet. *Journal of Physics: Condensed Matter*, 19(14):145255, 2007.

[6] D. N. Aristov. Luttinger liquids with curvature: Density correlations and coulomb drag effect. *Phys. Rev. B*, 76:085327, Aug 2007.

[7] A. Auerbach. *Interacting Electrons and Quantum Magnetism*. Springer-Verlag, 1994.

[8] L. Balents. Spin liquids in frustrated magnets. *Nature*, 464:199, 2010.

[9] B. Andrei Bernevig, Taylor L. Hughes, and Shou-Cheng Zhang. Quantum spin hall effect and topological phase transition in hgte quantum wells. *Science*, 314(5806):1757–1761, 2006.

[10] B. Andrei Bernevig, J. Orenstein, and Shou-Cheng Zhang. Exact $su(2)$ symmetry and persistent spin helix in a spin-orbit coupled system. *Phys. Rev. Lett.*, 97:236601, Dec 2006.

[11] B. Andrei Bernevig and Shou-Cheng Zhang. Quantum spin hall effect. *Phys. Rev. Lett.*, 96:106802, Mar 2006.

[12] F. Bert, D. Bono, P. Mendels, F. Ladieu, F. Duc, J.-C. Trombe, and P. Millet. Ground state of the kagomé-like $s = 1/2$ antiferromagnet volborthite cu3v2o7(oh)22h2o. 95(8):087203, 2005.

[13] G.S. Boebinger, A.M. Chang, H.L. Stormer, and D.C. Tsui. Magnetic field dependence of activation energies in the fractional quantum hall effect. *Phys. Rev. Lett.*, 55:1606, 1985.

[14] Yu.A. Bychkov and E.I. Rashba. Oscillatory effects and the magnetic susceptibility of carriers in inversion layers. *J. Phys. C*, 17:6039, 1984.

[15] M.A. Cazalilla. Bosonizing one-dimensional cold atomic gases. *J. of Phys. B: AMOP*, 37:S1, 2004.

[16] O. Cépas, C. M. Fong, P. W. Leung, and C. Lhuillier. Quantum phase transition induced by dzyaloshinskii-moriya interactions in the kagome antiferromagnet. *Phys. Rev. B*, 78:140405, Oct 2008.

[17] P.M. Chaikin and T.C. Lubensky. *Principles of Condensed Matter Physics*. Cambridge University Press, 1995.

[18] Victor Chua, Hong Yao, and Gregory A. Fiete. Exact chiral spin liquid with stable spin fermi surface on the kagome lattice. *Phys. Rev. B*, 83:180412, May 2011.

[19] R. H. Colman, F. Bert, D. Boldrin, A. D. Hillier, P. Manuel, P. Mendels, and A. S. Wills. Spin dynamics in the $s = \frac{1}{2}$ quantum kagome compound vesignieite, $\mathrm{cu_3ba}(vo_5h)_2$. *Phys. Rev. B*, 83:180416, May 2011.

[20] H.L. Stormer D.C. Tsui and A.C. Gossard. Two-dimensional magnetotransport in the extreme quantum limit. *Phys. Rev. Lett.*, 48:1559, 1982.

[21] P Debray, V Zverev, O Raichev, R Klesse, P Vasilopoulos, and R S Newrock. Experimental studies of coulomb drag between ballistic quantum wires. *Journal of Physics: Condensed Matter*, 13(14):3389, 2001.

[22] P Debray, V N Zverev, V Gurevich, R Klesse, and R S Newrock. Coulomb drag between ballistic one-dimensional electron systems. *Semiconductor Science and Technology*, 17(11):R21, 2002.

[23] G. Dresselhaus. Spin-orbit coupling effects in zinc blende structures. *Phys. Rev.*, 100:580, 1955.

[24] M. Dyakonov. Twenty years since the discovery of the fractional quantum hall effect: Current state of the theory. 2002.

[25] M.I. Dyakonov and V.I. Perel. Current-induced spin orientation of electrons in semiconductors. *Phys. Lett. A*, 35:459, 1971.

[26] M.I. Dyakonov and V.I. Perel. Possibility of orienting electron spins with current. *Sov. Phys. JETP Lett.*, 13:467, 1971.

[27] I.E. Dzyaloshinsky. A thermodynamic theory of "weak" ferromagnetism of antiferromagnetics. *J. Phys. Chem. Solids*, 4(4):241, 1958.

[28] M. Elhajal, B. Canals, and C. Lacroix. Symmetry breaking due to dzyaloshinsky-moriya interactions in the kagomé lattice. *Phys. Rev. B*, 66:014422, Jul 2002.

[29] N. Elstner and A. P. Young. Spin-1/2 heisenberg antiferromagnet on the kagome lattice: High-temperature expansion and exact-diagonalization studies. *Phys. Rev. B*, 50:6871–6876, Sep 1994.

[30] V. J. Emery, A. Luther, and I. Peschel. Solution of the one-dimensional electron gas on a lattice. *Phys. Rev. B*, 13:1272–1276, Feb 1976.

[31] G. Evenbly and G. Vidal. Frustrated antiferromagnets with entanglement renormalization: Ground state of the spin-$\frac{1}{2}$ heisenberg model on a kagome lattice. *Phys. Rev. Lett.*, 104:187203, May 2010.

[32] M. Fabrizio, A. Gogolin, and A. Nersesyan. Critical properties of the double-frequency sine-gordon model with applications. *Nucl. Phys. B*, 580:647, 2000.

[33] G.A. Fiete. *Science*, 323:546, 2011.

[34] Gregory A Fiete. Singular responses of spin-incoherent luttinger liquids. *Journal of Physics: Condensed Matter*, 21(19):193201, 2009.

[35] Gregory A. Fiete, Karyn Le Hur, and Leon Balents. Coulomb drag between two spin-incoherent luttinger liquids. *Phys. Rev. B*, 73:165104, Apr 2006.

[36] Liang Fu and C. L. Kane. Time reversal polarization and a Z_2 adiabatic spin pump. *Phys. Rev. B*, 74:195312, Nov 2006.

[37] Liang Fu and C. L. Kane. Topological insulators with inversion symmetry. *Phys. Rev. B*, 76:045302, Jul 2007.

[38] Liang Fu, C. L. Kane, and E. J. Mele. Topological insulators in three dimensions. *Phys. Rev. Lett.*, 98:106803, Mar 2007.

[39] Thomas Fuchs, Rochus Klesse, and Ady Stern. Coulomb drag between quantum wires with different electron densities. *Phys. Rev. B*, 71:045321, Jan 2005.

[40] Suhas Gangadharaiah, Jianmin Sun, and Oleg A. Starykh. Spin-orbital effects in magnetized quantum wires and spin chains. *Phys. Rev. B*, 78:054436, Aug 2008.

[41] Ion Garate and Ian Affleck. Interplay between symmetric exchange anisotropy, uniform dzyaloshinskii-moriya interaction, and magnetic fields in the phase diagram of quantum magnets and superconductors. *Phys. Rev. B*, 81:144419, Apr 2010.

[42] F. Ghahari, Y. Zhao, P. Cadden-Zimansky, K. Bolotin, and P. Kim. Measurement of the nu=1/3 fractional quantum hall energy gap in suspended graphene. *Phys. Rev. Lett.*, 106:046801, 2011.

[43] T. Giamarchi. *Quantum Physics in One Dimension.* Oxford Science Publications, 2003.

[44] R.R. Girvin and S.M. Girvin.

[45] S.M. Girvin and A.H. MacDonald. Off-diagonal long-range order, oblique confinement, and the fractional quantum hall effect. *Phys. Rev. Lett.*, 58:1252, 1987.

[46] A.O. Gogolin, A.A. Nersesyan, and A.M. Tsvelik. *Bosonization and Strongly Correlated Systems.* Cambridge University Press, 1998.

[47] F.D.M. Haldane. Effective harmonic-fluid approach to low-energy properties of one-dimensional quantum fluids. *Phys. Rev. Lett*, 47:1840, 1981.

[48] F.D.M. Haldane. Fractional quantization of the hall effect: A hierarchy of incompressible quantum fluid states. *Phys. Rev. Lett.*, 51:605, 1983.

[49] B.I. Halperin. Statistics of quasiparticles and the hierarchy of fractional quantized hall states. *Phys. Rev. Lett.*, 52:1583, 1984.

[50] B.I. Halperin, P.A. Lee, and N. Read. Theory of the half-filled landau level. *Phys. Rev. B*, 47:7312, 1993.

[51] T. H. Han, J. S. Helton, S. Chu, A. Prodi, D. K. Singh, C. Mazzoli, P. Müller, D. G. Nocera, and Y. S. Lee. Synthesis and characterization of single crystals of the spin-$\frac{1}{2}$ kagome-lattice antiferromagnets $\mathrm{zn}_x\mathrm{cu}_{4-x}(oh)_6\mathrm{cl}_2$. *Phys. Rev. B*, 83:100402, Mar 2011.

[52] Zhihao Hao, Yuan Wan, Ioannis Rousochatzakis, Julia Wildeboer, A. Seidel, F. Mila, and O. Tchernyshyov. Destruction of valence-bond order in a $s = \frac{1}{2}$ sawtooth chain with a dzyaloshinskii-moriya term. *Phys. Rev. B*, 84:094452, Sep 2011.

[53] M.Z. Hasan and C.L. Kane.

[54] J. S. Helton, K. Matan, M. P. Shores, E. A. Nytko, B. M. Bartlett, Y. Qiu, D. G. Nocera, and Y. S. Lee. Dynamic scaling in the susceptibility of the spin-$\frac{1}{2}$ kagome lattice antiferromagnet herbertsmithite. *Phys. Rev. Lett.*, 104:147201, Apr 2010.

[55] J. S. Helton, K. Matan, M. P. Shores, E. A. Nytko, B. M. Bartlett, Y. Yoshida, Y. Takano, A. Suslov, Y. Qiu, J.-H. Chung, D. G. Nocera, and Y. S. Lee. Spin dynamics of the spin-1/2 kagome lattice antiferromagnet $\mathrm{zncu}_3(oh)_6\mathrm{cl}_2$. 98(10):107204, 2007.

[56] Michael Hermele, Ying Ran, Patrick A. Lee, and Xiao-Gang Wen. Properties of an algebraic spin liquid on the kagome lattice. *Phys. Rev. B*, 77:224413, Jun 2008.

[57] J. E. Hirsch. Spin hall effect. *Phys. Rev. Lett.*, 83:1834–1837, Aug 1999.

[58] M. Hohenadler, T. C. Lang, and F. F. Assaad. Correlation effects in quantum spin-hall insulators: A quantum monte carlo study. *Phys. Rev. Lett.*, 106:100403, Mar 2011.

[59] Chang-Yu Hou, Eun-Ah Kim, and Claudio Chamon. Corner junction as a probe of helical edge states. *Phys. Rev. Lett.*, 102:076602, Feb 2009.

[60] Yejin Huh, Lars Fritz, and Subir Sachdev. Quantum criticality of the kagome antiferromagnet with dzyaloshinskii-moriya interactions. *Phys. Rev. B*, 81:144432, Apr 2010.

[61] J. Fabian I. Zutic and S. Das Sarma. Spintronics: Fundamentals and applications. *Rev. Mod. Phys.*, 76:323, 2004.

[62] Sin itiro Tomonaga. Remarks on bloch's method of sound waves applied to many-fermion problems. *Progress of Theoretical Physics*, 5(4):544–569, 1950.

[63] F. Bert J.A. Quilliam, A.S. Wills R.H. Colman, D. Boldrin, and P. Mendels. Ground State and Intrinsic Susceptibility of the Kagome Antiferromagnet Vesignieite as seen by 51V NMR. *ArXiv*.

[64] J.K. Jain. Composite-fermion approach for the fractional quantum hall effect. *Phys. Rev. Lett.*, 63:199, 1989.

[65] J.K. Jain. *Composite Fermions.* Cambridge University Press, 2007.

[66] T. Jungwirth and A.H. MacDonald. Electron-electron interactions and two-dimensionaltwo-dimensional tunneling. *Phys. Rev. B*, 53:7403, 1996.

[67] V. Kalmeyer and S.-C. Zhang. Metallic phase of the quantum hall system at even-denominator filling fractions. *Phys. Rev. B*, 46:9889, 1992.

[68] C. L. Kane and E. J. Mele. Quantum spin hall effect in graphene. *Phys. Rev. Lett.*, 95:226801, Nov 2005.

[69] C. L. Kane and E. J. Mele. Z_2 topological order and the quantum spin hall effect. *Phys. Rev. Lett.*, 95:146802, Sep 2005.

[70] C.L. Kane, R. Mukhopadhyay, and T.C. Lubensky. Fractional quantum hall effect in an array of quantum wires. *Phys. Rev. Lett.*, 88:036401, 2002.

[71] Michael Karbach, Gerhard Müller, A. Hamid Bougourzi, Andreas Fledderjohann, and Karl-Heinz Mütter. Two-spinon dynamic structure factor of the one-dimensional $s = \frac{1}{2}$ heisenberg antiferromagnet. *Phys. Rev. B*, 55:12510–12517, May 1997.

[72] Mehdi Kargarian, Jun Wen, and Gregory A. Fiete. Competing exotic topological insulator phases in transition-metal oxides on the pyrochlore lattice with distortion. *Phys. Rev. B*, 83:165112, 2011.

[73] Y. K. Kato, R. C. Myers, A. C. Gossard, and D. D. Awschalom. Observation of the spin hall effect in semiconductors. *Science*, 306(5703):1910–1913, 2004.

[74] E. Kermarrec, P. Mendels, F. Bert, R. H. Colman, A. S. Wills, P. Strobel, P. Bonville, A. Hillier, and A. Amato. Spin-liquid ground state in the frustrated kagome antiferromagnet $\mathrm{mgcu_3}(oh)_6\mathrm{cl_2}$. *Phys. Rev. B*, 84:100401, Sep 2011.

[75] V. S. Khrapai, A. A. Shashkin, M. G. Trokina, V. T. Dolgopolov, V. Pellegrini, F. Beltram, G. Biasiol, and L. Sorba. Direct measurements of fractional quantum hall effect gaps. *Phys. Rev. Lett.*, 99:086802, 2007.

[76] Rochus Klesse and Ady Stern. Coulomb drag between quantum wires. *Phys. Rev. B*, 62:16912–16925, Dec 2000.

[77] K. v. Klitzing, G. Dorda, and M. Pepper. New method for high-accuracy determination of the fine-structure constant based on quantized hall resistance. *Phys. Rev. Lett.*, 45:494–497, Aug 1980.

[78] Markus Konig, Steffen Wiedmann, Christoph Brne, Andreas Roth, Hartmut Buhmann, Laurens W. Molenkamp, Xiao-Liang Qi, and Shou-Cheng

Zhang. Quantum spin hall insulator state in hgte quantum wells. *Science*, 318(5851):766–770, 2007.

[79] J. D. Koralek, C. P. Weber, J. Orenstein, B. A. Bernevig, Shou-Cheng Zhang, S. Mack, and D. D. Awschalom. Emergence of the persistent spin helix in semiconductor quantum wells. *Nature*, 458:610, 2009.

[80] L.D. Landau and E.M. Lifshitz. *Quantum Mechanics: Non-Relativistic Theory*. Pergamon Press, 1977.

[81] R.B. Laughlin. Anomalous quantum hall effect: an incompressible quantum fluid with fractionally charged excitations. *Phys. Rev. Lett.*, 50:1395, 1983.

[82] K. T. Law, C. Y. Seng, Patrick A. Lee, and T. K. Ng. Quantum dot in a two-dimensional topological insulator: The two-channel kondo fixed point. *Phys. Rev. B*, 81:041305, Jan 2010.

[83] P. Lecheminant, B. Bernu, C. Lhuillier, L. Pierre, and P. Sindzingre. Order versus disorder in the quantum heisenberg antiferromagnet on the kagome lattice using exact spectra analysis. *Phys. Rev. B*, 56:2521–2529, Aug 1997.

[84] D.-H. Lee, G.-M. Zhang, and T. Xiang. Edge solitons of topological insulators and fractionalized quasiparticles in two dimensions. *Phys. Rev. Lett.*, 99:196805, 2007.

[85] P. W. Leung and Veit Elser. Numerical studies of a 36-site kagome antiferromagnet. *Phys. Rev. B*, 47:5459–5462, Mar 1993.

[86] Elliott H. Lieb. Exact analysis of an interacting bose gas. ii. the excitation spectrum. *Phys. Rev.*, 130:1616–1624, May 1963.

[87] Elliott H. Lieb and Werner Liniger. Exact analysis of an interacting bose gas. i. the general solution and the ground state. *Phys. Rev.*, 130:1605–1616, May 1963.

[88] J. M. Luttinger. An exactly soluble model of a many-fermion system. *Journal of Mathematical Physics*, 4(9):1154–1162, 1963.

[89] Joseph Maciejko, Chaoxing Liu, Yuval Oreg, Xiao-Liang Qi, Congjun Wu, and Shou-Cheng Zhang. Kondo effect in the helical edge liquid of the quantum spin hall state. *Phys. Rev. Lett.*, 102:256803, Jun 2009.

[90] J. B. Marston and C. Zeng. Spin-peierls and spin-liquid phases of kagom[e-acute] quantum antiferromagnets. *Journal of Applied Physics*, 69(8):5962–5964, 1991.

[91] K. Matan, D. Grohol, D. G. Nocera, T. Yildirim, A. B. Harris, S. H. Lee, S. E. Nagler, and Y. S. Lee. Spin waves in the frustrated kagomé lattice antiferromagnet $kfe_3(OH)_6(so_4)_2$. *Phys. Rev. Lett.*, 96:247201, Jun 2006.

[92] K. Matan, T. Ono, Y. Fukumoto, T. J. Sato, J. Yamaura, M. Yano, K. Morita, and H. Tanaka. *Nature Physics*, 6:865, 2010.

[93] Daniel C. Mattis and Elliott H. Lieb. Exact solution of a many-fermion system and its associated boson field. *Journal of Mathematical Physics*, 6(2):304–312, 1965.

[94] Philippe Mendels and Fabrice Bert. Quantum kagome antiferromagnet $zncu_3(oh)_6cl_2$. 79(1):011001, 2010.

[95] L. Messio, O. Cépas, and C. Lhuillier. Schwinger-boson approach to the kagome antiferromagnet with dzyaloshinskii-moriya interactions: Phase diagram and dynamical structure factors. *Phys. Rev. B*, 81:064428, Feb 2010.

[96] G. Misguich and B. Bernu. Specific heat of the $s = \frac{1}{2}$ heisenberg model on the kagome lattice: high-temperature series expansion analysis. *Phys. Rev. B*, 71:014417, Jan 2005.

[97] G. Moore and D. Green. Nonabelions in the fractional quantum hall effect. *Nucl. Phys. B*, 360:362, 1991.

[98] J.E. Moore. *Nature*, 464:194, 2010.

[99] Tôru Moriya. Anisotropic superexchange interaction and weak ferromagnetism. *Phys. Rev.*, 120:91–98, Oct 1960.

[100] B.M. Bartlett M.P. Shores, E.A. Nytko and D.G. Nocera. A structurally perfect s = 1/2 kagom antiferromagnet.

[101] Shuichi Murakami, Naoto Nagaosa, and Shou-Cheng Zhang. Dissipationless quantum spin current at room temperature. *Science*, 301(5638):1348–1351, 2003.

[102] Naoto Nagaosa, Jairo Sinova, Shigeki Onoda, A. H. MacDonald, and N. P. Ong. Anomalous hall effect. *Rev. Mod. Phys.*, 82:1539, 2010.

[103] Hiroki Nakano, Tokuro Shimokawa, and Toru Sakai. Collapse of ferrimagnetism in two-dimensional heisenberg antiferromagnet due to frustration. *Journal of the Physical Society of Japan*, 80(3):033709, 2011.

[104] Chetan Nayak, Steven H. Simon, Ady Stern, Michael Freedman, and Sankar Das Sarma. Non-abelian anyons and topological quantum computation. *Rev. Mod. Phys.*

[105] Yoshihiko Okamoto, Masashi Tokunaga, Hiroyuki Yoshida, Akira Matsuo, Koichi Kindo, and Zenji Hiroi. Magnetization plateaus of the spin-$\frac{1}{2}$ kagome antiferromagnets volborthite and vesignieite. *Phys. Rev. B*, 83:180407, May 2011.

[106] A. Olariu, P. Mendels, F. Bert, F. Duc, J. C. Trombe, M. A. de Vries, and A. Harrison. ^{17}O nmr study of the intrinsic magnetic susceptibility and spin dynamics of the quantum kagome antiferromagnet $\mathrm{zncu_3(OH)_6cl_2}$. *Phys. Rev. Lett.*, 100:087202, Feb 2008.

[107] P.K. Panigrahi and M. Sivakumar. Laughlin wave function and one-dimensional free fermions. *Phys. Rev. B*, 52:13742, 1995.

[108] O.A. Pankratov, S.V. Pakhomov, and B.A. Volkov. Supersymmetry in heterojunctions: Band-inverting contact on the basis of $pb(1-x)sn(x)te$ and $hg(1-x)cd(x)te$. *Solid State Communications*, 61:93, 1987.

[109] D. Pesin and L. Balents. *Nature Physics*, 6:376, 2010.

[110] V. V. Ponomarenko and D. V. Averin. Coulomb drag between one-dimensional conductors. *Phys. Rev. Lett.*, 85:4928–4931, Dec 2000.

[111] M. Pustilnik, M. Khodas, A. Kamenev, and L. I. Glazman. Dynamic response of one-dimensional interacting fermions. *Phys. Rev. Lett.*, 96:196405, May 2006.

[112] M. Pustilnik, E. G. Mishchenko, L. I. Glazman, and A. V. Andreev. Coulomb drag by small momentum transfer between quantum wires. *Phys. Rev. Lett.*, 91:126805, Sep 2003.

[113] M. Pustilnik, E. G. Mishchenko, and O. A. Starykh. Generation of spin current by coulomb drag. *Phys. Rev. Lett.*, 97:246803, Dec 2006.

[114] Xiao-Liang Qi and Shou-Cheng Zhang. The quantum spin hall effect and topological insulators. *Physics Today*, 63(1):33–38, 2010.

[115] Xiao-Liang Qi and Shou-Cheng Zhang. Topological insulators and superconductors. *Rev. Mod. Phys.*, 83:1057, 2011.

[116] Stephan Rachel and Karyn Le Hur. Topological insulators and mott physics from the hubbard interaction. *Phys. Rev. B*, 82:075106, Aug 2010.

[117] Ying Ran, Michael Hermele, Patrick A. Lee, and Xiao-Gang Wen. Projected-wave-function study of the spin-1/2 heisenberg model on the kagomé lattice. *Phys. Rev. Lett.*, 98:117205, Mar 2007.

[118] N. Read. Excitation structure of the hierarchy scheme in the fractional quantum hall effect. *Phys. Rev. Lett.*, 65:1502, 1990.

[119] Marcos Rigol and Rajiv R. P. Singh. Kagome lattice antiferromagnets and dzyaloshinsky-moriya interactions. *Phys. Rev. B*, 76:184403, Nov 2007.

[120] Marcos Rigol and Rajiv R. P. Singh. Magnetic susceptibility of the kagome antiferromagnet $zncu_3(OH)_6cl_2$. *Phys. Rev. Lett.*, 98:207204, May 2007.

[121] Andreas Roth, Christoph Brne, Hartmut Buhmann, Laurens W. Molenkamp, Joseph Maciejko, Xiao-Liang Qi, and Shou-Cheng Zhang. Nonlocal transport in the quantum spin hall state. *Science*, 325(5938):294–297, 2009.

[122] Ioannis Rousochatzakis, Salvatore R. Manmana, Andreas M. Läuchli, Bruce Normand, and Frédéric Mila. Dzyaloshinskii-moriya anisotropy and nonmagnetic impurities in the $s = \frac{1}{2}$ kagome system $zncu_3(OH)_6cl_2$. *Phys. Rev. B*, 79:214415, Jun 2009.

[123] Andreas Rüegg and Gregory A. Fiete. Topological order and semions in a strongly correlated quantum spin hall insulator. *Phys. Rev. Lett.*,

108:046401, Jan 2012.

[124] S. Sachdev. *Quantum Phase Transitions.* Cambridge University Press, 1999.

[125] Subir Sachdev. Kagome- and triangular-lattice heisenberg antiferromagnets: Ordering from quantum fluctuations and quantum-disordered ground states with unconfined bosonic spinons. *Phys. Rev. B*, 45:12377–12396, Jun 1992.

[126] Andreas P. Schnyder, Oleg A. Starykh, and Leon Balents. Spatially anisotropic heisenberg kagome antiferromagnet. *Phys. Rev. B*, 78:174420, Nov 2008.

[127] H.J. Schulz. *The Metal-Insulator Transition in One Dimension.* 1993.

[128] H.J. Schulz, G. Cuniberti, and P. Pieri. *Fermi liquids and Luttinger liquids.* Springer, 2000.

[129] L. Shekhtman, O. Entin-Wohlman, and Amnon Aharony. Moriya's anisotropic superexchange interaction, frustration, and dzyaloshinsky's weak ferromagnetism. *Phys. Rev. Lett.*, 69:836–839, Aug 1992.

[130] P. Sindzingre, G. Misguich, C. Lhuillier, B. Bernu, L. Pierre, Ch. Waldtmann, and H.-U. Everts. Magnetothermodynamics of the spin- $\frac{1}{2}$ kagome antiferromagnet. *Phys. Rev. Lett.*, 84:2953–2956, Mar 2000.

[131] Rajiv R. P. Singh and David A. Huse. Three-sublattice order in triangular- and kagome-lattice spin-half antiferromagnets. *Phys. Rev. Lett.*, 68:1766–1769, Mar 1992.

[132] Rajiv R. P. Singh and David A. Huse. Ground state of the spin-1/2 kagome-lattice heisenberg antiferromagnet. *Phys. Rev. B*, 76:180407, Nov 2007.

[133] O. A. Starykh, A. W. Sandvik, and R. R. P. Singh. Dynamics of the spin- heisenberg chain at intermediate temperatures. *Phys. Rev. B*, 55:14953–14967, Jun 1997.

[134] Oleg A. Starykh and Leon Balents. Dimerized phase and transitions in a spatially anisotropic square lattice antiferromagnet. *Phys. Rev. Lett.*, 93:127202, Sep 2004.

[135] Oleg A. Starykh and Leon Balents. Ordering in spatially anisotropic triangular antiferromagnets. *Phys. Rev. Lett.*, 98:077205, Feb 2007.

[136] Oleg A. Starykh, Akira Furusaki, and Leon Balents. Anisotropic pyrochlores and the global phase diagram of the checkerboard antiferromagnet. *Phys. Rev. B*, 72:094416, Sep 2005.

[137] Oleg A. Starykh, Hosho Katsura, and Leon Balents. Extreme sensitivity of a frustrated quantum magnet: cs_2Cucl_4. *Phys. Rev. B*, 82:014421, Jul 2010.

[138] H.L. Stormer, A. Chang, D.C. Tsui, J.C.M. Hwang, A.C. Gossard, and W. Wiegmann. Fractional quantization of the hall effect. *Phys. Rev. Lett.*, 50:1953, 1983.

[139] E. M. Stoudenmire and Leon Balents. Ordered phases of the anisotropic kagome-lattice antiferromagnet in a magnetic field. *Phys. Rev. B*, 77:174414, May 2008.

[140] Anders Ström and Henrik Johannesson. Tunneling between edge states in a quantum spin hall system. *Phys. Rev. Lett.*, 102:096806, Mar 2009.

[141] Jianmin Sun, Suhas Gangadharaiah, and Oleg A. Starykh. Spin-orbit-induced spin-density wave in a quantum wire. *Phys. Rev. Lett.*, 98:126408, Mar 2007.

[142] Yukio Tanaka and Naoto Nagaosa. Two interacting helical edge modes in quantum spin hall systems. *Phys. Rev. Lett.*, 103:166403, Oct 2009.

[143] J.C.Y. Teo and C.L. Kane. From luttinger liquid to non-abelian quantum hall states. *arXiv:1111.2617*, 2011.

[144] Jeffrey C. Y. Teo and C. L. Kane. Critical behavior of a point contact in a quantum spin hall insulator. *Phys. Rev. B*, 79:235321, Jun 2009.

[145] Mayra Tovar, Kumar S. Raman, and Kirill Shtengel. Dzyaloshinskii-moriya interactions in valence-bond systems. *Phys. Rev. B*, 79:024405, Jan 2009.

[146] J Voit. One-dimensional fermi liquids. *Rep. Prog. Phys.*, 58:977, 1995.

[147] G. E. Volovik. *The Universe in a Helium Droplet.* Clarendon Press, 2003.

[148] Fa Wang, Ashvin Vishwanath, and Yong Baek Kim. Quantum and classical spins on the spatially distorted kagomé lattice: Applications to volborthite $cu_3v_2o_7(OH)_2 2h_2O$. *Phys. Rev. B*, 76:094421, Sep 2007.

[149] X.-G. Wen. *Quantum Field Theory of Many-Body Systems.* Oxford Science Publications, 2004.

[150] William Witczak-Krempa, Ting Pong Choy, and Yong Baek Kim. Gauge field fluctuations in three-dimensional topological mott insulators. *Phys. Rev. B*, 82:165122, Oct 2010.

[151] Congjun Wu, B. Andrei Bernevig, and Shou-Cheng Zhang. Helical liquid and the edge of quantum spin hall systems. *Phys. Rev. Lett.*, 96:106401, Mar 2006.

[152] W. Wu, S. Rachel, W.-M. Liu, and K. Le Hur. Quantum Spin Hall Insulators with Interactions and Lattice Anisotropy. *ArXiv e-prints*, June 2011.

[153] Dirk Wulferding, Peter Lemmens, Patric Scheib, Jens Röder, Philippe Mendels, Shaoyan Chu, Tianheng Han, and Young S. Lee. Interplay of thermal and quantum spin fluctuations in the kagome lattice compound herbertsmithite. *Phys. Rev. B*, 82:144412, Oct 2010.

[154] J. Wunderlich, B. Kaestner, J. Sinova, and T. Jungwirth. Experimental observation of the spin-hall effect in a two-dimensional spin-orbit coupled semiconductor system. *Phys. Rev. Lett.*, 94:047204, Feb 2005.

[155] Cenke Xu and Liang Fu. Fractionalization in josephson junction arrays hinged by quantum spin hall edges. *Phys. Rev. B*, 81:134435, Apr 2010.

[156] Cenke Xu and J. E. Moore. Stability of the quantum spin hall effect: Effects of interactions, disorder, and Z_2 topology. *Phys. Rev. B*, 73:045322, Jan 2006.

[157] Youhei Yamaji and Masatoshi Imada. Mott physics on helical edges of two-dimensional topological insulators. *Phys. Rev. B*, 83:205122, May 2011.

[158] M. Yamamoto, M. Stopa, Y. Tokura, Y. Hirayama, and S. Tarucha. Negative coulomb drag in a one-dimensional wire. *Science*, 313(5784):204–207, 2006.

[159] Simeng Yan, David A. Huse, and Steven R. White. Spin-liquid ground state of the s = 1/2 kagome heisenberg antiferromagnet. *Science*, 332(6034):1173–1176, 2011.

[160] T. Yavors'kii, W. Apel, and H.-U. Everts. Heisenberg antiferromagnet with anisotropic exchange on the kagomé lattice: Description of the magnetic properties of volborthite. *Phys. Rev. B*, 76:064430, Aug 2007.

[161] M. Yoshida, M. Takigawa, H. Yoshida, Y. Okamoto, and Z. Hiroi. Phase diagram and spin dynamics in volborthite with a distorted kagome lattice. 103(7):077207, 2009.

[162] M. Yoshida, M. Takigawa, H. Yoshida, Y. Okamoto, and Z. Hiroi. Heterogeneous spin state in the field-induced phase of volborthite as seen via ^{51}v nuclear magnetic resonance. *Phys. Rev. B*, 84:020410, Jul 2011.

[163] Hiroyuki Yoshida Yoshihiko Okamoto and Zenji Hiroi. Vesignieite $\mathrm{bacu_3v_2o_8}(oh)_2$ as a candidate spin-1/2 kagome antiferromagnet. 78(3):033701, 2009.

[164] Michael W. Young, Sung-Sik Lee, and Catherine Kallin. Fractionalized quantum spin hall effect. *Phys. Rev. B*, 78:125316, Sep 2008.

[165] Chen Zeng and Veit Elser. Numerical studies of antiferromagnetism on a kagome net. *Phys. Rev. B*, 42:8436–8444, Nov 1990.

[166] Naoya Kobayashi Minoru Nohara Hidenori Takagi Yoshitomo Kato Zenji Hiroi, Masafumi Hanawa and Masashi Takigawa. Spin-1/2 *Kagomé*-like lattice in volborthite
$cu_3v_2o_7(oh)_2 \cdot 2h_2o$. 70(11):3377, 2001.

[167] A. Zorko, S. Nellutla, J. van Tol, L. C. Brunel, F. Bert, F. Duc, J.-C. Trombe, M. A. de Vries, A. Harrison, and P. Mendels. Dzyaloshinsky-moriya anisotropy in the spin-1/2 kagome compound $\mathrm{zncu_3(OH)_6cl_2}$. *Phys. Rev. Lett.*, 101:026405, Jul 2008.

[168] V.A. Zyuzin, E.G. Mishchenko, and M.E. Raikh. Tunneling between two-dimensional electron layers with correlated disorder: Anomalous sensitivity to spin-orbit coupling. *Phys. Rev. B*, 74:205322, 2006.

Vita

Vladimir Alexandrovich Zyuzin was born in Leningrad, USSR on 6 December 1982, the son of Alexander Yu. Zyuzin and Klavdia I. Shestak. He received the Master of Science degree in Physics from the Saint Petersburg State Polytechnical University in June 2005. During the 2005-2008 academic years he was a graduate student at the University of Utah. He then entered the Graduate School of the University of Texas at Austin in August 2008.

Permanent address: 1905 Nueces str, apt 225
Austin, Texas 78705

This dissertation was typeset with LaTeX[†] by the author.

[†]LaTeX is a document preparation system developed by Leslie Lamport as a special version of Donald Knuth's TeX Program.